INL/EXT-14-32661

Fast Neutron Spectrum Potassium Worth for Space Power Reactor Design Validation

John D. Bess, Margaret A. Marshall, J. Blair Briggs, Anatoli Tsiboulia, Yevgeniy Rozhikhin, John T. Mihalczo

March 2015

The INL is a U.S. Department of Energy National Laboratory
operated by Battelle Energy Alliance

INL/EXT-14-32661

Fast Neutron Spectrum Potassium Worth for Space Power Reactor Design Validation

John D. Bess, Margaret A. Marshall, J. Blair Briggs, Anatoli Tsiboulia, Yevgeniy Rozhikhin, John T. Mihalczo

March 2015

Idaho National Laboratory

Idaho Falls, Idaho 83415

http://www.inl.gov

Prepared for the
U.S. Department of Energy
Office of Nuclear Energy
Under DOE Idaho Operations Office
Contract DE-AC07-05ID14517

NEA/NSC/DOC(2006)1

Space Reactor - SPACE

ORCEF-SPACE-EXP-001
CRIT-REAC

Fast Neutron Spectrum Potassium Worth for Space Power Reactor Design Validation

Evaluator

John D. Bess
Idaho National Laboratory

Internal Reviewers

Margaret A. Marshall
J. Blair Briggs
Idaho National Laboratory

Independent Reviewers

Anatoli Tsiboulia
Yevgeniy Rozhikhin
Institute of Physics and Power Engineering

John T. Mihalczo
Oak Ridge National Laboratory

Space Reactor - SPACE

ORCEF-SPACE-EXP-001
CRIT-REAC

Status of Compilation / Evaluation / Peer Review

Section 1	Compiled	Independent Review	Working Group Review	Approved
1.0 DETAILED DESCRIPTION				
1.1 Description of the Critical and / or Subcritical Configuration	YES	YES	YES	YES
1.2 Description of Buckling and Extrapolation Length Measurements	NA	NA	NA	NA
1.3 Description of Spectral Characteristics Measurements	NA	NA	NA	NA
1.4 Description of Reactivity Effects Measurements	YES	YES	YES	YES
1.5 Description of Reactivity Coefficient Measurements	NA	NA	NA	NA
1.6 Description of Kinetics Measurements	NA	NA	NA	NA
1.7 Description of Reaction-Rate Distribution Measurements	NA	NA	NA	NA
1.8 Description of Power Distribution Measurements	NA	NA	NA	NA
1.9 Description of Isotopic Measurements	NA	NA	NA	NA
1.10 Description of Other Miscellaneous Types of Measurements	NA	NA	NA	NA
Section 2	**Evaluated**	**Independent Review**	**Working Group Review**	**Approved**
2.0 EVALUATION OF EXPERIMENTAL DATA				
2.1 Evaluation of Critical and / or Subcritical Configuration Data	YES	YES	YES	YES
2.2 Evaluation of Buckling and Extrapolation Length Data	NA	NA	NA	NA
2.3 Evaluation of Spectral Characteristics Data	NA	NA	NA	NA
2.4 Evaluation of Reactivity Effects Data	YES	YES	YES	YES
2.5 Evaluation of Reactivity Coefficient Data	NA	NA	NA	NA
2.6 Evaluation of Kinetics Measurements Data	NA	NA	NA	NA
2.7 Evaluation of Reaction Rate Distributions	NA	NA	NA	NA
2.8 Evaluation of Power Distribution Data	NA	NA	NA	NA
2.9 Evaluation of Isotopic Measurements	NA	NA	NA	NA
2.10 Evaluation of Other Miscellaneous Types of Measurements	NA	NA	NA	NA

Section 3	Compiled	Independent Review	Working Group Review	Approved
3.0 BENCHMARK SPECIFICATIONS				
3.1 Benchmark-Model Specifications for Critical and / or Subcritical Measurements	YES	YES	YES	YES
3.2 Benchmark-Model Specifications for Buckling and Extrapolation Length Measurements	NA	NA	NA	NA
3.3 Benchmark-Model Specifications for Spectral Characteristics Measurements	NA	NA	NA	NA
3.4 Benchmark-Model Specifications for Reactivity Effects Measurements	YES	YES	YES	YES
3.5 Benchmark-Model Specifications for Reactivity Coefficient Measurements	NA	NA	NA	NA
3.6 Benchmark-Model Specifications for Kinetics Measurements	NA	NA	NA	NA
3.7 Benchmark-Model Specifications for Reaction-Rate Distribution Measurements	NA	NA	NA	NA
3.8 Benchmark-Model Specifications for Power Distribution Measurements	NA	NA	NA	NA
3.9 Benchmark-Model Specifications for Isotopic Measurements	NA	NA	NA	NA
3.10 Benchmark-Model Specifications of Other Miscellaneous Types of Measurements	NA	NA	NA	NA
Section 4	**Compiled**	**Independent Review**	**Working Group Review**	**Approved**
4.0 RESULTS OF SAMPLE CALCULATIONS				
4.1 Results of Calculations of the Critical or Subcritical Configurations	YES	YES	YES	YES
4.2 Results of Buckling and Extrapolation Length Calculations	NA	NA	NA	NA
4.3 Results of Spectral Characteristics Calculations	NA	NA	NA	NA
4.4 Results of Reactivity Effect Calculations	YES	YES	YES	YES
4.5 Results of Reactivity Coefficient Calculations	NA	NA	NA	NA
4.6 Results of Kinetics Parameter Calculations	NA	NA	NA	NA
4.7 Results of Reaction-Rate Distribution Calculations	NA	NA	NA	NA
4.8 Results of Power Distribution Calculations	NA	NA	NA	NA
4.9 Results of Isotopic Calculations	NA	NA	NA	NA
4.10 Results of Calculations of Other Miscellaneous Types of Measurements	NA	NA	NA	NA
Section 5	**Compiled**	**Independent Review**	**Working Group Review**	**Approved**
5.0 REFERENCES	YES	YES	YES	YES
Appendix A: Computer Codes, Cross Sections, and Typical Input Listings	YES	YES	YES	YES

Space Reactor - SPACE

ORCEF-SPACE-EXP-001
CRIT-REAC

FAST NEUTRON SPECTRUM POTASSIUM WORTH FOR SPACE POWER REACTOR DESIGN VALIDATION

IDENTIFICATION NUMBER: ORCEF-SPACE-EXP-001
CRIT-REAC

KEY WORDS: acceptable, annuli, critical experiment, fast-spectrum, highly enriched, metal, oralloy, ORCEF, potassium, reactivity, stainless steel can, uranium, vertical assembly

SUMMARY

1.0 DETAILED DESCRIPTION

A variety of critical experiments were constructed of enriched uranium metal (oralloy[a]) during the 1960s and 1970s at the Oak Ridge Critical Experiments Facility (ORCEF) in support of criticality safety operations at the Y-12 Plant. The purposes of these experiments included the evaluation of storage, casting, and handling limits for the Y-12 Plant and providing data for verification of calculation methods and cross-sections for nuclear criticality safety applications. These included solid cylinders of various diameters, annuli of various inner and outer diameters, two and three interacting cylinders of various diameters, and graphite and polyethylene reflected cylinders and annuli.

Of the hundreds of delayed critical experiments, one was performed that consisted of uranium metal annuli surrounding potassium-filled, stainless steel cans. The outer diameter of the annuli was approximately 13 inches (33.02 cm) with an inner diameter of 7 inches (17.78 cm). The diameter of the stainless steel can was 7 inches (17.78 cm). The critical height of the configurations was approximately 5.6 inches (14.224 cm). The uranium annulus consisted of multiple stacked rings, each with radial thicknesses of 1 inch (2.54 cm) and varying heights. A companion measurement was performed using empty stainless steel cans. The experimental measurements were performed on July 11, 1963, by J. T. Mihalczo, J. J. Lynn, and R. G. Taylor (Ref. 1). Additional information may be found in the corresponding logbook.[b]

The primary purpose of these experiments was to test the fast neutron cross sections of potassium as it was a candidate for coolant in some early space power reactor designs. A series of small, compact critical assembly (SCCA) experiments had been performed from 1962-65 at ORCEF[c,d,e] in support of the Medium-Power Reactor Experiments (MPRE) program.[f] In the late 1950s, efforts were made to study "power plants for the production of electrical power in space vehicles." The MPRE program was a part of those efforts and studied the feasibility of a stainless-steel system, boiling potassium 1 MWt, or about 140 kWe, reactor. This program was carried out until 1967. Experiments at ORCEF supported a UO_2 variant of the SNAP reactor fuel, and were indicated as the SNAP UO_2 experiments in the SCCA logbook.[g]

---

[a] Oralloy stands for Oak Ridge Alloy, and consists of HEU metal with a ^{235}U enrichment of more than 93 %.
[b] Experimental data for these experiments can be found on page 9 of ORNL logbook 12R (East Cell – Logbook 1, E-19), and pages 49-54 and 60 of ORNL logbook 13R (East Cell – Logbook 2, E-20).
[c] J. T. Mihalczo, "A Small Beryllium-Reflected UO_2 Assembly," ORNL-TM-655, Oak Ridge National Laboratory (1964).
[d] J. T. Mihalczo, "A Small, Beryllium-Reflected UO_2 Critical Assembly," *Trans. Am. Nucl. Soc.*, **72**, 196-198 (1995).
[e] M. A. Marshall, "Critical Configuration and Physics Measurements for Beryllium-Reflected Assemblies of U(93.15)O_2 Fuel Rods (1.506-cm Pitch and 7-Tube Clusters)," SCCA-SPACE-EXP-003, *International Handbook of Evaluated Reactor Physics Benchmark Experiments*, OECD-NEA, Paris, France (2015).
[f] A. P. Fraas, "Summary of the MPRE Design and Development Program," ORNL-4048, Oak Ridge National Laboratory (1967).
[g] ORNL logbook 75r (SNAP UO_2, E-2).

Unreflected and unmoderated experiments with the same set of highly enriched uranium metal parts were performed at ORCEF in the 1960s and are evaluated in the *International Handbook for Evaluated Criticality Safety Benchmark Experiments* (ICSBEP Handbook)[a] with the identifier HEU-MET-FAST-051. Thin graphite reflected (2 inches or less) experiments also using the same set of highly enriched uranium metal parts are evaluated in HEU-MET-FAST-071. Polyethylene-reflected configurations are evaluated in HEU-MET-FAST-076. A stack of highly enriched metal discs with a thick beryllium top reflector is evaluated in HEU-MET-FAST-069, and two additional highly enriched uranium annuli with beryllium cores are evaluated in HEU-MET-FAST-059.

Both detailed and simplified model specifications are provided in this evaluation. Both of these fast neutron spectra assemblies were determined to be acceptable benchmark experiments. The calculated eigenvalues for both the detailed and the simple benchmark models are within ~0.26 % of the benchmark values for Configuration 1 (calculations performed using MCNP6 with ENDF/B-VII.1 neutron cross section data), but under-calculate the benchmark values by ~7σ because the uncertainty in the benchmark is very small (~0.0004, 1σ); for Configuration 2, the under-calculation is ~0.31 % and ~8σ. There is significant variability between results using different neutron cross section libraries, the greatest being within ~0.6 % (~17σ) of the benchmark values for both configurations using JEFF-3.1.

Comparison of detailed and simple model calculations, for both the potassium worth measurement and potassium mass coefficient, yield results approximately 70 – 80 % lower (~6σ to 10σ) than the benchmark values for the various nuclear data libraries utilized. Both the potassium worth and mass coefficient measurements are also adequately described and deemed to be acceptable benchmark experiment measurements. Please note that this benchmark experiment value is derived from the two near-critical benchmark experiment configurations.

1.1 Description of the Critical and / or Subcritical Configuration

1.1.1 Overview of Experiment

Two near-critical configurations have been evaluated. The first configuration consisted of stacked HEU metal annuli around empty stainless steel cans. The second configuration consisted of the same stacks of HEU metal annuli around stainless steel cans containing potassium. Both configurations have been evaluated as acceptable benchmark experiments.

1.1.2 Geometry of the Experiment Configuration and Measurement Procedure

These experiments were performed on a vertical assembly machine located in the 35 × 35 × 30-ft-high East Cell of the ORCEF, and the assemblies of uranium were located approximately 11.7 ft from the five-ft-thick concrete west wall, 12.7 ft from the two-ft-thick concrete north wall, and 9.2 ft above the concrete floor.

The two annular experiments consisted of a stack of annular uranium discs with a nominal inside diameter of ~7 inches (~17.78 cm), which was filled with stainless steel (Type 304) cans with a nominal outer diameter of ~7 inches (~7.62 cm).[b] The outer diameter of the uranium annuli was ~13 inches (~33.02 cm) with a height of ~5.6 inches (~14.224 cm). The stainless steel cans were either empty (Configuration 1) or filled with potassium (Configuration 2). See Figure 1.1-1 for a sketch of the assembly arrangement from Ref. 1 for Configuration 2, as well as a 3D image created to help visualize the experiment assembly. The combined height of the steel cans was ~5.5 inches (~13.97 cm) in each

[a] *International Handbook of Evaluated Criticality Safety Benchmark Experiments*, OECD-NEA, Paris, France (2014).

[b] Incorrectly reported as having a diameter of 2.99 in. in Ref. 1; this value was verified as incorrect by the lead experimenter. (Personal communication with John T. Mihalczo, January 2014.)

experiment. A thin stainless steel (Type 304) diaphragm separated the top and bottom halves of each experiment.

The general measurement procedure for all HEU oralloy experiments includes the following details. Detectors used for reactor period measurements were placed 10 to 15 ft (3.048 to 4.572 m) away and consisted of BF_3 proportional counters and boron-lined ionization chambers. The reactivity worth was obtained from the difference in two measurements; one without the change and the other with the change. The inhour equation was then used to convert reactor period to reactivity. A neutron source was near the assemblies for startup only and was withdrawn ~4 ft (~1.2192 m) away into a borated paraffin shield during the measurements. Measurements were performed at fission rates such that the neutrons coming out of the shield from the startup source were insignificant.[a]

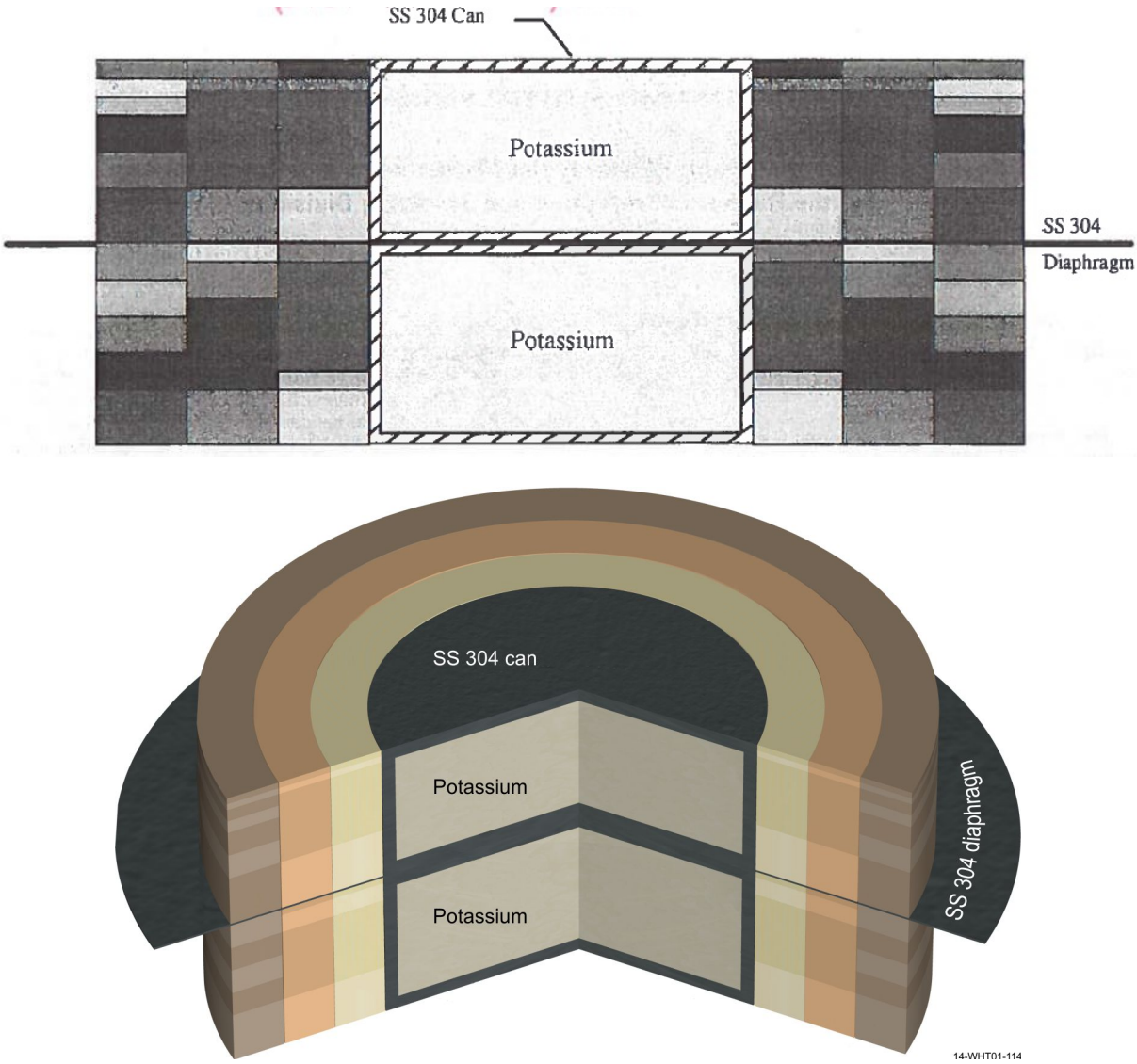

Figure 1.1-1. Oralloy Metal Annuli with Potassium-Filled Stainless Steel Cans (Configuration 2). Configuration 1 is identical in design, but the cans were empty. Top figure copied from Ref. 1; bottom figure provided for additional clarity regarding assembly.

[a] Personal communication with John T. Mihalczo, March 2010.

1.1.2.1 General Assembly Procedure

In general, all HEU oralloy experiments were constructed on a vertical assembly machine (shown in Figure 1.1-2), which primarily consisted of a hydraulic lift with 22-inch (55.88-cm) vertical motion, to support the lower section and a stationary upper section (The upper support shown in Figure 1.1-2 was not used in this experiment).

For unreflected experiments (i.e., no significant amounts of reflector material were placed around the periphery of the experiment), the lower support stand held the uranium metal of the lower section in place. The lower section was supported on 0.125-inch-(0.3175-cm)-thick aluminum edges, oriented vertically 120 degrees apart (visible in Figure 1.1-3). The upper section was supported by four vertical posts, which held a low-mass support consisting of two 30-inch-(76.2-cm)-ID, 2-inch (5.08-cm) wide, 0.5-inch-(1.27-cm)-thick, aluminum clamping rings bolted together and supported off vertical poles by aluminum tubing; see Figure 1.1-3. Note that Figure 1.1-3 shows an unreflected uranium metal assembly; these critical experiments were assembled on the same vertical lift with the same support structure as shown in this figure. The 30-inch-diameter clamping rings held a 0.010-inch-(0.0254-cm)-thick stainless steel (304L) diaphragm on which the upper uranium metal section was supported. The lower section was supported on a low-mass support stand (sometimes referred to as a support tower) mounted in the vertical position and also shown in Figure 1.1-3. The 0.5-inch-(1.27-cm)-thick, 18-inch-(45.72-cm)-diameter aluminum base of this support stand was bolted to the 1-inch-(2.54-cm)-thick, 18-inch-(45.72-cm)-diameter stainless steel table of the vertical lift as shown in Figure 1.1-3. The lower surface of the uranium was at a height of 36 inches (91.44 cm) above the aluminum base. Small aluminum pieces bolted to the 120° vertical members restrained lateral motion of the lower section. These low mass supports were used to minimize the reflection effects of support structure. The aluminum base of the support stand is type Al6061 and the stainless steel table is Type 304L.[a] Additional structural detail for the lower support stand and diaphragm clamping ring are given in Appendix E.

Experiments were assembled by mounting a fixed height of uranium metal parts on the lower section with lower steel can, after which uranium and the upper can were added to the upper section until near delayed criticality was achieved. For these experiments, the lower section was raised until it made contact with the diaphragm and actually slightly lifted the upper section of material mounted on the diaphragm. The lifting of the top section slightly by the bottom section was used to compensate for the sag of the diaphragm due to the weight of the upper material. The lifting of the diaphragm was monitored to the nearest 0.001 inches (0.00254 cm) and the lower section was moved up only until the diaphragm was level. Due to the thickness of the smallest uranium parts, the system could rarely be adjusted to exactly delayed criticality. For most assemblies the uranium mass of the upper section was adjusted until a self-sustaining fission chain reaction occurred with a measurable positive stable reactor period. For assemblies that were slightly subcritical, an additional hydrogenous reflector (small piece of Plexiglas) was added as a reflector to achieve a self-sustaining chain reaction. When the fission rate achieved a value from which a negative reactor period could be measured, the Plexiglas was quickly (within a fraction of a second)[b] removed to measure the resulting negative reactor period.

1.1.2.2 Stack Height of Annuli

Assembly heights at different angular locations for HEU oralloy experiments were measured to within ±0.001 inches by stacking them on a precision flat surface and measuring the distance between the upper surface of uranium and the precision flat surface. Multiple measurements were performed with all parts assembled in the same vertical order and orientation that they were in the critical experiment, which stacked uranium cylinders and annuli azimuthally such that the part numbers were always oriented towards the north wall. The part numbers were scribed on the upper surface of the part. This operation

[a] Personal communication with John T. Mihalczo, February 2010.
[b] Personal communication with John T. Mihalczo in HEU-MET-FAST-076 (ICSBEP Handbook), June 2006.

presented no criticality safety problems in hand stacking since the annuli were only one-inch-thick radially.

For the experiments with uranium metal on the lower support stand, the heights were measured with the uranium on the lower support stand as the assemblies were disassembled. For example, for a typical 15-inch-(38.1-cm)-OD cylinder, the height of the outer annulus (15-13 inches, 38.1-33.02 cm) was measured at several locations azimuthally. After the height measurements for this annular ring were made, the annular ring was removed from the support stand and the height of the 13-11 inch (33.02-27.94 cm) annular ring measured. This process continued until the height of the central 7-inch (17.78-cm) diameter disc stack was measured. The stack height was measured directly with the lower support table in the withdrawn position since the top and bottom of the stacks are accessible. The micrometer read out to 0.001 inches (0.00254 cm) and was repeatable at any azimuthal location. The standard deviation associated with the averages of the azimuthal measurements provides the uncertainty in the thickness.[a]

Reported heights (Ref. 1) for the stacked annuli for these HEU/K experiments are given in Table 1.1-1. The series of stack height measurements recorded in the logbook are shown in Table 1.1-2. The average stack heights were calculated and reported in the original logbooks. The standard deviation has been calculated using the original data.

[a] Personal communication with John T. Mihalczo, March 2010.

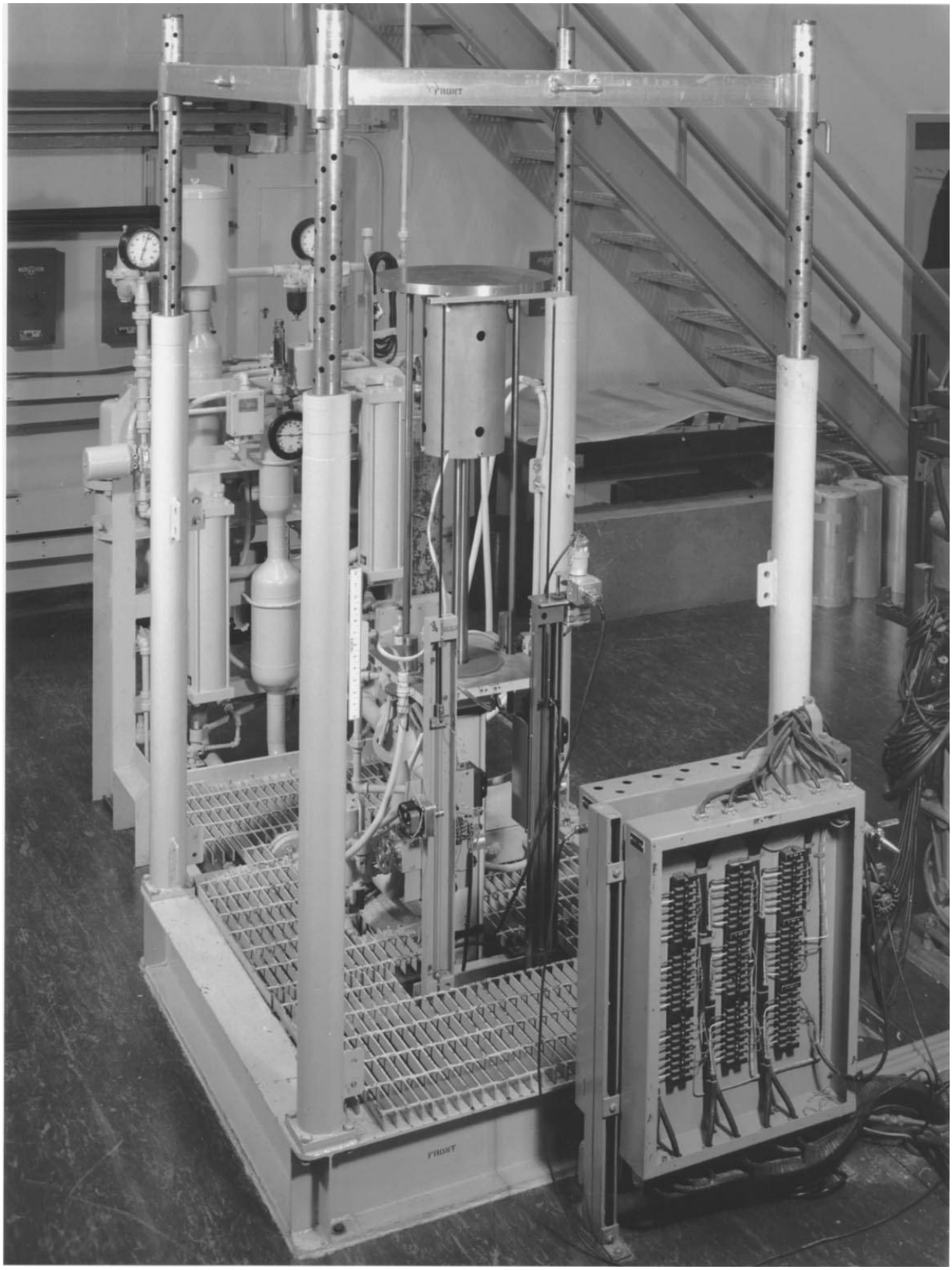

Figure 1.1-2. Photograph of the Vertical Assembly Machine with the Movable Table Up.
(The upper support shown in this photograph was not used in these measurements.)

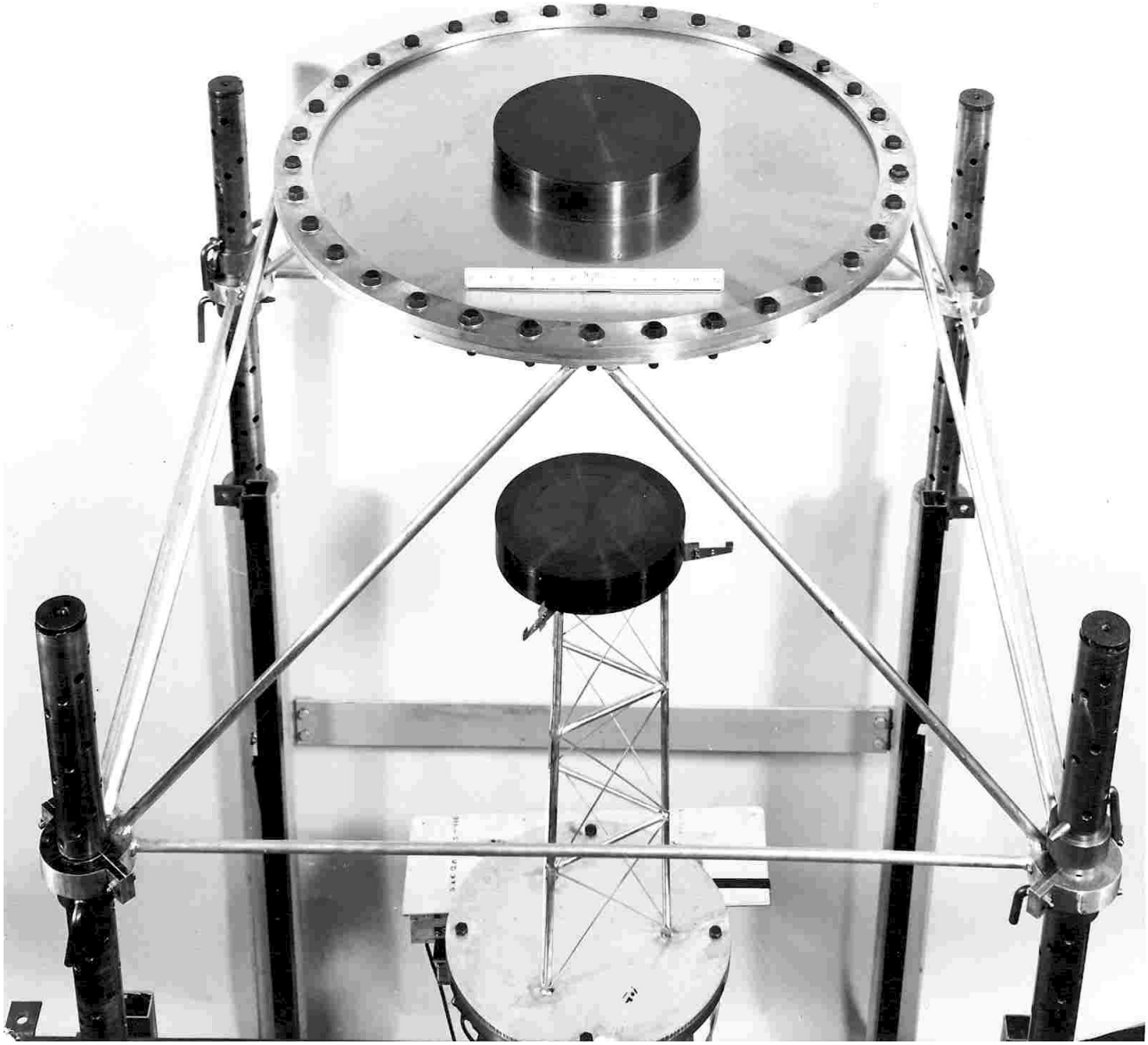

Figure 1.1-3. A Typical Uranium Metal Assembly of Two Interacting 11-inch-Diameter Cylinders at Close Spacing on the Vertical Assembly Machine (Not a Photo of the Current Experiment).[a]
(Similar supports were used in these measurements and are described in Appendix E.)

[a] Photo 39380, Oak Ridge National Laboratory photo of a bare uranium assembly. This same support structure was used for these measurements.

Table 1.1-1. Reported Stack Height Measurements (Ref. 1).

Assembly Parts Nominal Dimensions (OD-ID, in.)	Measured Height As Assembled (in.)[a]	Material Height[b] (in.)[a]	Average Void Between Rings of the Same Diameters (in.)[c]	Mass (g)
Upper Section of the Assembly				
13-11 ring	2.5147	2.50695	0.0013	28,962
11-9 ring	2.6338	2.63015	0.0018	25,344
9-7 ring	2.6230	2.62385	0.0000	20,224
Lower Section of the Assembly				
13-11 ring	3.0183	3.0119	0.0016	34,808
11-9 ring	3.0108	3.0008	0.0034	28,910
9-7 ring	3.0120	3.0025	0.0032	23,135

(a) Average of several measurements.
(b) The sum of the individual heights for all annuli in a given stack.
(c) From inspection reports the average radial voids are 0.0053 in. for the top section between the outer and middle ring and 0.0057 for the bottom section; between the middle and inner ring, 0.0064 for the top section and 0.0055 for the lower section. The average outside and inside diameters, respectively, for the three rings of the upper section were 12.9957 and 11.0026, 10.9968 and 9.0019, and 8.9962 and 7.0034 in. and for the lower section were 12.9959 and 11.0028, 10.9960 and 9.0024, and 8.9963 and 7.0031 in. *Note: the value 7.0034 in. was incorrectly reported as 77.0034 in. in Ref. 1.*

Table 1.1-2. Logbook Oralloy Stack Height Measurements (in.).

Experiment	Stack Edge	13-11 in.	11-9 in.	9-7 in.
1 & 2 (Top)[a]	N	2.516	2.635	2.623
	NE	2.513	2.635	2.622
	E	2.514	2.634	2.624
	S	2.513	2.633	2.623
	SW	2.515	2.633	2.623
	W	2.517	2.633	2.623
Average[b]	--	2.5147	2.6338	2.6230
1σ[b]	--	0.0016	0.0010	0.0006
Experiment	**Stack Edge**	**13-11 in.**	**11-9 in.**	**9-7 in.**
1 & 2 (Bottom)[a]	N	3.018	3.011	3.011
	NE	3.017	3.012	3.012
	E	3.018	3.012	3.012
	S	3.018	3.011	3.011
	SW	3.019	3.010	3.013
	W	3.020	3.009	3.013
Average[b]	--	3.0183	3.0108	3.012
1σ[b]	--	0.0010	0.0012	0.0009

(a) Stack height measurements for the top and bottom halves of Configurations 1 and 2 were obtained from pages 52 and 60, respectively, from ORNL logbook 13R (East Cell – Logbook 2, E-20).
(b) The average stack heights were calculated and reported in the original logbooks. The standard deviation has been calculated using the original data.

1.1.2.3 Assembly Alignment

Radial Alignment of Upper Section: For assembly of the upper section, uranium metal was placed on the Type 304L stainless steel diaphragm. Uranium was positioned, with a ruler, the appropriate distance from the inside of the aluminum clamping ring, which held the 0.010-inch-(0.0254-cm)-thick stainless diaphragm. For example, a layer of uranium metal for an 11-inch-(27.94-cm)-diameter annulus typically consists of a 7-inch-(17.78-cm)-ID / 9-inch-(22.86-cm)-OD annulus, and a 9-inch-(22.86-cm)-ID / 11-inch-(27.94-cm)-OD annulus. About half of the material was added to the diaphragm and the location of the material was continuously adjusted with a precise high-quality level in one direction and then the level was rotated 90° on the top of the uranium. If the assembly was not exactly centered on the diaphragm, it would not be precisely level because of the sag in the diaphragm as it was loaded. Two precisely machined steel blocks (±0.0001 inches, ±0.000254 cm) were used to squeeze the outside radial surface of the uranium metal until it was aligned. An edge of the machined block was then held at one outside radial location, squeezing the uranium together until no light was visible between the machined block and the uranium metal. This process was repeated 90° from the position of the original adjustment, rechecked again at the original position, and small adjustments made if necessary. This process continued until the outside radii of the parts were precisely aligned and the upper section assembly was complete. The squeezing procedure was performed by one individual while another person observed the light coming through small gaps between the blocks and the uranium metal.[a] The alignment of outer radii of the upper or lower section was less than ±0.001 inches. Of course, if two positions 90° apart are adjusted, the positions at 180° and 270° can be off only by the difference in the diameters of the outside parts.

Radial Alignment of Lower Section: For the lower section, the uranium parts were centrally located on the lower support stand and the same procedure was used except that the leveling of the parts was accomplished by shimming with aluminum foil (various thicknesses of aluminum foil were available). The foil was placed between the three 120° upper edges of the lower support stand and the lowest parts.

Radial Alignment Accuracy Summary: Uncertainty in radial alignment of uranium metal parts on each half is ±0.001 inch.

Lateral Alignment of Upper Section with the Lower Section: For these experiments, the alignment of the upper and lower sections was adjusted and verified using the Lateral Alignment Fixture shown in Figure 1.1-4. There were two identical fixtures used for lateral alignment between the upper section and the lower section. They were U-shaped and were machined out of 0.375-inch-(0.9525-cm)-thick aluminum. The end pieces were carefully machined by the Y-12 shops to be perpendicular to the long direction of the fixture and coplanar with each other. When leveled properly, the front face of the 4×4×½-inch-(10.16×10.16×1.27-cm)-thick end pieces were vertical and in the same plane to within ±0.001 inch (±0.00254 cm). In use, the lower side of the upper leg rested on the top surface of the clamping ring for the diaphragm. The fixture was perpendicular to the outer radial surface of the annuli and was moved inward until it touched the uranium of the top section. The leveling screws were adjusted until the fixture was level.

The second fixture was placed 90° apart from the first in a similar manner. Both fixtures were moved back slightly, and the lower section was raised until it was at the height of the lower leg of the U-shaped fixtures. Both fixtures were then nearly adjusted properly. Removal or additions of material from the upper section sometimes required small leveling adjustments. The fixtures were moved in until they touched uranium (either on the upper or the lower section). When lack of contact was observed at either of the front faces of the fixture, the lower section was lowered to the full-out position, and the position of the uranium on the lower support stand was adjusted. Finally, the lower lift table was raised and the alignment was checked.

[a] Personal communication with John T. Mihalczo, March 2010.

The process was repeated several times as necessary. The final 0.005-inch (0.0127-cm) adjustments were usually made by moving the upper section. This was a long and tedious procedure, which took one to two hours or more as needed but was always performed and resulted in uranium metal of the upper and lower sections being aligned within ±0.005 inch (±0.0127 cm).

Lateral Alignment Accuracy Summary: Upper and lower assembly uranium metal alignment uncertainty is ±0.005 inch (±0.0127 cm).

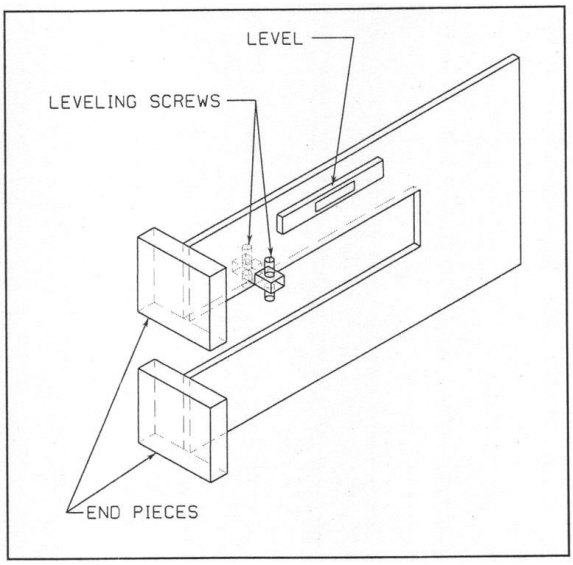

Figure 1.1-4. Sketch of Fixture for Lateral Alignment of Uranium.

1.1.2.4 Reactivity Effects of Support Structure

The support structure that was used to assemble these experiments was made up of the 0.010-inch-(0.0254-cm)-thick Type 304L stainless steel diaphragm, low-mass aluminum support stand, and two 30-inch-diameter, 2-inch-(5.08-cm)-wide, 0.5-inch-(1.27-cm)-thick diaphragm clamping rings bolted together. The support structure reactivity worth consisted primarily of the reactivity effects of the diaphragm, the diaphragm support rings, and the low-mass support stand. The reactivity worth of each of these three parts of the support structure was measured.

Additional figures depicting the assembly support structure are provided in Appendix E.

A positive reactivity effect means that the reactivity of the critical assembly increased due to the inclusion of that item in the assembly. Therefore, removing that particular item from the experiment resulted in a decrease in the neutron multiplication factor. A negative reactivity effect means that the reactivity of the assembly decreased due to the item's inclusion. The Type 304L stainless steel diaphragm in all experiments typically reduced the k_{eff} of the system since it separated uranium metal halves and introduced neutron absorbing material between them. The presence of the diaphragm support ring and low-mass support stand of the lower section generally resulted in a positive reactivity addition. The presence of the support ring and low-mass stand provided neutron reflection to the system. The combined reactivity effect of all other supports, such as the four vertical poles and tubing for the diaphragm support ring, was reported to be less than one cent and was not evaluated.

The reactivity of the support structure, when measured, was evaluated by assembling the system to delayed criticality or a known measured reactivity, adding additional support structure, and obtaining the

reactivity of the support structure from the measured reactor period for the assembly with and without the additional support structure. The effect of the lower support stand was evaluated using an inverted support stand, like that for the lower section, which was added to the top of the upper section. Care was taken in suspending it so that it would not compress the materials of the assembly. To estimate the effect of the diaphragm and clamping ring, their thicknesses were doubled and the reactivity change was measured. Where multiple instruments were used to measure the reactor period, the reactivity values obtained were averaged. These effects were measured for the components listed in Table 1.1-3. The reactivity worth of the entire support structure is obtained by adding the worth of the three components of the support structure: annular diaphragm rings, stainless steel diaphragm, and low-mass support stand. Multiple measurements for the reactivity effects of the support structure were unavailable. The measured worth of the diaphragm includes the separation distance between the two halves of the experiment.[a]

Table 1.1-3. Reactivity (cents) Effects Measurements.

Measurement	Detector 1	Detector 2	Reported Average	Reported Worth
Configuration 1 (Empty Steel Cans)	-6.34	-6.80	-6.57	--
Configuration 2 (Potassium-Filled Cans)	3.83	3.67	3.75	10.32
Second Diaphragm and Support Rings Added[(a)]	-4.4	-4.55	-4.47[(b)]	-8.22[(b)]
Second Fuel Support Stand Added to Top[(a)]	11.62	11.6	11.61	16.18[(b)]

(a) Measurements were performed using Configuration 2 but assumed to apply to both configurations.
(b) These measurements were recalculated by the evaluator to be -4.475, -8.225, and +16.085 ¢, respectively.

The effective delayed-neutron fraction, β_{eff}, reported for similar experiment in the series (HEU-MET-FAST-069 of the ICSBEP Handbook) is 0.0066±0.00033 (±5 %), and can also be applied to these two configurations. For Configuration 1, the full assembly was 6.57¢ below delayed critical (k_{eff} of 0.99957) and had an adjusted worth of 14.43¢ below delayed critical (k_{eff} of 0.99905) with all the support structure removed. For Configuration 2, the full assembly was 3.75¢ above delayed critical (k_{eff} of 1.00025), and 4.11¢ below delayed critical (k_{eff} of 0.99973) when all the support structure was removed.

The diaphragm bolts were not included in the experimental analysis of the support structure worth. The 304L stainless steel bolts are 0.5 in. (1.27 cm) in diameter and 1.5 in. (3.81 cm) long; their effective worth is believed to be negligible and within the measurement uncertainty of ±2¢, which is the reproducibility uncertainty for a given configuration.[b]

1.1.2.5 Uranium Components

The assembly contained a total of 26 annular rings: 12 outer rings, 7 middle rings, and 7 inner rings.[c] The total height of the outer rings was ~5.5 in. (~13.97 cm). The height of the smaller rings was ~5.62

[a] Personal communication with John T. Mihalczo, February 2010.
[b] Personal communication with John T. Mihalczo, June-July 2010.
[c] Ref. 1 incorrectly reports the number of annular rings in the outer, middle, and inner stacks as 13, 11, and 9, respectively.

in. (~14.2748 cm). The assembly was divided into two halves with the lower half being ~3.0 in. (~7.62 cm) in height. The upper half was supported on the steel diaphragm.
The average dimensions and masses of the uranium metal parts for these experiments are given in Table 4 and come from the Y-12 database; the dimensions are traditionally reported as having been measured to within 1×10^{-4} inches (2.54×10^{-4} cm) with an uncertainty of 5×10^{-5} inches (1.27×10^{-4} cm) and the masses of the parts are accurate to within 0.5 grams. All dimensional measurements for the parts were measured at 70° F at the Y-12 plant. The readout of the measuring device was calibrated to 0.0001 in. (0.000254 cm) using standards traceable back to the National Bureau of Standards (now NIST). An average of more than one measurement could result in the recording of a fifth digit.[a]

The density of each part can be obtained by dividing the reported mass of the part by the volume, which is calculated using the values provided in Table 1.1-4.

The average axial gaps between uranium metal annular parts were obtained by subtracting the sum of the heights of the individual parts in a given stack from the measured stack height, and then dividing this value by the number of parts in the stack minus one. The axial gap heights between the uranium annuli were reported in Table 1.1-1; the annular gap thicknesses between the uranium annuli are also reported in Table 1.1-1.

Table 1.1-4. Measured Properties of Uranium Metal Annuli.

Annulus (Stack)	Part Number	Mass (g)	Height (in.)	Inner Diameter (in.)	Outer Diameter (in.)
13-11 (Upper)	2781	1449	0.1252	11.0025	12.99675
	2780	1440	0.12485	11.002	12.99605
	2783	2888	0.25075	11.003	12.9956
	2782	2914	0.25175	11.0035	12.9956
	2750	4336	0.37545	11.0015	12.9945
	2749	4360	0.3774	11.003	12.9955
	2757	11575	1.00155	11.0025	12.996
11-9 (Upper)	2746	1238	0.12865	9.00175	10.9965
	2748	14462	1.5	9.0025	10.9975
	2776	9644	1.0015	9.0015	10.9965
9-7 (Upper)	2763	953	0.1243	7.0038	8.9958
	2741	11568	1.5003	7.0025	8.9965
	2762	7703	0.99925	7.00375	8.99625
13-11 (Lower)	2754	5826	0.5036	11.004	12.9953
	2753	5782	0.5013	11.003	12.99675
	2752	5811	0.50325	11.0025	12.9955
	2751	5822	0.50355	11.0015	12.9958
	2756	11567	1.0002	11.0036	12.9967
11-9 (Lower)	2744	1223	0.12675	9.0065	10.9968
	2742	3617	0.3751	9.0015	10.9968
	2747	14436	1.4999	9.002	10.9968
	2745	9634	0.999	9.001	10.9965
9-7 (Lower)	2829	2895	0.37625	7.00315	8.99625
	2740	11568	1.5	7.0025	8.99625
	2773	962	0.125	7.0015	8.997
	2738	7710	1.0012	7.00375	8.99575

[a] Personal communication with John T. Mihalczo, March 2010.

1.1.2.6 Stainless Steel Cans and Potassium

A total of four stainless steel cans were utilized in this pair of critical experiments, with each configuration comprised of HEU annuli surrounding a lower can and an upper can. The only difference between these two experiments is the contents of the cans (air in Configuration 1 and potassium in Configuration 2).

The stainless steel can for the lower section was approximately 6.99 in. (17.7546 cm) in diameter,[a] 0.062 in. (0.15748 cm) in radial wall thickness, and 0.201 in. (0.51054 cm) in top and bottom thickness; the steel can for the upper section had approximately the same dimensions as the lower can. The can for the lower section was 3.000 in. (7.62 cm) in total height, and that for the upper section was 2.500 in. (6.35 cm) in total height, slightly lower than the uranium height. Multiple measurements reported for various dimensions of the stainless steel cans were also recorded in the logbooks; all reported measurements are summarized in Table 1.1-5.

The stainless steel cans, which are initially fabricated with a fill tube, were filled by inserting a tube with a smaller diameter than the can fill tube to pump liquid potassium from a fill tub into the cans. During the filling process, air would escape through the void between the can fill tube and the inserted potassium tube. The can was tilted so that the fill tube was the highest point and thus no air would be trapped in the can during filling. The potassium would then be left to solidify and the fill tube would be pinched off and welded shut. The potassium was solidified slowly from the bottom up to prevent trapped voids. Any excess fill tube would have been cut off and the cans were effectively sealed.[b]

[a] Incorrectly reported as having a diameter of 2.99 in. in Ref. 1; this value was verified as incorrect by the lead experimenter. The diameter of the upper can was not directly reported in Ref. 1 (Personal communication with John T. Mihalczo, January 2014.
[b] Personal communication with John T. Mihalczo, August 2014.

Table 1.1-5. Stainless Steel Can Measurements.

Can	Source	Height (in.)	Weight (g)	Outer Diameter (in.)
Upper	Ref. 1	2.500	2360 (empty) 1064 (K only)	--
	E-19, p. 9	2.5	2360 (empty)	6.973 6.973
	E-20, p. 49	2.5	2354 (empty)	7
	E-20, p. 51	2.5	2360 (empty) 3424 (filled) 1064 (K only)	--
Lower	Ref. 1	3.000	2421 (empty) 1334 (K only)	6.99[(a)]
	E-19, p. 9	2.990 2.982 2.995 2.975 2.9855 (avg)	2435 (empty)	6.969 6.976
	E-20, p. 49	3	2416 (empty)	7
	E-20, p. 51	3	2421 (empty) 3755 (filled) 1334 (K only)	--

Can	Source	Height (in.)	Radial Wall Thickness (in.)	Top and Bottom Thickness (in.)
Upper	E-20, p. 54	2.5	0.062 0.062 0.0615 0.062 0.063 0.062 0.062 (avg)	0.209 0.208 0.198 0.195 0.211 0.2095 0.1945 0.197 0.196 0.201 (avg)
Lower	E-20, p. 54	3	0.062 0.062 0.061 0.062 0.062 0.062 (avg)	0.202 0.202 0.204 0.202 0.199 0.199 0.200 0.200 0.203 0.201 (avg)

(a) Incorrectly reported as having a diameter of 2.99 in. in Ref. 1; this value was verified as incorrect by the lead experimenter, and replaced with the number shown in this table.

1.1.2.7 Experimental Configurations

The system was assembled to delayed criticality with the empty stainless steel cans placed within the annulus. A small additional reflector was placed near the assembly to raise the system reactivity. Then the reflector was removed and the negative reactor period was measured. The reactivity of the assembly was obtained using the Inhour equation and Keepin, et al. delayed neutron data.[a] The reactivity of the assembly with empty cans was -6.57 ± 0.20 ¢. The empty cans were then replaced with identical potassium-filled cans and the positive reactor period was measured. The reactivity of the assembly with potassium-filled cans was +3.75 ± 0.10 ¢. The total reported potassium reactivity was +10.32 ± 0.40 ¢, or a reactivity mass coefficient of $+4.30 \times 10^{-3}$ ¢/g K.

The HEU pieces were arranged in the stack order provide in Tables 1.1-4 and 1.1-6. A sketch was provided in the logbook but the quality of the digitized image is poor. The lead experimenter verified the parts and arrangement provided in this evaluation.[b]

1.1.3 Material Data

1.1.3.1 Uranium Components

The density of the annular right circular cylindrical assembly of uranium metal was reported to be 18.76 g/cm^3. The average isotopics of the uranium metal in weight percent were ^{234}U = 0.97, ^{235}U = 93.15, ^{236}U = 0.24, and ^{238}U = 5.64. The uranium material contained 0.9995 g of uranium per gram of material with negligible impurities, mainly consisting of aluminum, copper, molybdenum, iron, silicon, nickel, carbon, oxygen, and nitrogen.

The uranium metal parts for these critical experiments were carefully cast and machined at the Oak Ridge Y-12 Plant in the early 1960s. Each uranium metal part was a separate casting which was then machined. Dimensions, masses, uranium isotopic, and impurity content were measured after machining. Uranium part masses and dimensions can be found in Table 1.1-4. The total uranium mass is 161.383 kg for both Configurations 1 and 2, which is the sum of the individual part masses.

The uranium isotopic content obtained from Y-12 spectrographic analyses are given in Table 1.1-6. The uncertainty in the measured values for ^{234}U, ^{235}U, and ^{236}U are traditionally reported as 5×10^{-3} wt.%. The ^{238}U values were obtained by subtracting the sum of the other three from 100 %.

The impurities from the 11 spectrographic analyses performed are given in Table 1.1-7 for uranium parts; only average and variation information were initially recorded.[c] These 11 randomly sampled uranium parts include discs and annular parts (from the series of oralloy experiments and not solely from this HEU/K experiment). As such, the information presented is a representative average of the impurity content in all uranium parts. These values are consistent with the nominal impurity content of highly enriched uranium metal at the Oak Ridge Y-12 Plant at the time the parts were made (i.e., 99.95 g of U per l00 g of material). Oxygen and nitrogen content was assumed by the experimentalist to be 20 and 30 ppm, respectively, consistent with highly enriched uranium produced at the time of these experiments.[d]

The HEU parts were coated annually in a very thin film of lightweight fluorocarbon oil to decrease mass loss due to oxidation. This oil has negligible effect upon the experiment conditions. After oiling, the

[a] G. R. Keepin, T. F. Wimett, and R. K. Zeigler, *Phys. Rev.*, **107**, 1044 (1957).
[b] Personal communication with John T. Mihalczo, June 2014.
[c] J. T. Mihalczo, "Graphite and Polyethylene Reflected Uranium-Metal Cylinders and Annuli," Union Carbide Corporation Nuclear Division, Oak Ridge Y-12 Plant, Y-DR-81 (1972).
[d] HEU-MET-FAST-076 in the ICSBEP Handbook.

parts were wiped with a dry rag to remove most of the oil. The oralloy parts were then handled by leather gloves, which further reduced the oil on the surface.[a]

Table 1.1-6. Uranium Disc Isotopic Content.[(a)]

Annulus (Stack)	Part Number	^{234}U (wt.%)	^{235}U (wt.%)	^{236}U (wt.%)	^{238}U (wt.%)[(b)]
13-11 (Upper)	2781	0.98	93.19	0.25	5.58
	2780	0.98	93.13	0.25	5.64
	2783	0.93	93.18	0.25	5.64
	2782	0.96	93.20	0.23	5.61
	2750	0.95	93.12	0.25	5.68
	2749	0.98	93.19	0.25	5.58
	2757	0.96	93.20	0.23	5.61
11-9 (Upper)	2746	1.00	93.09	0.22	5.69
	2748	1.00	93.09	0.22	5.69
	2776	0.96	93.16	0.23	5.65
9-7 (Upper)	2763	0.96	93.18	0.25	5.61
	2741	0.96	93.18	0.25	5.61
	2762	0.97	93.13	0.27	5.63
13-11 (Lower)	2754	0.96	93.10	0.28	5.66
	2753	0.95	93.12	0.25	5.68
	2752	0.98	93.13	0.24	5.65
	2751	0.98	93.13	0.24	5.65
	2756	0.93	93.18	0.25	5.64
11-9 (Lower)	2744	0.98	93.14	0.23	5.65
	2742	0.98	93.14	0.23	5.65
	2747	0.98	93.16	0.19	5.67
	2745	0.96	93.20	0.22	5.62
9-7 (Lower)	2829	0.99	93.10	0.24	5.67
	2740	0.97	93.17	0.24	5.62
	2773	0.97	93.17	0.24	5.62
	2738	0.98	93.15	0.24	5.63

(a) Mass spectrographic analysis.
(b) By difference from 100 % pure uranium.

[a] Personal communication with John T. Mihalczo, June-July 2010.

Table 1.1-7. Measured Impurity Content of Uranium Metal Cylinders, Annuli, and Plates.[a]

Element [a]	Parts per Million by Weight (ppm) [b]	Variation (ppm)	Standard Deviation (ppm) [c]
Ag	8	3-25	3.2
Ba	< 0.01 [d]	-	0.005
Bi	164	81-311	52.9
C	< 10	-	2.4
Ca	0.1	-	0.05
Cd	< 1	-	0.5
Co	5	2-15	1.9
Cr	7	4-12	1.9
Cu	25	10-40	8
K	< 0.2	0.2-0.8	0.1
Li	< 2	-	1
Mg	3	2-3	1.7
Mn	56	25-89	17.1
Mo	< 1	< 1 – 1	0.5
Na	27	15-50	7.7
Ni	100	-	10
Sb	38	10-80	17.4
Ti	1	-	0.5

(a) Mass spectrographic analysis except for oxygen and nitrogen using data in J. T. Mihalczo, "Graphite and Polyethylene Reflected Uranium-Metal Cylinders and Annuli," Union Carbide Corporation Nuclear Division, Oak Ridge Y-12 Plant, Y-DR-81 (April 28, 1972). Oxygen and nitrogen content was assumed by the principal experimentalist to be 20 and 30 ppm, respectively, consistent with highly enriched uranium produced at the time of these experiments. Total impurity content is consistent with stated values at that time of 500 ppm which gives 99.95 grams of U per 100 grams of material. Minor differences in the impurities exist between values listed in Table 8 and the impurity values provided in HEU-MET-FAST-051 in the ICSBEP Handbook.

(b) Except for the values shown as less than the detection limit, impurity data are average values from 11 randomly sampled uranium parts.

(c) Personal communication, J. A. Mullens to John Mihalczo in HEU-MET-FAST-076 in the ICSBEP Handbook, June 2004.

(d) Less than (<) indicates lower detection limit and not necessarily that the impurity is present.

1.1.3.2 Stainless Steel Cans and Potassium

The measured masses of the empty upper and lower stainless steel Type 304 cans reported in Ref. 1 were 2360 and 2421 g, respectively. The upper potassium-filled can contained 1064 g of potassium; the lower can contained 1334 g of potassium, which resulted in a total potassium mass of 2398 g. Additional reported masses for the stainless steel cans were reported in the logbook, as well as the potassium mass measurements; these values are reported in Table 1.1-5.

1.1.4 Temperature Data

Room and assembly temperature measurements were not recorded during the course of the experiments. The ORCEF operated in a controlled environment.[a] The fission rate in the measurements corresponded to usually much less than 0.01 watts, so there was no appreciable heating of the experiment components. The dimensions of the uranium were measured at 70 ºF and the experiments were generally performed at the ORCEF room temperature of 72 ºF. The reactivity coefficient for a temperature change for these assemblies is approximately -0.3¢/ºC.[b]

1.1.5 Additional Information Relevant to Critical and Subcritical Measurements

Additional information is not available.

1.2 Description of Buckling and Extrapolation Length Measurements

Buckling and extrapolation length measurements were not made.

1.3 Description of Spectral Characteristics Measurements

Spectral characteristics measurements were not made.

1.4 Description of Reactivity Effects Measurements

1.4.1 Overview of Experiment

The difference between the two critical configurations provided in Section 1.1 is the addition of 2.398 kg of potassium. The worth of the potassium was measured and evaluated as an acceptable benchmark experiment. Please note that this benchmark experiment value is derived from the two near-critical benchmark experiment configurations.

1.4.2 Geometry of the Experiment Configuration and Measurement Procedure

The geometry of the experimental configurations is provided in Section 1.1.2.

The system was assembled to delayed criticality with the empty stainless steel cans placed within the annulus. A small additional reflector was placed near the assembly to raise the system reactivity. Then the reflector was removed and the negative reactor period was measured. The reactivity of the assembly was obtained using the Inhour equation and Keepin, et al. delayed neutron data.[c] The reactivity of the assembly with empty cans was -6.57 ± 0.20 ¢. The empty cans were then replaced with identical

[a] Personal communication with John T. Mihalczo, February 2010.
[b] Personal communication with John T. Mihalczo, March 2010.
[c] G. R. Keepin, T. F. Wimett, and R. K. Zeigler, *Phys. Rev.*, **107**, 1044 (1957).

potassium-filled cans and the positive reactor period was measured. The reactivity of the assembly with potassium-filled cans was +3.75 ± 0.10 ¢. The total reported potassium reactivity was +10.32 ± 0.40 ¢, or a mass reactivity coefficient of $+4.30 \times 10^{-3}$ ¢/g K (2398 g K).

1.4.3 Material Data

The materials utilized in this experiment are provided in Section 1.1.3.

1.4.4 Temperature Data

Temperature data for this experiment are provided in Section 1.1.4.

1.4.5 Additional Information Relevant to Reactivity Effects Measurements

Additional information is not available.

1.5 Description of Reactivity Coefficient Measurements

Reactivity coefficient measurements were not made.

1.6 Description of Kinetics Measurements

Kinetics measurements were not made.

1.7 Description of Reaction-Rate Distribution Measurements

Reaction-rate distribution measurements were not made.

1.8 Description of Power Distribution Measurements

Power distribution measurements were not made.

1.9 Description of Isotopic Measurements

Isotopic measurements were not made.

1.10 Description of Other Miscellaneous Types of Measurements

Other miscellaneous types of measurements were not made.

2.0 EVALUATION OF EXPERIMENTAL DATA

Monte Carlo n-Particle (MCNP) version 6.1 calculations were utilized to estimate the biases and uncertainties associated with the experimental results in this evaluation. MCNP is a general-purpose, continuous-energy, generalized-geometry, time-dependent, coupled n-particle Monte Carlo transport code.[a] The Evaluated Neutron Data File library, ENDF/B-VII.1,[b] was utilized in analysis of the experiment and benchmark model biases and uncertainties. The statistical uncertainty in k_{eff} and Δk_{eff} is 0.00002 and 0.00003, respectively. Calculations were performed with 1,050 generations with 1,000,000 neutrons per generation. The k_{eff} estimates did not include the first 50 generations and are the result of 1,000,000,000 neutron histories.

Elemental data such as molecular weights and isotopic abundances were taken from the 17th edition of the Chart of the Nuclides.[c]

Room return effects with its associated uncertainty are addressed in Section 3.1.1.3.

2.1 Evaluation of Critical and / or Subcritical Configuration Data

Variations of the benchmark models provided in Section 3 were utilized with perturbations of the model parameters to estimate uncertainties in k_{eff} due to uncertainties in values defining the benchmark experiment. Where applicable, comparison of the upper and lower perturbation k_{eff} values to evaluate the uncertainty in the eigenvalue were utilized to minimize correlation effects, if any, induced by comparing all perturbations to the original benchmark model configuration, as discussed elsewhere.[d]

Unless specifically stated otherwise, all uncertainty values in this section correspond to 1σ. When the change in k_{eff} between the base case and the perturbed model (single-sided perturbation), or two perturbed models (double-sided perturbation directly comparing an upper and a lower perturbation from the base case), is less than the statistical uncertainty of the Monte Carlo results, the changes in the variable are amplified, if possible, and the calculations repeated. The resulting calculated change is then scaled to a value corresponding to the given uncertainty using a scaling factor, assuming linearity, which should be adequate for these small changes in k_{eff}. Throughout Section 2, the difference in eigenvalues computed using the perturbation method described is denoted with Δk_p; the scaled 1σ uncertainty is denoted as Δk_{eff}. All Δk_{eff} uncertainties are considered to be absolute values whose magnitude applies both positively and negatively to the experimental k_{eff}, as shown in Tables 2.1-27 and 2.1-28. Negative signs are retained in other tables in Section 2, where the effective uncertainty is reported for a given uncertainty perturbation, to demonstrate whether the effect in k_{eff} was directly or indirectly proportional to the uncertainty.

When evaluating parameters such as measured diameters, heights, and mass, all parts of a given type are perturbed at the same time: e.g., the uranium mass in all annuli is simultaneously increased or decreased. The calculated uncertainty is then reduced by the square root of the number of components perturbed, representative of a random uncertainty. When appropriate, a systematic component of the evaluated uncertainty is retained, which is considered to not be impacted by the perturbation of the number of parts perturbed for its assessment. It should be noted, however, that typically when parameters of multiple parts are evaluated, the parts are nearly identical in every aspect. The uranium annuli utilized in this

[a] J. T. Goorley, et al., "Initial MCNP6 Release Overview – MCNP6 version 1.0," LA-UR-13-22934, Los Alamos National Laboratory (2013).
[b] M. B. Chadwick, et al., "ENDF/B-VII.1: Nuclear Data for Science and Technology: Cross Sections, Covariances, Fission Product Yields and Decay Data," *Nucl. Data Sheets*, **112**: 2887-2996 (2011).
[c] E. M. Baum, M. C. Ernesti, H. D. Knox, T. R. Miller, and A. M. Watson, *Nuclides and Isotopes, Chart of the Nuclides: 17th Edition*, Knolls Atomic Power Laboratory (2009).
[d] D. Mennerdahl, "Statistical Noise for Nuclear Criticality Safety Specialists," *Trans. Am. Nucl. Soc.*, **101**: 465-466 (2009).

experiment vary in mass and dimensions; as such, the relative importance of the annuli varies throughout the assembly. In general, perturbation of many components of varying dimensions and mass would not be appropriate and should be replaced instead with multiple individualized perturbation analyses. In the case of the precisely-measured annuli for these experiments, perturbation of individual component parameters without their respective uncertainties would produce negligible results. Simultaneous perturbation of the various parameters for all annuli parts is performed, even though the parts are not identical, to demonstrate that the combined effect of the uncertainties is still negligible.

Uncertainties less than 0.00003 Δk_{eff} are treated as negligible. When calculated uncertainties in Δk_{eff} are less than or equal to their statistical uncertainties, and an increased parameter scaling cannot be performed, the statistical uncertainties are added to the calculated uncertainty to assess the magnitude of the total uncertainty; however, the absolute magnitude of any uncertainty combined in this way is less than 0.00003 Δk_{eff}, therefore they are treated as negligible.

The total evaluated uncertainty in k_{eff} for this experiment is provided in Section 2.1.4; the square root of the sum of the squares of all the individual uncertainties assessed in this section is used to obtain the total uncertainty in the experimental k_{eff}.

2.1.1 Experimental Measurements

2.1.1.1 Temperature

These experiments were performed at a room temperature of ~295 K. Part measurements were performed at a room temperature of ~294 K. The uncertainty in each of these two temperatures is unknown. Any variations in temperature for the experiments and room environment were small. Heating effects in the experiment components were negligible. The temperature reactivity coefficient is approximately -0.3 ¢/ºC. It is assumed that a temperature variation of 2 ºC (1σ) adequately describes the temperature uncertainty. A temperature uncertainty of ±2 ºC in k_{eff} results in a Δk_{eff} of ±0.00004 for both configurations.

2.1.1.2 Experiment Reproducibility and Measurement

The experimenter indicated that to completely dismantle a system and reassemble it on a different day, the reactivity differences are ~2 ¢ or less; measurements repeated on the same day exhibited much less of a difference.[a] The experimenter indicated that reproducibility of experiments performed with the vertical lift is even better. The corresponding uncertainty of ±0.00013 Δk_{eff} is treated as a 1σ value for both configurations.

The uncertainty in the actual measurement of the reactivity, which is determined by positive period measurements, is considered very accurate. There is some uncertainty in fitting data and evaluation of the period. Careful measurements and rigorous fitting procedures can yield estimate uncertainties of ~0.2 pcm, which is negligible.[b] It is assumed that uncertainty in the actual measurement of the reactivity is already included in the reproducibility uncertainty already discussed in the previous paragraph.

2.1.1.3 Measured Reactivity of Support Structure Removal

Reactivity values for the worth of the support structure are given in Table 1.1-3. Multiple measurements to assess the uncertainty in the support structure worth were not performed. Prior benchmarks in this experimental series (HEU-MET-FAST-051, HEU-MET-FAST-071, and HEU-MET-FAST-076 in the ICSBEP Handbook) assumed a 1σ standard deviation of 10 % of each measured value of the support

[a] Personal communication with John T. Mihalczo, July 2014.
[b] Personal communication with Dick McKnight, July 2010.

structure worth and the delayed critical measurement worth was sufficient. A slightly more rigorous approach is utilized in this evaluation.
The individual worth measurements were obtained using modified experiments from the clean critical experimental configuration. Each of these configurations would have a repeatability uncertainty of, at most, ~2 ¢ if the assembly had been completely disassembled between measurements (as discussed in the previous section). Therefore the uncertainty in the adjustment for the removal of the assembly support structure from the experiment configuration would be obtained by taking the square root of the number of measured worths, multiplied by the square root of the number of experiment configurations needed to evaluate a given measured worth, and multiplied by the reproducibility uncertainty for a single configuration. A total of three experimental configurations were needed to obtain two worth measurement corrections to represent the removal of the support structure from each configuration: $\sqrt{3}\times\sqrt{2}\times 2$ ¢. The uncertainty in the repeatability of the clean critical experiments is already discussed in the previous section.

The calculated uncertainty associated with the uncertainty in the measured reactivity for support structure removal is ±0.00032 Δk_{eff} for both configurations.

Although the measured corrections were performed using only Configuration 2 and then applied equally to Configuration 1, it is not believed that this assumption would add any additional significant uncertainty.

2.1.1.3 Effective Delayed Neutron Fraction, β_{eff}

A typical effective delayed neutron fraction for bare HEU metal systems is 0.0066 (see HEU-MET-FAST-051 in the ICSBEP Handbook). Typically the uncertainty in β_{eff} is around 5 %, which, when propagated, results in a Δk_{eff} of approximately ±0.00005 and ±0.00001 for Configurations 1 and 2, respectively, which is considered negligible ($\Delta k_{eff} < 0.00003$) for Configuration 2. This uncertainty was obtained by taking the difference between the experimental eigenvalue calculated for the actual experiment using the reported delayed neutron fraction, and an eigenvalue calculated using the delayed neutron fraction perturbed by ±5 %.

Two methods were utilized to assess the calculation of β_{eff}. First, calculations were performed using the adjoint-weighted point kinetics capabilities of MCNP,[a] ENDF/B-VII.1 nuclear data, and the benchmark models provided in Section 3.1. Second, eigenvalue calculations were performed both with and without the delayed neutron component (TOTNU card in MCNP set to "no"); these calculated eigenvalues were incorporated in the following equation to estimate β_{eff} values:[b]

$$\beta_{eff} = 1 - \frac{k_{prompt}}{k_{eff}}.$$

Averages of the calculated results from the two methods and both detailed and simple models are 0.00641±0.00004 and 0.00641±0.00001, for Configurations 1 and 2, respectively, and, while lower than expected, are within the ±5 % uncertainty in β_{eff}.

2.1.2 Geometrical Properties

2.1.2.1 Uranium Annuli

[a] B. C. Kiedrowski, T. E. Booth, F. B. Brown, J. S. Bull, J. A. Favorite, R. A. Forster, and R. L. Martz, "MCNP5-1.60 Feature Enhancements & Manual Clarifications," LA-UR-10-06217, Los Alamos National Laboratory (2010).
[b] R. K. Meulekamp and S. C. van der Marck, "Calculating the Effective Delayed Neutron Fraction with Monte Carlo," *Nucl. Sci. Eng.*, **152**, 142-148 (2006).

Traditionally, the uncertainties in the ORCEF Oralloy experiments have been as follows in regards to geometrical properties. The measurement uncertainties in the stack heights can be calculated using the standard deviation of the average from multiple measurements, which are typically about ±0.001 inches (±0.00254 cm). The manufacturing tolerances of the Y-12 HEU parts are ±0.0001 inches (±0.000254 cm). When multiple measurements of the dimensions of a part were taken, the average was typically within ±0.00005 inches (±0.000127 cm) of all the individual measurements.[a]

More recently a document has been prepared to examine the uncertainties pertaining to critical experiments performed at ORCEF using HEU metal components.[b] This document will be the basis for the uncertainty analysis in this evaluation; however, the results for many of the calculations are negligible, which is what would be expected if the traditional approach to calculate the geometrical uncertainties were implemented.

There may be effects on the system k_{eff} values associated with correlations between uncertainties in stack heights, gap thicknesses, and the height of the individual parts in an assembly. However, except for the k_{eff} uncertainty associated with the uranium stack height uncertainties, the individual evaluated uncertainties in k_{eff} are negligible. Therefore, a possible increase in the uncertainty in k_{eff} due to correlation, if any, between the individual uncertainties is considered negligible.

There are a total of 26 individual uranium annuli in Configurations 1 and 2. When evaluating the uncertainty for a given parameter, all uranium components are simultaneously modified. The calculated change in the eigenvalue for the perturbation of a given parameter is scaled by the square root of the number of annuli, N, to represent the randomness of the actual variation amongst the individual pieces.

Diameter

The diameters of each uranium annulus was measured after machining at the Y-12 Plant and reported to an accuracy of 0.0001 inches (0.000254 cm) at several locations (~8) and then averaged. All measurements were at 70° Fahrenheit and are traceable back to the National Bureau of Standards (i.e. measurement systems were calibrated with standards produced by the NBS). While these measurements were performed using a Moore machine (high-performance ultra-precision manufacturing equipment, typically a jig borer or jig grinder with accompanying high-accuracy measurement capability)[c] accurate to this quantity, other sources have since indicated that the accuracy of the Moore machine utilized at that time was between 0.0003 and 0.0005 in. (0.000762 to 0.00127 cm).[a] The maximum value is taken to represent the accuracy of the measurement of the diameter for the oralloy parts instead of the average. Additionally, the uncertainty in the reported diameter of each annulus included a rounding uncertainty of ±0.00005 inches (±0.000127 cm). These two uncertainties are both considered to represent bounding uncertainties with uniform probability distribution and are combined in quadrature to obtain a total bounding uncertainty of ±0.0005025 in. (±0.001276 cm).

To find the effect of this diametral uncertainty on the k_{eff} value, the diameters of the annuli (Table 1.1-4) were adjusted by a factor of 5 times the bounding uncertainty. In order to keep the uranium mass of each experiment constant, the density of each of the uranium parts was adjusted accordingly. Effectively the entire uranium volume in the system was expanded and contracted while maintaining the total uranium mass constant. Outer and inner diameters were simultaneously increased to find an upper perturbation k_p value and then simultaneously decreased to find a lower perturbation k_p value. Half of the difference between the upper and lower perturbation k_p values was used to represent the variation in k_p due to perturbing the annuli diameters. The 1σ uncertainty in k_{eff} associated with the uncertainty in the diameter

[a] Personal communication with John T. Mihalczo, March 2010.
[b] J. T. Mihalczo and T. Gregory Schaaff, "Uncertainties in Masses, Dimensions, Impurities, and Isotopics of HEU Metal Used in Critical Experiments at ORCEF," ORNL/TM-2012/32, Oak Ridge National Laboratory (2012).
[c] Moore Precision Tools, http://mooretool.com/, Moore Tool Company, Bridgeport, CT, USA (last accessed September 18, 2014).

of the uranium annuli is found from the following formula, where Δk_p is one-half the difference between the upper and lower perturbation k_p values, SF is the scaling factor, N is the number of uranium annuli in each configuration which for both configurations is 26), and the factor of square root of two is present because the inner and outer diameters were simultaneously perturbed:

$$\Delta k_{eff}(1\sigma) = \frac{\Delta k_p}{SF}\sqrt{\left[\gamma_{sys}\right]^2 + \left[\frac{\gamma_{ran}}{\sqrt{2}\times\sqrt{N}}\right]^2}.$$

In the above equation, both systematic, γ_{sys}, and random, γ_{ran}, components are accounted for in the calculation of the total uncertainty in k_{eff} due to the uncertainty in the oralloy part diameters. It is estimated that the systematic component of this uncertainty is roughly equivalent to the ratio of the rounding uncertainty to the uncertainty in the accuracy of the Moore machine; therefore, the systematic component of the uncertainty is estimated to be approximately 10 %. The fraction of the uncertainty attributed to the random component is then 90 %; it should be noted that the random component of the uncertainty is not computed using the ratio of non-systematic uncertainty to the total uncertainty. Results are provided in Table 2.1-1, and are considered negligible ($\Delta k_{eff} < 0.00003$) for both configurations.

Table 2.1-1. Effect of Uncertainty in Uranium Annuli Diameters.

Case	Deviation (cm)	Δk_p	±	$\sigma_{\Delta kp}$	SF	Δk_{sys} (γ_{sys}=10%)	Δk_{ran} (γ_{ran}=90%)	Δk_{eff} (1σ)	±	$\sigma_{\Delta keff}$
1	±0.006382	-0.00009	±	0.00001	5√3	<0.00001	<0.00001	<0.00001	±	<0.00001
2	±0.006382	-0.00007	±	0.00001	5√3	<0.00001	<0.00001	<0.00001	±	<0.00001

Height

The height of each uranium annulus was measured after machining at the Y-12 Plant to an accuracy of 0.0001 inches (0.000254 cm) at several radial locations (~8) and then averaged. The same detailed discussion of measurement uncertainties and the method of analysis provided regarding the analysis of the diameters of the uranium annuli in the previous subsection also apply to the uranium heights.

To find the effect of this uncertainty on the k_{eff} value, the heights of the annuli (Table 1.1-4) were adjusted by a factor of 3 times the bounding uncertainty, while reducing the effective gap thicknesses between each component. The measured stack height, where possible, was conserved. When the increase in the combined heights of the individual parts was greater than the stack height, the parts were modeled in contact, with no gaps, and the effective stack height was increased. In order to keep the uranium mass of each experiment constant, the density of each of the uranium parts was adjusted accordingly. Effectively the entire uranium volume in the system was expanded and contracted while maintaining the total uranium mass constant. Heights were simultaneously increased to find an upper perturbation k_p value and then simultaneously decreased to find a lower perturbation k_p value. Half of the difference between the upper and lower perturbation k_p values was used to represent the variation in k_p due to perturbing the annuli heights. The 1σ uncertainty in k_{eff} associated with the uncertainty in the heights of the uranium annuli is found from the following formula:

$$\Delta k_{eff}(1\sigma) = \frac{\Delta k_p}{SF}\sqrt{\left[\gamma_{sys}\right]^2 + \left[\frac{\gamma_{ran}}{\sqrt{N}}\right]^2}.$$

Results are provided in Table 2.1-2, and are considered negligible ($\Delta k_{eff} < 0.00003$) for both configurations.

Table 2.1-2. Effect of Uncertainty in Uranium Annuli Heights.

Case	Deviation (cm)	Δk_p	±	$\sigma_{\Delta kp}$	SF	Δk_{sys} (γ_{sys}=10%)	Δk_{ran} (γ_{ran}=90%)	Δk_{eff} (1σ)	±	$\sigma_{\Delta keff}$
1	±0.003829	0.00013	±	0.00001	3√3	<0.00001	<0.00001	<0.00001	±	<0.00001
2	±0.003829	0.00013	±	0.00001	3√3	<0.00001	<0.00001	<0.00001	±	<0.00001

Stack Height

The stack heights of the uranium annuli placed above and below the stainless steel diaphragm were measured with a standard deviation of the average of approximately ±0.001 in. (±0.00254 cm) for most measurements, which is also the uncertainty of the measurement device for taking stack height measurements, and assumed to represent a 1σ uncertainty. Additionally, the uncertainty in the reported stack height included a rounding uncertainty of ±0.0005 inches (±0.00127 cm), which is considered to represent a bounding uncertainty with uniform probability distribution (i.e. ÷√3). These two uncertainty components are combined in quadrature to obtain a total 1σ uncertainty of ±0.001041 in. (±0.002644 cm).

To find the effect of this uncertainty on the k_{eff} value, the stack height of these annuli (Tables 1.1-2 and 2.1-10) was adjusted by increasing the effective gap thicknesses between each component. The stack height was increased by a factor of 10 times the 1σ uncertainty to find an upper perturbation k_p value. The difference between the upper perturbation k_p value and the unperturbed model k_{eff} value was used to represent the variation in k_p due to perturbing the annuli stack heights. The 1σ uncertainty in k_{eff} associated with the uncertainty in the measured stack heights of the uranium annuli is found from the following formula, where Δk_p is the difference between the upper perturbation and unperturbed model k_{eff} values, and N is the number of uranium annuli stacks in each configuration, which for both configurations is 6:

$$\Delta k_{eff}(1\sigma) = \frac{\Delta k_p}{SF}\sqrt{\left[\gamma_{sys}\right]^2 + \left[\frac{\gamma_{ran}}{\sqrt{N}}\right]^2}.$$

It is estimated that the systematic component of this uncertainty is roughly equivalent to the ratio of the rounding uncertainty to the uncertainty in the measurement of the stack height; therefore, the systematic component of the uncertainty is estimated to be approximately 29 % The fraction of the uncertainty attributed to the random component is then 71 %; it should be noted that the random component of the uncertainty is not computed using the ratio of non-systematic uncertainty to the total uncertainty. Results are provided in Table 2.1-3.

Table 2.1-3. Effect of Uncertainty in Uranium Stack Heights.

Case	Deviation (cm)	Δk_p	±	$\sigma_{\Delta kp}$	SF	Δk_{sys} (γ_{sys}=29%)	Δk_{ran} (γ_{ran}=71%)	Δk_{eff} (1σ)	±	$\sigma_{\Delta keff}$
1	+0.02644	-0.00014	±	<0.00001	10	-0.00004	-0.00004	0.00006	±	<0.00001
2	+0.02644	-0.00014	±	<0.00001	10	-0.00004	-0.00004	0.00006	±	<0.00001

2.1.2.2 Stainless Steel Cans

A total of four stainless steel cans were utilized in this pair of critical experiments, with each configuration comprised of HEU annuli surrounding a lower can with a nominal height of 3 in. (7.62 cm) and an upper can with a nominal height of 2.5 in. (6.35 cm). The nominal outer diameter of each can is 7 in. (17.78 cm) with a nominal radial thickness of 0.062 in. (0.15748 cm), and a nominal top/bottom end thickness of 0.202 in. (0.51308 cm). The only difference between these two experiments is the contents of the cans (air in Configuration 1 and potassium in Configuration 2).

The can dimension values provided in Table 1.1-5 seem to indicate that some values were measured on at least one of each can type and often designation of the can dimensions was truncated to the nominal dimensions for convenience. The non-rounded values in this table were averaged to obtain mean can dimensions for use in detailed models of the experiment. The upper and lower cans were respectively assumed to have the same dimensions in both configurations. These detailed dimensions are provided in Table 2.1-4.

Table 2.1-4. Mean Stainless Steel Can Properties.

Property	Upper Can	Lower Can
Height	2.5 in. (6.35 cm)	2.9855 in. (7.58317 cm)
Outer Diameter	6.973 in. (17.71142 cm)	6.9725 in. (17.71015 cm)
Radial Thickness	0.062083 in. (0.15769082 cm)	0.0618 in. (0.156972 cm)
End Thickness	0.202 in. (0.51308 cm)	0.201222 in. (0.51110388 cm)
Steel Mass	2358 g	2424 g
Potassium Mass	1064 g	1334 g

Further investigation of the measured values reported in Table 1.1-5 indicates that the standard deviation in the repeated measurements is relatively small. The largest standard deviation is in the measured height of the lower steel can, which is ±0.0044 in. (±0.011176 cm). An uncertainty in the height of the upper can could not be evaluated; however, it is believed that a 1σ uncertainty of ±0.005 in. (±0.0127 cm) should be adequate to represent the uncertainty in the measurement of the stainless steel can dimensions. An additional uncertainty can also be included to account for rounding of ±0.0005 inches (±0.00127 cm), which is considered to represent a bounding uncertainty with uniform probability distribution (i.e. ÷√3). These two uncertainties are combined in quadrature to obtain a total 1σ uncertainty of ±0.005008 in. (±0.012721 cm).

To find the effect of any of the dimensional uncertainties on the k_{eff} value, the dimensions of the steel cans (Table 2.1-4) were adjusted by a factor of 10 times the 1σ uncertainty. For all geometric perturbations of the stainless steel can dimensions, the mass of the stainless steel and potassium were conserved, which equated to an adjustment of the material densities in the simulations. Both upper and lower can dimensions of the same type were simultaneously increased to find an upper perturbation k_p value and then simultaneously decreased to find a lower perturbation k_p value. Half of the difference between the upper and lower perturbation k_p values was used to represent the variation in k_p due to perturbing the various dimensional properties. The 1σ uncertainty in k_{eff} associated with the uncertainty in a given can dimension is found from the following formula, where Δk_p is one-half the difference between the upper and lower perturbation k_p values, SF is the scaling factor, and N is the number of steel cans in each configuration:

$$\Delta k_{eff}(1\sigma) = \frac{\Delta k_p}{SF}\sqrt{\left[\gamma_{sys}\right]^2 + \left[\frac{\gamma_{ran}}{\sqrt{N}}\right]^2}.$$

It is estimated that the systematic component of this uncertainty is roughly equivalent to the ratio of the rounding uncertainty to the uncertainty attributed to the measurement of a given dimension; therefore, the systematic component of the uncertainty is estimated to be approximately 6 %. The fraction of the uncertainty attributed to the random component is then 94 %; it should be noted that the random component of the uncertainty is not computed using the ratio of non-systematic uncertainty to the total uncertainty. Results are provided in Table 2.1-5 for the outer diameter of the steel cans, Table 2.1-6 for the radial wall thickness, Table 2.1-7 for the height of the steel cans, and Table 2.1-8 for the top and bottom end thickness. Results and are considered negligible ($\Delta k_{eff} < 0.00003$) in both configurations for most of these parameters.

Outer Diameter

Table 2.1-5. Effect of Uncertainty in Steel Can Outer Diameters.

Case	Deviation (cm)	Δk_p	±	$\sigma_{\Delta kp}$	SF	Δk_{sys} (γ_{sys}=6%)	Δk_{ran} (γ_{ran}=94%)	Δk_{eff} (1σ)	±	$\sigma_{\Delta keff}$
1	±0.127211	0.00009	±	0.00001	10	<0.00001	0.00001	0.00001	±	<0.00001
2	±0.127211	0.00012	±	0.00001	10	<0.00001	0.00001	0.00001	±	<0.00001

Radial Wall Thickness

Table 2.1-6. Effect of Uncertainty in Steel Can Radial Wall Thickness.

Case	Deviation (cm)	Δk_p	±	$\sigma_{\Delta kp}$	SF	Δk_{sys} (γ_{sys}=6%)	Δk_{ran} (γ_{ran}=94%)	Δk_{eff} (1σ)	±	$\sigma_{\Delta keff}$
1	±0.127211	0.00039	±	0.00001	10	<0.00001	0.00003	0.00003	±	<0.00001
2	±0.127211	0.00030	±	0.00001	10	<0.00001	0.00002	0.00002	±	<0.00001

Height

Table 2.1-7. Effect of Uncertainty in Steel Can Heights.

Case	Deviation (cm)	Δk_p	±	$\sigma_{\Delta kp}$	SF	Δk_{sys} (γ_{sys}=6%)	Δk_{ran} (γ_{ran}=94%)	Δk_{eff} (1σ)	±	$\sigma_{\Delta keff}$
1	±0.127211	0.00016	±	0.00001	10	<0.00001	0.00001	0.00001	±	<0.00001
2	±0.127211	0.00020	±	0.00001	10	<0.00001	0.00001	0.00001	±	<0.00001

Top and Bottom End Thickness

Table 2.1-8. Effect of Uncertainty in Steel Can End Thickness.

Case	Deviation (cm)	Δk_p	±	$\sigma_{\Delta kp}$	SF	Δk_{sys} (γ_{sys}=6%)	Δk_{ran} (γ_{ran}=94%)	Δk_{eff} (1σ)	±	$\sigma_{\Delta keff}$
1	±0.127211	-0.00033	±	0.00001	10	<0.00001	-0.00002	0.00002	±	<0.00001
2	±0.127211	-0.00035	±	0.00001	10	<0.00001	-0.00002	0.00002	±	<0.00001

Can Lateral Placement

There is limited space within the central cavity of the HEU annulus for placement of the stainless steel cans. Variations in the lateral placement would be minimal and have negligible impact upon neutron streaming paths and the total reactivity of the system.

2.1.2.3 Potassium

All dimensional perturbations of the potassium within the stainless steel cans in Configuration 2 were included in the evaluation of the different geometrical uncertainties of the cans in the previous subsections of this evaluation. The mass of the potassium was conserved throughout the perturbation analysis and evaluation of the uncertainties in the dimensions of the cans.

2.1.2.4 Lateral Alignment

Lateral alignment measurements were made to within ±0.005 inches (±0.0127 cm). To find the effect of this uncertainty on the k_{eff} value, the lower half of each configuration was moved laterally (in a model) by a factor of 10 times this reported uncertainty to find a perturbed k_{eff} value. The difference between the perturbed k_p value and the unperturbed model k_{eff} value was used to represent the variation in k_{eff} due to perturbing the lateral assembly alignment. The 1σ uncertainty associated with the uncertainty in the lateral alignment is found from the following formula, where Δk_p is the difference between the upper perturbation and unperturbed model k_{eff} values, and SF is the parameter scaling factor:

$$\Delta k_{eff}(1\sigma) = \frac{\Delta k_p}{SF}.$$

This uncertainty is treated as a one-sided bounding uncertainty with uniform probability distribution (i.e. ÷2√3). Furthermore, this uncertainty is treated as 100 % systematic with no random uncertainty component. Results are provided in Table 2.1-9, and are considered negligible (Δk_{eff} < 0.00003) for both configurations.

Table 2.1-9. Effect of Uncertainty in Assembly Lateral Alignment.

Case	Deviation (cm)	Δk_p	±	$\sigma_{\Delta kp}$	SF	Δk_{eff} (1σ)	±	$\sigma_{\Delta keff}$
1	+0.127	-0.00006	±	0.00003	10×2√3	<0.00001	±	<0.00001
2	+0.127	-0.00003	±	0.00003	10×2√3	<0.00001	±	<0.00001

2.1.2.5 Vertical Assembly Alignment

The uncertainty of axial symmetry was not considered in this evaluation since it is embedded within the uranium and stainless steel can diameter uncertainties.

2.1.2.6 Gaps between Parts

The uncertainty in gap heights was not considered in this evaluation since it is embedded within the uranium stack height and diameter uncertainties.

The total height of the gaps between the stacks of uranium annuli was obtained by taking the difference between the measured stack height and the summation of the heights of the individual uranium annuli in each stack. The total gap height was then divided by the number of annuli minus one, to represent the number of gaps between the uranium annuli. There is no gap between the bottom of the top uranium annuli stacks and the stainless steel diaphragm. The gap heights for Configurations 1 and 2 can be seen in Figure 3.1-2 and Table 2.1-10.

The tallest stack of uranium annuli in the lower section was modeled "in contact with" the bottom of the stainless steel diaphragm. The gaps between the diaphragm and the remaining stacks were adjusted such that the bottoms of all the lower stacks were collocated on the same plane. This effectively models each of these stacks as having been "raised" as a single configuration on a planar surface (as was performed in the actual experiment).

The measured worth of the diaphragm includes the separation distance between the two halves of the experiment. Therefore, when the diaphragm is removed from the model, the parts adjacent to the diaphragm are brought closer together and the separation distance of 0.010 in. (0.0254 cm) that represents the diaphragm thickness would be eliminated.[a]

It should be noted that the gaps calculated using the experimental data do not necessarily match exactly with those in Table 1.1-1; however, they are approximately the same within rounding of digits. It is unclear for what purpose the annular gaps in Table 1.1-1 were presented other than to demonstrate the very close fit of the annuli, effectively producing a "solid" annulus of HEU material.

Table 2.1-10. Reported Vertical Gaps between Uranium Metal Annuli.

Annular Ring Stack	Average Stack Height (in.)[(a)]	Combined Height of Annuli (in.)[(b)]	Number of Annuli	Number of Gaps	Average Gap Height (in.)	Average Gap Height (cm)
Upper 13-11	2.514667	2.50695	7	6	0.001286	0.003267
Upper 11-9	2.633833	2.63015	3	2	0.001842	0.004678
Upper 9-7	2.623	2.62385	3	2	~0[(c)]	~0[(c)]
Lower 13-11	3.018333	3.0119	5	4	0.001608	0.004085
Lower 11-9	3.010833	3.00075	4	3	0.003361	0.008537
Lower 9-7	3.012	3.00245	4	3	0.003183	0.008086

(a) The average stack height was recalculated from the measurement data provided.
(b) The sum of the individual heights for all annuli in a given stack.
(c) The sum of the heights of the individual parts was greater than the measured stack height.

[a] Personal communication with John T. Mihalczo, February 2010.

2.1.2.7 Assembly Separation

The uncertainty for the separation of the upper and lower assemblies is based upon the accuracy of vertical placement measurement when bringing the two experiment halves into contact, ±0.001 in. (±0.00254 cm). This uncertainty, however, would be included within the measurement uncertainty of the worth of the stainless steel diaphragm.

2.1.3 Compositional Variations

2.1.3.1 Uranium Annuli

Traditionally, the uncertainties in the ORCEF Oralloy experiments have been as follows in regards to material properties. The uranium mass of each part measured at the Y-12 Plant is traceable back to the Bureau of Standards to less than 0.5 gram accuracy and then rounded to the nearest gram yielding a mass uncertainty for each uranium annuli is ±0.5 g. Based on the accuracy of isotopic ratios from the mass spectrometry laboratory at the Y-12 Plant, uncertainty for the uranium isotopic content is ±0.005 wt.% for ^{234}U, ^{235}U, and ^{236}U. The ^{238}U content was obtained by subtracting the sum of the ^{234}U, ^{235}U, and ^{236}U contents from one.

More recently a document has been prepared to examine the uncertainties pertaining to critical experiments performed at ORCEF using HEU metal components.[a] This document will be the basis for the uncertainty analysis in this evaluation; however, the results for many of the calculations are negligible, which is what would be expected if the traditional approach to calculate the material uncertainties were implemented using the uncertainty values provided in Section 1.1.3.1.

Mass

The uranium mass of each part measured at the Y-12 Plant is traceable back to the Bureau of Standards to less than 0.5 gram accuracy and then rounded to the nearest gram, thus the uncertainty for the mass of each uranium annuli is ±0.5 g. Additionally, the scale in the metrology laboratory of the Y-12 Plant had a mass accuracy of 0.089 g in 1960 for 20 kg calibration measurements.[b] These two uncertainties are both considered to represent bounding uncertainties with uniform probability distribution and are combined in quadrature to obtain a total bounding uncertainty of ±0.507859 g. A mass measurement of multiple uranium annuli was not performed.

To find the effect of this uncertainty on the k_{eff} value, the masses of the annuli (Table 1.1-4) were adjusted by a factor of 10 times the bounding uncertainty. In order to keep the uranium volume of the experiment constant, the density of each of the uranium annuli was adjusted accordingly. Uranium masses were simultaneously increased to find an upper perturbation k_p value and then simultaneously decreased to find a lower perturbation k_p value. Half of the difference between the upper and lower perturbation k_p values was used to represent the variation in k_p due to perturbing the annuli masses. The 1σ uncertainty in k_{eff} associated with the uncertainty in the mass of the uranium annuli is found from the following formula, where Δk_p is one-half the difference between the upper and lower perturbation k_{eff} values, N is the number of uranium annuli in each configuration, and SF is the parameter scaling factor:

$$\Delta k_{eff}(1\sigma) = \frac{\Delta k_p}{SF}\sqrt{\left[\gamma_{sys}\right]^2 + \left[\frac{\gamma_{ran}}{\sqrt{N}}\right]^2}.$$

[a] J. T. Mihalczo and T. Gregory Schaaff, "Uncertainties in Masses, Dimensions, Impurities, and Isotopics of HEU Metal Used in Critical Experiments at ORCEF," ORNL/TM-2012/32, Oak Ridge National Laboratory (2012).
[b] J. T. Mihalczo and T. Gregory Schaaff, "Uncertainties in Masses, Dimensions, Impurities, and Isotopics of HEU Metal Used in Critical Experiments at ORCEF," ORNL/TM-2012/32, Oak Ridge National Laboratory (2012).

It is estimated that the systematic component of this uncertainty is roughly equivalent to the ratio of the accuracy of the metrology laboratory scale to the rounding uncertainty of the final value after performing multiple measurements; therefore, the systematic component of the uncertainty is estimated to be approximately 18 %. The fraction of the uncertainty attributed to the random component is then 82 %; it should be noted that the random component of the uncertainty is not computed using the ratio of non-systematic uncertainty to the total uncertainty. Results are provided in Table 2.1-11, and are considered negligible ($\Delta k_{eff} < 0.00003$) for both configurations.

Table 2.1-11. Effect of Uncertainty in Uranium Mass.

Case	Deviation (g)	Δk_p	±	$\sigma_{\Delta kp}$	SF	Δk_{sys} (γ_{sys}=18%)	Δk_{ran} (γ_{ran}=72%)	Δk_{eff} (1σ)	±	$\sigma_{\Delta keff}$
1	±5.078592 × 26	0.00055	±	0.00001	10√3	0.00001	0.00001	0.00001	±	<0.00001
2	±5.078592 × 26	0.00056	±	0.00001	10√3	0.00001	0.00001	0.00001	±	<0.00001

Isotopic Content

Based on the accuracy of isotopic ratios from the mass spectrometry laboratory at the Y-12 Plant, uncertainty for the uranium isotopic content is ±0.005 wt.% for ^{234}U, ^{235}U, and ^{236}U, which represents a rounding uncertainty that can also be considered a bounding uncertainty with uniform probability distribution (i.e. ÷√3). The ^{238}U content was obtained by subtracting the sum of the ^{234}U, ^{235}U, and ^{236}U contents from one. The weight percent uncertainty in isotopic content of the oralloy for measurement using a standard traceable back to the Bureau of Standards and the standard deviation of the mean for these parts were assessed.[a] The individual contributors to the total uncertainty in the uranium isotopic content are summarized in Table 2.1-12.

Table 2.1-12. Weight Percent (wt.%) Uncertainty (1σ) in Oralloy Isotopic Content.

Isotope	Uncertainty in Traceable Standard Measurement[(a)]	Standard Deviation of the Mean for As-Measured Parts[(a)]	Rounding	Total Uncertainty
^{234}U	0.0017	0.00203	0.005/√3	0.003917
^{235}U	0.0177	0.00346	0.005/√3	0.018265
^{236}U	0.0130	0.00218	0.005/√3	0.013494

(a) J. T. Mihalczo and T. Gregory Schaaff, "Uncertainties in Masses, Dimensions, Impurities, and Isotopics of HEU Metal Used in Critical Experiments at ORCEF," ORNL/TM-2012/32, Oak Ridge National Laboratory (2012).

To find the effect of this uncertainty on the k_{eff} value, the isotopic contents of the annuli (Table 1.1-6) were adjusted by a factor of 10 times the 1σ uncertainty. An upper perturbation k_p value was found by simultaneously increasing the isotopic contents of ^{234}U, ^{235}U, or ^{236}U and adjusting the ^{238}U isotopic content accordingly. The isotopic contents of ^{234}U, ^{235}U, or ^{236}U were then simultaneously decreased, again with the ^{238}U content adjusted, to find the lower perturbation k_p value. Typically, the isotopic content of all components in a system would be varied individually so as to isolate any parts with

[a] J. T. Mihalczo and T. Gregory Schaaff, "Uncertainties in Masses, Dimensions, Impurities, and Isotopics of HEU Metal Used in Critical Experiments at ORCEF," ORNL/TM-2012/32, Oak Ridge National Laboratory (2012).

significant merit. As this is a small system and relatively large perturbations of the combined isotopic content yield a negligible change in k_{eff}, all oralloy isotopic contents for a given isotope (^{234}U, ^{235}U, or ^{236}U) were adjusted simultaneously in all uranium parts. Half of the difference between the upper and lower perturbation k_p values was used to represent the variation in k_p due to perturbing the isotopic content. The 1σ uncertainty in k_{eff} associated with the uncertainty in the isotopic content of the uranium annuli is found from the following formula, where Δk_p is one-half the difference between the upper and lower perturbation k_p values and SF is the parameter scaling factor:

$$\Delta k_{eff}(1\sigma) = \frac{\Delta k_p}{SF}.$$

This uncertainty is treated as 100 % systematic with no random uncertainty component because the impact due to the variability in measurement of multiple oralloy components was already accounted for in the derivation of the standard deviation of the mean reported in Table 2.1-12. Results are provided in Tables 2.1-13 through 2.1-15 for the uncertainties in ^{234}U, ^{235}U, and ^{236}U, respectively; the uncertainties are considered negligible ($\Delta k_{eff} < 0.00003$) for both configurations for the ^{234}U and ^{236}U isotopic contents.

Table 2.1-13. Effect of Uncertainty in ^{234}U Isotopic Content.

Case	Deviation (wt.%)	Δk_p	±	$\sigma_{\Delta kp}$	SF	Δk_{eff} (1σ)	±	$\sigma_{\Delta keff}$
1	±0.039172	0.00015	±	0.00001	10	0.00001	±	<0.00001
2	±0.039172	0.00016	±	0.00001	10	0.00002	±	<0.00001

Table 2.1-14. Effect of Uncertainty in ^{235}U Isotopic Content.

Case	Deviation (wt.%)	Δk_p	±	$\sigma_{\Delta kp}$	SF	Δk_{eff} (1σ)	±	$\sigma_{\Delta keff}$
1	±0.182646	0.00097	±	0.00001	10	0.00010	±	<0.00001
2	±0.182646	0.00098	±	0.00001	10	0.00010	±	<0.00001

Table 2.1-15. Effect of Uncertainty in ^{236}U Isotopic Content.

Case	Deviation (wt.%)	Δk_p	±	$\sigma_{\Delta kp}$	SF	Δk_{eff} (1σ)	±	$\sigma_{\Delta keff}$
1	±0.134939	0.00013	±	0.00001	10	0.00001	±	<0.00001
2	±0.134939	0.00015	±	0.00001	10	0.00001	±	<0.00001

Impurities

The uranium impurities listed in Table 1.1-7 are given as the average of a spectrographic analysis from randomly sampled components for each impurity (assuming the values to be normally distributed) or listed as less than a minimum value. In the latter case, they are less than the detectable limit. The impurity content, as specified in Table 1.1-7, is accepted as the nominal composition for the oralloy parts utilized at ORCEF. A summary of the nominal impurity composition is found in Table 11. The oxygen and nitrogen content was included at the experimentalist-specified quantities of 20 and 30 ppm, respectively. For impurities below a detectable limit, the content is selected as half the detectable limit and the detection limit as a bounding uncertainty. The concentration of metallic impurities in the oralloy

was determined by DC-Arc emission spectroscopy, and the concentration of "gas" species was determined by combustion analyses, similar to modern Leco-type measurements. It was established that the uncertainty in these methods was 70 % for values measured below 10 μg/g-U and 20 % for values measured above 10 μg/g-U. However, for the measurement of oralloy materials, the uncertainty was about 20 % and 6 %, respectively.[a] The mean impurity content and revised uncertainty assessment are provided in Table 2.1-16.

Table 2.1-16. Impurity Content of Uranium Metal Annuli.

Element	Impurity Content (ppm)	1σ Uncertainty (ppm)
Ag	8	1.6
Ba	0.005	0.005/√3
Bi	164	9.84
C	5	5/√3
Ca	0.1	0.02
Cd	0.5	0.5/√3
Co	5	1
Cr	7	1.4
Cu	25	1.5
K	0.1	0.1/√3
Li	1	1/√3
Mg	3	0.6
Mn	56	3.36
Mo	0.5	0.5/√3
Na	27	1.62
Ni	100	6
Sb	38	2.28
Ti	1	0.2
O	20	1.8
N	30	1.2
Total	491.205	~35

To find the effect of this uncertainty on the k_{eff} value, the impurities were all simultaneously increased by 3σ to find an upper perturbation k_p value and then all simultaneously decreased to find a lower perturbation k_p value. Perturbation of the content of individual impurities was not performed as their content and the uncertainty in the content is already quite small; furthermore, the primary effect of this uncertainty would be the impact of adjusting the total uranium content in the oralloy metal. The weight fraction of the uranium metal was adjusted, as appropriate, to compensate for the adjustments in impurity content. Half of the difference between the upper and lower perturbation k_p values was used to represent the variation in k_p due to perturbing the uranium impurity content. The 1σ uncertainty in k_{eff} associated with the impurity content of the uranium annuli is found from the following formula, where Δk_p is one-half the difference between the upper and lower perturbation k_p values and SF is the parameter scaling factor:

[a] J. T. Mihalczo and T. Gregory Schaaff, "Uncertainties in Masses, Dimensions, Impurities, and Isotopics of HEU Metal Used in Critical Experiments at ORCEF," ORNL/TM-2012/32, Oak Ridge National Laboratory (2012).

$$\Delta k_{eff}(1\sigma) = \frac{\Delta k_p}{SF}.$$

This uncertainty is treated as 100 % systematic with no random uncertainty component because there is insufficient information to assess any randomness in the impurity content between manufactured oralloy components. Results are provided in Table 2.1-17, and are considered negligible ($\Delta k_{eff} < 0.00003$) for both configurations.

Table 2.1-17. Effect of Uncertainty in Uranium Impurity Content.

Case	Deviation (ppm)	Δk_p	±	$\sigma_{\Delta kp}$	SF	Δk_{eff} (1σ)	±	$\sigma_{\Delta keff}$
1	±3σ (see Table 2.1-16)	-0.00001	±	0.00001	3	<0.00001	±	<0.00001
2	±3σ (see Table 2.1-16)	-0.00004	±	0.00001	3	0.00001	±	<0.00001

2.1.3.2 Stainless Steel Cans

Mass

A total of three pairs of masses are recorded for the empty stainless steel cans in the logbooks, with only a single pair mentioned in Ref. 1 (see Table 1.1-5). The average of these values is used in Table 2.1-4 to represent the mass of each stainless steel can in detailed models of the experiment. The standard deviation in the averaged can masses is ±1.16 g in the upper can and ±9.85 g in the lower can; propagation of these two uncertainties yields a total stainless steel mass uncertainty, due to the variation in reported can mass measurements, of ±9.92 g. Assuming that the steel cans were weighed on the plant scale, which had a mass measurement uncertainty of ±0.30 g[a] and that the mass measurements of the steel cans were also subject to the same rounding uncertainty as the HEU annuli (±0.5/√3 g), these three uncertainties were combined in quadrature to obtain a total 1σ uncertainty of ±9.93 g, which is rounded to ±10 g (1σ) for the evaluation of the mass uncertainty in the stainless steel cans. The actual uncertainty is most likely on the order of <1 g; however, as can be seen below, the impact of the larger perturbation is negligible.

To find the effect of this uncertainty on the k_{eff} value, the total mass of the steel cans (Table 2.1-4) was adjusted by a factor of 3 times the 1σ uncertainty. In order to keep the steel can volumes constant, the density of each of the steel cans was adjusted accordingly. Steel masses were simultaneously increased to find an upper perturbation k_p value and then simultaneously decreased to find a lower perturbation k_p value. Half of the difference between the upper and lower perturbation k_p values was used to represent the variation in k_p due to perturbing the steel can masses. The 1σ uncertainty in k_{eff} associated with the uncertainty in the mass of the steel cans is found from the following formula, where Δk_p is one-half the difference between the upper and lower perturbation k_{eff} values, N is the number of steel cans in each configuration, and SF is the parameter scaling factor:

$$\Delta k_{eff}(1\sigma) = \frac{\Delta k_p}{SF}\sqrt{\left[\gamma_{sys}\right]^2 + \left[\frac{\gamma_{ran}}{\sqrt{N}}\right]^2}.$$

It is estimated that the systematic component of this uncertainty is roughly equivalent to the ratio of the accuracy of the plant laboratory scale combined in quadrature with the rounding uncertainty of the reported mass value over the approximate uncertainty in the reported mass measurements (~±10 g);

[a] J. T. Mihalczo and T. Gregory Schaaff, "Uncertainties in Masses, Dimensions, Impurities, and Isotopics of HEU Metal Used in Critical Experiments at ORCEF," ORNL/TM-2012/32, Oak Ridge National Laboratory (2012).

therefore, the systematic component of the uncertainty is estimated to be approximately 6 %. The fraction of the uncertainty attributed to the random component is then 94 %; it should be noted that the random component of the uncertainty is not computed using the ratio of non-systematic uncertainty to the total uncertainty. Results are provided in Table 2.1-18, and are considered negligible ($\Delta k_{eff} < 0.00003$) for both configurations.

Table 2.1-18. Effect of Uncertainty in Steel Can Mass.

Case	Deviation (g)	Δk_p	±	$\sigma_{\Delta kp}$	SF	Δk_{sys} (γ_{sys}=6%)	Δk_{ran} (γ_{ran}=94%)	Δk_{eff} (1σ)	±	$\sigma_{\Delta keff}$
1	30	0.00004	±	0.00001	3	<0.00001	0.00001	0.00001	±	<0.00001
2	30	0.00005	±	0.00001	3	<0.00001	0.00001	0.00001	±	<0.00001

Composition

A composition was not reported for the stainless steel 304 cans. Composition ranges and a nominal content for stainless steel 304 to be used in this evaluation are summarized in Table 2.1-19 from handbook data for stainless steel 304, 304L, and 304H.[a]

Table 2.1-19. Composition of Stainless Steel 304.

Element	Minimum wt.%	Maximum wt.%	Nominal wt.%
C	--	0.1	0.05
Cr	18	20	19
Ni	8	12	10
Mn	--	2	1
Si	--	0.75	0.375
P	--	0.045	0.0225
S	--	0.03	0.015
N	--	0.1	0.05
Fe	--	Balance	69.4875

To find the effect of this uncertainty on the k_{eff} value, the compositions of the steel cans (Table 2.1-19) were adjusted by the bounding weight percent limits. An upper perturbation k_p value was found by increasing the contents of Cr, Ni, Mn, or (C, Si, P, S, & N) and adjusting the Fe content accordingly. The contents of Cr, Ni, Mn, or (C, Si, P, S, & N) were then decreased, again with the Fe content adjusted, to find the lower perturbation k_p value. Half of the difference between the upper and lower perturbation k_p values was used to represent the variation in k_p due to perturbing the steel can compositions. The 1σ uncertainty in k_{eff} associated with the uncertainty in the compositions of the steel cans is found from the following formula, where Δk_p is one-half the difference between the upper and lower perturbation k_p values and SF is the parameter scaling factor:

[a] R. Perry and D. W. Green (editors), *Perry's Chemical Engineers' Handbook*, 8th edition, McGraw-Hill, New York, NY (2007).

$$\Delta k_{eff}(1\sigma) = \frac{\Delta k_p}{SF}.$$

This uncertainty is treated as 100 % systematic with no random uncertainty component because the same stainless steel sheeting is assumed to have been used to form all cans in this experiment. Results are provided in Tables 2.1-20 through 2.1-23 for the uncertainties in Cr, Ni, Mn, and (C, Si, P, S, & N), respectively; the uncertainties are considered negligible ($\Delta k_{eff} < 0.00003$) for both configurations.

Table 2.1-20. Effect of Uncertainty in Steel Can Chromium Content.

Case	Deviation (wt.%)	Δk_p	±	$\sigma_{\Delta kp}$	SF	Δk_{eff} (1σ)	±	$\sigma_{\Delta keff}$
1	±1	0.00003	±	0.00001	√3	0.00002	±	0.00001
2	±1	0.00001	±	0.00001	√3	<0.00001	±	0.00001

Table 2.1-21. Effect of Uncertainty in Steel Can Nickel Content.

Case	Deviation (wt.%)	Δk_p	±	$\sigma_{\Delta kp}$	SF	Δk_{eff} (1σ)	±	$\sigma_{\Delta keff}$
1	±2	0.00003	±	0.00001	√3	0.00002	±	0.00001
2	±2	0.00002	±	0.00001	√3	0.00001	±	0.00001

Table 2.1-22. Effect of Uncertainty in Steel Can Manganese Content.

Case	Deviation (wt.%)	Δk_p	±	$\sigma_{\Delta kp}$	SF	Δk_{eff} (1σ)	±	$\sigma_{\Delta keff}$
1	±1	<0.00001	±	0.00001	√3	<0.00001	±	0.00001
2	±1	<0.00001	±	0.00001	√3	<0.00001	±	0.00001

Table 2.1-23. Effect of Uncertainty in Steel Can C, Si, P, S, & N Content.

Case	Deviation (wt.%)	Δk_p	±	$\sigma_{\Delta kp}$	SF	Δk_{eff} (1σ)	±	$\sigma_{\Delta keff}$
1	±0.1375 combined	0.00001	±	0.00001	√3	<0.00001	±	0.00001
2	±0.1375 combined	<0.00001	±	0.00001	√3	<0.00001	±	0.00001

Impurities

The effect of possible impurities in the stainless steel was evaluated. An example reference for impurities in stainless steel 304 was investigated and the reported content is provided in Table 2.1-24.[a] The effect of including these impurities within the steel composition for detailed models of both configurations had a negligible impact on the calculation of k_{eff} ($\Delta k_{eff} < 0.00003$); therefore, it was concluded that any uncertainty in the impurity content of the stainless steel would also be negligible.

[a] S. Danyluk, I. Wolke, J. H. Hong, and E. A. Loria, "Intergranular Fracture, Corrosion Susceptibility, and Impurity Segregation in Sensitized Type 304 Stainless Steel," *J. Mater. Energy Syst*, **7**, 6-15 (1985).

Table 2.1-24. Example Impurity Content for Stainless Steel 304.

Element	wt.%
Cu	0.133
Mo	0.25
V	0.096
Co	0.181
O	0.008
Ti	<0.01
Nb	<0.01
Zr	<0.01
Al	<0.01

2.1.3.3 Potassium

Mass

An uncertainty in the mass of potassium added in Configuration 2 was not provided. Without additional information to support a smaller mass uncertainty, the mass uncertainty evaluated for the mass of the stainless steel cans (see Section 2.1.3.2) of ±10 g (1σ) was applied as the uncertainty in the potassium mass. The actual uncertainty is most likely on the order of <1 g; however, as can be seen below, the impact of the larger perturbation is negligible.

To find the effect of this uncertainty on the k_{eff} value, the total mass of the potassium (Table 2.1-4) was adjusted by a factor of 3 times the 1σ uncertainty. In order to keep the steel can volumes constant, the density of each of the potassium was adjusted accordingly. Potassium masses were simultaneously increased to find an upper perturbation k_p value and then simultaneously decreased to find a lower perturbation k_p value. Half of the difference between the upper and lower perturbation k_p values was used to represent the variation in k_p due to perturbing the potassium masses. The 1σ uncertainty in k_{eff} associated with the uncertainty in the mass of the potassium is found from the following formula, where Δk_p is one-half the difference between the upper and lower perturbation k_{eff} values, N is the number of potassium-filled cans in each configuration, and SF is the parameter scaling factor:

$$\Delta k_{eff}(1\sigma) = \frac{\Delta k_p}{SF}\sqrt{\left[\gamma_{sys}\right]^2 + \left[\frac{\gamma_{ran}}{\sqrt{N}}\right]^2}.$$

It is estimated that the systematic component of this uncertainty is roughly equivalent to the ratio of the accuracy of the plant laboratory scale combined in quadrature with the rounding uncertainty of the reported mass value over the approximate uncertainty in the reported mass measurements (~±10 g); therefore, the systematic component of the uncertainty is estimated to be approximately 6 %. The fraction of the uncertainty attributed to the random component is then 94 %; it should be noted that the random component of the uncertainty is not computed using the ratio of non-systematic uncertainty to the total uncertainty. Results are provided in Table 2.1-25, and are considered negligible (Δk_{eff} < 0.00003) for Configuration 2 (potassium was not present in Configuration 1).

Table 2.1-25. Effect of Uncertainty in Potassium Mass.

Case	Deviation (g)	Δk_p	±	$\sigma_{\Delta kp}$	SF	Δk_{sys} (γ_{sys}=6%)	Δk_{ran} (γ_{ran}=94%)	Δk_{eff} (1σ)	±	$\sigma_{\Delta keff}$
1	--		--		--	--	--		--	
2	30	<0.00001	±	0.00001	3	<0.00001	<0.00001	<0.00001	±	<0.00001

Impurities

The effect of possible impurities in the potassium was evaluated. An example reference for impurities in purified potassium from Oak Ridge National Laboratory was investigated and the reported content is provided in Table 2.1-26.[a] The effect of including these impurities within the potassium composition for a detailed model of Configuration 2 had a negligible impact on the calculation of k_{eff} ($\Delta k_{eff} < 0.00003$); therefore, it was concluded that any uncertainty in the impurity content of the potassium would also be negligible.

Table 2.1-26. Example Impurity Content for Potassium.

Element	wppm
B	10
Ca	11
Cs	20
Cr	1
Fe	20
Li	1
Mg	2
Mo	5
Ni	7
Nb	5
Si	10
Na	60
Rb	130
Ti	5
V	1
Zr	20
O	35
H	115

Bubbles

Care was taken during filling of the stainless steel cans to minimize void spaces and the production of bubbles. The total mass of potassium added to the system was measured. The inclusion of small bubbles

[a] J. J. Zuckerman and A. P. Hagen (editors), *Inorganic Reactions and Methods*, Volume 13, Section 7.2.2.3.3, VCH Publishers, Salem, MA (1991).

or voids is expected have a negligible impact on system reactivity as this is a fast system with total mass conserved.

2.1.4 Total Experimental Uncertainty

The total k_{eff} uncertainty for each experiment was calculated by taking the square root of the sum of the squares of all the individual uncertainties discussed in this section; they are summarized in Tables 2.1-27 and 2.1-28 for Configurations 1 and 2, respectively; these are acceptable benchmark experiments. Uncertainties < 0.00003 Δk_{eff} are reported as negligible (neg).

Table 2.1-27. Total Experimental Uncertainty for Configuration 1 (Empty Cans).

Perturbed Parameter	**Parameter Value**	**1σ Uncertainty**	**Δk_{eff}**
Temperature (K)	294	±2	0.00004
Experiment reproducibility (¢)	--	±2	0.00013
Measured reactivity worth (¢)	--	±√3×√2×2	0.00032
β_{eff}	0.0066	±5 %	0.00005
Uranium diameter (cm)	Tables 1.1-4 and 3.1-2	±0.001276/√3	neg
Uranium height (cm)	Tables 1.1-4 and 3.1-2	±0.001276/√3	neg
Uranium stack height (cm)	Table 2.1-10	±0.002644	0.00006
Steel can diameter (cm)	Table 2.1-4	±0.012721	neg
Steel can radial thickness (cm)	Table 2.1-4	±0.012721	0.00003
Steel can height (cm)	Table 2.1-4	±0.012721	neg
Steel can end thickness (cm)	Table 2.1-4	±0.012721	neg
Steel can lateral placement (cm)	Not Applicable – See Section 2.1.2.2		
Lateral assembly alignment (cm)	0	±0.0127/2√3	neg
Vertical assembly alignment (cm)	Not Applicable – See Section 2.1.2.5		
Gaps between parts (cm)	Not Applicable – See Section 2.1.2.6		
Assembly separation (cm)	Not Applicable – See Section 2.1.2.7		
Uranium mass (g)	Table 1.1-4	±0.507859/√3	neg
^{234}U content (wt.%)	Table 1.1-6	±0.039172	neg
^{235}U content (wt.%)	Table 1.1-6	±0.182646	0.00010
^{236}U content (wt.%)	Table 1.1-6	±0.134939	neg
Uranium impurities (ppm)	Table 2.1-16		neg
Stainless steel mass (g)	Table 2.1-4	±10	neg
Stainless steel Cr content (wt.%)	Table 2.1-19	±1/√3	neg
Stainless steel Ni content (wt.%)	Table 2.1-19	±2/√3	neg
Stainless steel Mn content (wt.%)	Table 2.1-19	±1/√3	neg
Stainless steel (C, Si, P, S, & N) content (wt.%)	Table 2.1-19	±0.1375/√3	neg
Stainless steel impurities (ppm)	See Section 2.1.3.2		neg
Potassium mass (g)	Not Applicable – No Potassium		
Potassium impurities (ppm)	Not Applicable – No Potassium		
Potassium bubbles or voiding	Not Applicable – No Potassium		
Total Experimental Uncertainty	**--**	**--**	**0.00037**

Table 2.1-28. Total Experimental Uncertainty for Configuration 2 (Potassium-Filled Cans).

Perturbed Parameter	**Parameter Value**	**1σ Uncertainty**	**Δk_{eff}**
Temperature (K)	294	±2	0.00004
Experiment reproducibility (¢)	--	±2	0.00013
Measured reactivity worth (¢)	--	±√3×√2×2	0.00032
β_{eff}	0.0066	±5 %	neg
Uranium diameter (cm)	Tables 1.1-4 and 3.1-2	±0.001276/√3	neg
Uranium height (cm)	Tables 1.1-4 and 3.1-2	±0.001276/√3	neg
Uranium stack height (cm)	Table 2.1-10	±0.002644	0.00006
Steel can diameter (cm)	Table 2.1-4	±0.012721	neg
Steel can radial thickness (cm)	Table 2.1-4	±0.012721	neg
Steel can height (cm)	Table 2.1-4	±0.012721	neg
Steel can end thickness (cm)	Table 2.1-4	±0.012721	neg
Lateral assembly alignment (cm)	0	±0.0127/2√3	neg
Steel can lateral placement (cm)	Not Applicable – See Section 2.1.2.2		
Vertical assembly alignment (cm)	Not Applicable – See Section 2.1.2.5		
Gaps between parts (cm)	Not Applicable – See Section 2.1.2.6		
Assembly separation (cm)	Not Applicable – See Section 2.1.2.7		
Uranium mass (g)	Table 1.1-4	±0.507859/√3	neg
^{234}U content (wt.%)	Table 1.1-6	±0.039172	neg
^{235}U content (wt.%)	Table 1.1-6	±0.182646	0.00010
^{236}U content (wt.%)	Table 1.1-6	±0.134939	neg
Uranium impurities (ppm)	Table 2.1-16		neg
Stainless steel mass (g)	Table 2.1-4	±10	neg
Stainless steel Cr content (wt.%)	Table 2.1-19	±1/√3	neg
Stainless steel Ni content (wt.%)	Table 2.1-19	±2/√3	neg
Stainless steel Mn content (wt.%)	Table 2.1-19	±1/√3	neg
Stainless steel (C, Si, P, S, & N) content (wt.%)	Table 2.1-19	±0.1375/√3	neg
Stainless steel impurities (ppm)	See Section 2.1.3.2		neg
Potassium mass (g)	Table 2.1-4	±10	neg
Potassium impurities (ppm)	See Section 2.1.3.3		neg
Potassium bubbles or voiding	Not Applicable – See Section 2.1.3.3		
Total Experimental Uncertainty	**--**	**--**	**0.00037**

2.2 Evaluation of Buckling and Extrapolation Length Data

Buckling and extrapolation length measurements were not made.

2.3 Evaluation of Spectral Characteristics Data

Spectral characteristics measurements were not made.

2.4 Evaluation of Reactivity Effects Data

The two critical configurations performed to measure the worth of potassium are very highly correlated measurements with small total experimental uncertainty (see Section 2.1.4). As such, many of the uncertainties are assumed to be correlated and of negligible impact on the measurement and subsequent calculation of the potassium worth measurement. A summary of the uncertainties evaluated in Section 2.1 that are assumed to be correlated or uncorrelated are summarized in Table 2.4-1. Uncertainties assumed to not be 100 % fully correlated are treated as fully uncorrelated for the purpose of this uncertainty analysis except in the case of reproducibility. The two configurations are highly correlated yet it is believed some uncertainty would still be introduced during the transition from one configuration to the second; it is assumed that 20 % of the reproducibility uncertainty for each critical configuration would be applicable for assessing the reproducibility uncertainty in the worth measurement. The uncertainties from Tables 2.1-27 and 2.1-28 that are thus treated as uncorrelated are combined (square root of the sum of the squares) and provided in the table below to obtain a total uncertainty in the potassium worth measurement. The ±5 % uncertainty in β_{eff} is propagated into the calculation of the total uncertainty reported in Table 2.4-1.

It is unclear how the reported uncertainty in the worth measurements of ±0.40 ¢ (Ref. 1) was derived. It is less than the uncertainty determined in Table 2.4-1; the larger of the two uncertainties will be used to represent the uncertainty in the potassium worth measurement.

A secondary method was utilized to verify the experimental uncertainty obtained as explained above. The eigenvalues for the uncorrelated uncertainty parameters between Configurations 1 and 2 of the critical configurations evaluated in Section 2.1 were compared against each other. For example, the computed eigenvalue for the upper perturbation of Configuration 1 for increasing the outer diameter of the stainless steel cans was compared against the lower perturbation of Configuration 2 for decreasing the outer diameter of the stainless steel cans to obtain a worth difference. Similarly this was performed for the opposing perturbations of reducing the outer diameter for Configuration 1 and increasing the outer diameter for Configuration 2; the larger of the two differences was retained as the uncertainty in the stainless steel can outer diameter. Similar perturbation comparisons were performed for the other uncorrelated uncertainties. The results were combined in quadrature to obtain a bounding uncertainty of ±0.00010 $\Delta\rho$, or a 1σ uncertainty of ±0.00006 $\Delta\rho$. This equates to a 1σ uncertainty of ±0.87 ¢, which is ±1.01 ¢ when including the ±5 % uncertainty in β_{eff}. As the results using this second method are comparable, within rounding, with the uncertainty obtained in Table 2.4-1, no additional uncertainty analysis was performed and the results are deemed acceptable for this measurement.

Worths were measured via their stable reactor period and converted into reactivity in units of ρ\$ using the Inhour equation. Any systematic uncertainties in the measurement and conversion of the stable reactor period would have a negligible effect on the reactivity worth ($\Delta\rho$), especially when compared against the total experimental uncertainty derived in Table 2.4-1.

Table 2.4-1. Uncertainty Contribution to the Potassium Worth Measurement.

Uncertainty Parameters	**Fully Correlated?**	**Δρ**
Temperature	Yes	--
Experiment reproducibility	No	0.00004
Measured reactivity worth	Yes	--
β_{eff}	Yes	--
Uranium diameter	Yes	--
Uranium height	Yes	--
Uranium stack height	Yes	--
Steel can diameter	No	0.00001
Steel can radial thickness	No	0.00003
Steel can height	No	0.00002
Steel can end thickness	No	0.00003
Steel can lateral placement	Yes	--
Lateral assembly alignment	Yes	--
Vertical assembly alignment	Yes	--
Gaps between parts	Yes	--
Assembly separation	Yes	--
Uranium mass	Yes	--
^{234}U content	Yes	--
^{235}U content	Yes	--
^{236}U content	Yes	--
Uranium impurities	Yes	--
Stainless steel mass	No	0.00002
Stainless steel Cr content	Yes	--
Stainless steel Ni content	Yes	--
Stainless steel Mn content	Yes	--
Stainless steel (C, Si, P, S, & N) content	Yes	--
Stainless steel impurities	Yes	--
Potassium mass	No	<0.00001
Potassium impurities	No	Section 3.4.1
Potassium bubbles or voiding	No	Section 2.1.3.3
Total Experimental Uncertainty	--	0.00006 (0.98 ¢)
Total Experimental Uncertainty (Including ±5 % β_{eff} Uncertainty)	**--**	**0.00006 (1.10 ¢)**

An additional small step is needed for the uncertainty evaluation of the potassium worth in units of ¢/g. The total experimental uncertainty in the potassium mass coefficient is the total uncertainty in the worth measurement divided by the total mass of potassium used in the experiment, 2398 g. This equates to a total experimental uncertainty of ±0.00041 ¢/g, which is ±0.00046 ¢/g when a ±5 % uncertainty in β_{eff} is also applied and propagated as part of the uncertainty analysis The 1σ uncertainty in the mass of potassium was estimated to be ±10 g (see Section 2.1.3.3); propagation of this uncertainty into the total uncertainty in the potassium mass coefficient yields a negligible impact on the total uncertainty in this measurement. The actual mass uncertainty is most likely on the order of <1 g; however, as just explained, the impact of the larger perturbation is negligible.

2.5 Evaluation of Reactivity Coefficient Data

Reactivity Coefficient measurements were not made.

2.6 Evaluation of Kinetics Measurements Data

Kinetics measurements were not made.

2.7 Evaluation of Reaction-Rate Distributions

Reaction-rate distribution measurements were not made.

2.8 Evaluation of Power Distribution Data

Power distribution measurements were not made.

2.9 Evaluation of Isotopic Measurements

Isotopic measurements were not made.

2.10 Evaluation of Other Miscellaneous Types of Measurements

Other miscellaneous types of measurements were not made.

3.0 BENCHMARK SPECIFICATIONS

3.1 Benchmark-Model Specifications for Critical and / or Subcritical Measurements

Two benchmark models were developed to represent each of the HEU metal annuli experiments; Case 1 has empty stainless steel cans placed in the center of the HEU annuli and Case 2 uses a nearly identical pair of cans but filled with potassium. The detailed benchmark model represents, as much as possible, the experiment described in Reference 1. Some approximation is necessary to estimate the height of gaps between the individual components of the experiment and reproduce the measured stack heights; however, any uncertainty in the gap height would be negligible compared with the total experimental uncertainty (see Sections 2.1.2.1, 2.1.2.6, and 2.1.4). The simple benchmark model reduces the experiments to a basic cylindrical structure comprised of three single materials: HEU annulus, stainless steel cans, and potassium (Case 2 only).

The experimental assembly, including the stainless steel diaphragm and the room itself, are not included in the benchmark models.

These two near-critical configurations have been evaluated as acceptable benchmark experiments. Furthermore, they can be utilized to evaluate the worth of the added potassium (see Section 3.4) and the associated mass coefficient (see Section 3.5).

3.1.1 Description of the Benchmark Model Simplifications

3.1.1.1 Detailed Model

The detailed benchmark model is comprised of stacks of uranium metal annuli. There are three sets of rings in both Cases 1 and 2. The center core of the annuli contains two stainless steel cans; these cans are empty in Case 1 and filled with potassium in Case 2. Small gaps exist between adjacent components of the experiment and each component has unique dimensions and composition that reproduce, as closely as possible, the actual component dimensions and compositions (see Figures 3.1-1 and 3.1-2).

Very small gaps exist between the components of the experiment, as the top and bottom surfaces of the discs are not perfectly smooth. However, it is not easy to exactly model the imperfect surfaces of the experiment components. The measured stack height and individual heights of each part are preserved in the detailed benchmark model. To preserve the stack height, small gaps must be placed between the discs. These gap heights are exaggerated in Figure 3.1-2 so that the gap heights can be easily noticed. The effect of eliminating the gaps between parts is quite small compared to effects such as adjusting the overall stacked height dimension of the experiment, which is then, much less than the uncertainty in the measurements of system reactivity and corrections for removal of experiment support structure (see section 2.1.4). Further discussion of the gaps between discs is provided in Section 2.1.2.6

3.1.1.2 Simple Model

The simple benchmark model consists of a single HEU metal annulus with an inner diameter of 17.78 cm (7 in.) and an outer diameter of 33.02 cm (13 in.) for both Cases 1 and 2 (see Figure 3.1-3). The core of the annulus is two stainless steel 304 cans with an outer diameter of 17.78 cm (7 in.); the height of the lower can is 7.62 cm (3 in.) and the height of the upper can is 6.35 cm (2.5 in.). The height of the HEU annulus is 14.181666 cm (2.583333 in.), which is the average height of the three stacks of HEU annuli in the detailed model. The steel cans in Case 1 is empty; the cans in Case 2 is filled with potassium. There are no gaps present between the uranium, steel, or potassium components. The total mass for the potassium, steel, and uranium is conserved in the simple model. The simple model dimensions correspond to the nominal experimental dimensions.

3.1.1.3 Evaluation of Benchmark Model Biases

A discussion of the individual benchmark model biases is provided below with a summary of the evaluated results in Table 3.1-1.

Room Return

The properties and dimensions of the room in which the experiment was performed were not provided in Reference 1, but they are well known and available from other ORCEF East Cell experiment reports. The dimensions were obtained from a similar benchmark report: HEU-MET-FAST-076 (in the ICSBEP Handbook). Room return effects were estimated using the room and experiment placement dimensions provided in Section 1.2 and assuming that the other concrete wall, floor, and ceiling thicknesses are 2 feet. The concrete was modeled as Oak Ridge Concrete with a density of 2.3 g/cm^3 and the room containing air with a density of 1.2 kg/m^3. The use of either Oak Ridge Concrete or Magnuson Concrete was previously demonstrated to provide similar results as shown in HEU-MET-FAST-076. Both concretes were prepared using crushed limestone instead of sand due to the unavailability of sand at the time.[a]

Support Structure Removal

The benchmark models do not include the support structure of the experimental assembly or the stainless steel diaphragm. Removal of the support structure materials was included in the experimental assessment of the reported eigenvalue and the uncertainty in their worth is discussed in Section 2.1.1.3.

The diaphragm bolts were not included in the experimental analysis of the support structure worth.[b] A calculation was performed previously in HEU-MET-FAST-069 of the ICSBEP Handbook to evaluate a "ring" of steel material where the bolts would have been located in the actual experiment. The calculated bias in that benchmark evaluation was negligible and is also assumed to have a negligible effect upon this set of experiments.

Temperature

The temperature reactivity coefficient is reported by the experimenter to be approximately -0.3¢/ºC. The parts were measured at ~294 K and the original experiments were performed at ~295 K. The uncertainty in either of these two temperatures is unknown. The benchmark models use dimensions as measured at room temperature conditions, ~294 K, and ENDF/B-VII.1 cross sections evaluated at 300 K. No bias for temperature effects was included in the benchmark model, however an uncertainty in the temperature of the experiments and evaluation are provided in Section 2.1.1.1.

Impurities in Stainless Steel Cans and Potassium

As discussed in Sections 2.1.3.2 and 2.1.3.3, impurities were not reported for these components. Analyses to assess the impact of adding impurities to the stainless steel and potassium were inconclusive as the results were negligible ($\Delta k_{eff} < 0.00003$) and within the statistical uncertainty in the Monte Carlo calculations. No additional bias is included for not including impurities in the steel and potassium (i.e. both were assumed to be 100 % pure), but a small bias uncertainty of ±0.00003 Δk_{eff} is included for each case.

[a] Personal communication with John T. Mihalczo, February 2010.
[b] Personal communication with John T. Mihalczo, June 2010.

Model Simplifications

Additional simplifications were performed to facilitate the application of a simple model in place of the detailed model. Simplifications include the removal of impurities from the uranium annuli, development of a uranium annulus with uniform material properties, development of two stainless steel cans with similar dimensions and the same material density, and modifying the potassium density to be identical within both cans. The adjusted dimensions are provided in the simple benchmark model described in Section 3.1.2.2 (see Figure 3.1-3 and Table 3.1-4). There are no gaps between the individual annuli in a stack, as they are modeled as a single homogenous annulus. These adjustments in dimensions were performed to match the approximate measurement descriptions for the experiment. The density of the individual stacks was computed using the total measured mass (161.383 kg) divided by the total adjusted volume (~8623.15 cm^3). The mass densities for the simple model is provided in Tables 3.1-8 through 3.1-10. These densities are less than those for the individual parts due to the absorption of gaps into the total volume. The weight fraction of isotopes in the uranium annulus was obtained by taking the weight-averaged isotopic contents of the individual annuli. The mass of the uranium annulus was also reduced by replacing the impurities with void (uranium weight fraction of 0.9995088). Results for these simplifications are shown in Table 3.1-1. MCNP6 and ENDF/B-VII.1 was utilized to estimate the biases, with a statistical uncertainty in Δk_{eff} of 0.00003.

Total Bias Adjustment

The total bias for the detailed benchmark model includes room return effects, experimentally measured corrections for the removal of support structure, and possible impurities in the steel cans and potassium.

The total bias for the simple benchmark model includes those for the detailed benchmark model as well as the model simplifications discussed earlier in this section for homogenization, impurity removal, and implementing standard material densities.

A list of the individually evaluated biases, with their respective bias uncertainties, and the total bias for both detailed and simple benchmark models are provided in Table 3.1-1.

Table 3.1-1. Calculated Biases (Δk_{eff}) for Benchmark Model Simplifications.

Bias/*Correction*	**Case 1 (Empty Cans)**	**Case 2 (Potassium)**
1. Room Return Effects	-0.00093 ± 0.00003	-0.00086 ± 0.00003
2. Removal of Stainless Steel Diaphragm	0.00054 --[(d)]	0.00054 --[(d)]
3. Removal of Support Structure	-0.00106 --[(d)]	-0.00106 --[(d)]
4. Temperature	--	--
5. Stainless Steel Impurities	-- ± 0.00003	-- ± 0.00003
6. Potassium Impurities	--	-- ± 0.00003
Total Bias for Detailed Model[(a)]	**-0.00145 ± 0.00004**	**-0.00138 ± 0.00005**
7. Removal of HEU Impurities	-0.00021 ± 0.00003	-0.00022 ± 0.00003
7. Removal of HEU Impurities with 8. Homogenization of HEU Annuli	-0.00027 ± 0.00003	-0.00023 ± 0.00003
9. Simplification of Steel Cans	0.00013 ± 0.00003	0.00006 ± 0.00003
7-9. Calculated Simplification Bias[(b)]	-0.00012 ± 0.00003	-0.00015 ± 0.00003
Total Bias for Simplified Model[(c)]	**-0.00157 ± 0.00005**	**-0.00153 ± 0.00006**

(a) Bias is the arithmetic sum of Items 1 through 6; bias uncertainty is the square root of the sum of the squares of each uncertainty for items 1 through 6.

(b) Bias is the difference between calculated k_{eff} of the detailed model and the simplified model (Items 7 through 9); bias uncertainty is the statistical uncertainty associated with the Monte Carlo calculations $\times \sqrt{2}$.

(c) Bias is the arithmetic sum of the total bias of the detailed model and the calculated simplification bias; bias uncertainty is the square root of the sum of the squares of the uncertainty in the bias for the detailed model and the uncertainty in the calculated simplification bias.

(d) The uncertainties in the measured corrections are already accounted for in evaluation of the total experimental uncertainty (see Section 2.1.1.3).

3.1.2 Dimensions

3.1.2.1 Detailed Model

The detailed benchmark model is shown in Figures 3.1-1 and 3.1-2 for the part dimensions and gaps between HEU parts, respectively, of both Cases 1 and 2. They are labeled with part identifiers and dimensions. Part dimensions for the HEU annuli are also summarized in Table 3.1-2. Detailed dimensions of the stainless steel cans are provided in Table 3.1-3. The bottom of the lower stainless steel can is on the same plane as the bottom of the lower stacks of HEU annuli; this produces a gap of 0.083397 cm between the top of the lower can and the bottom of the upper can.

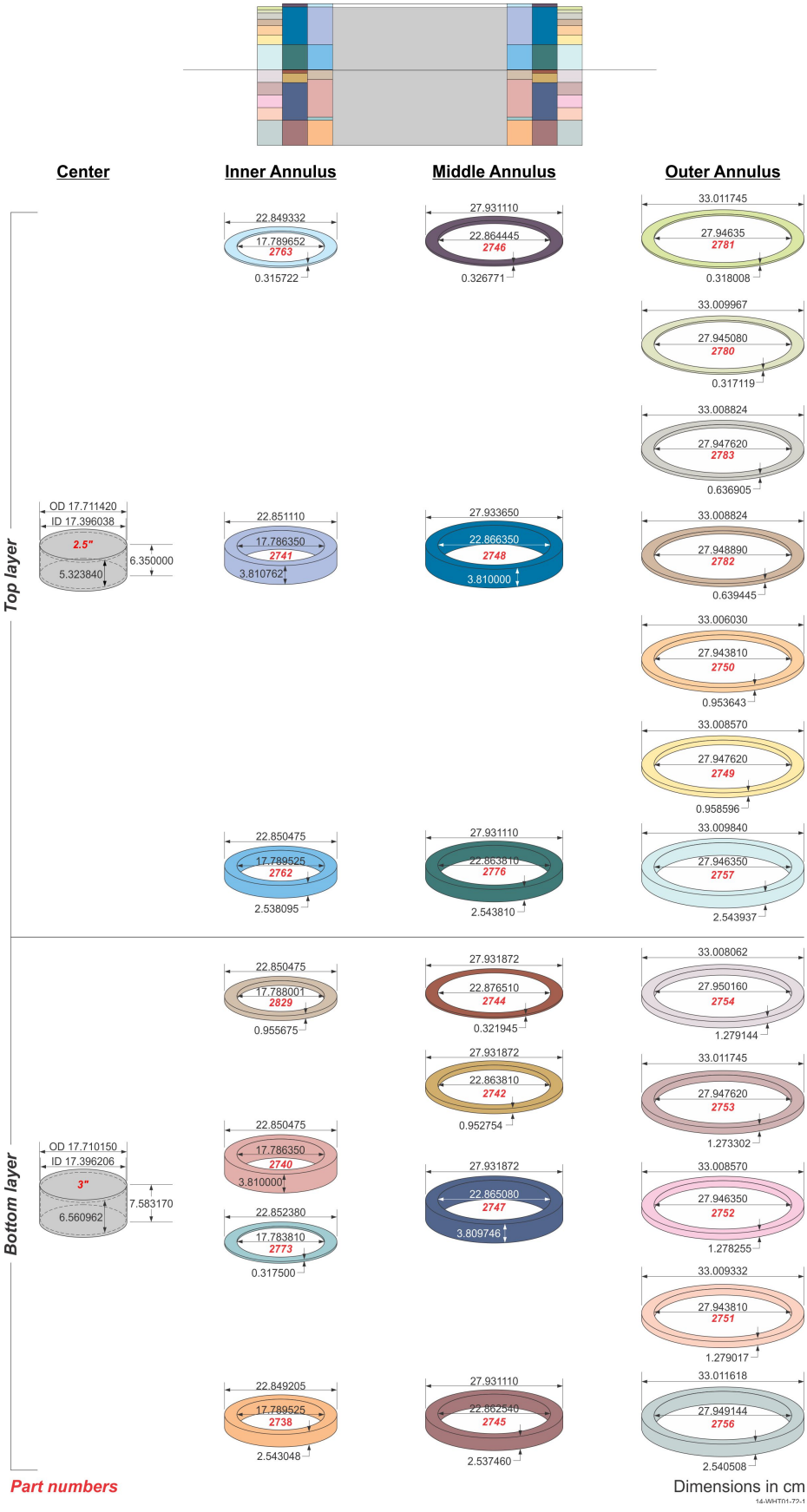

Figure 3.1-1. Detailed Benchmark Model of Cases 1 and 2.

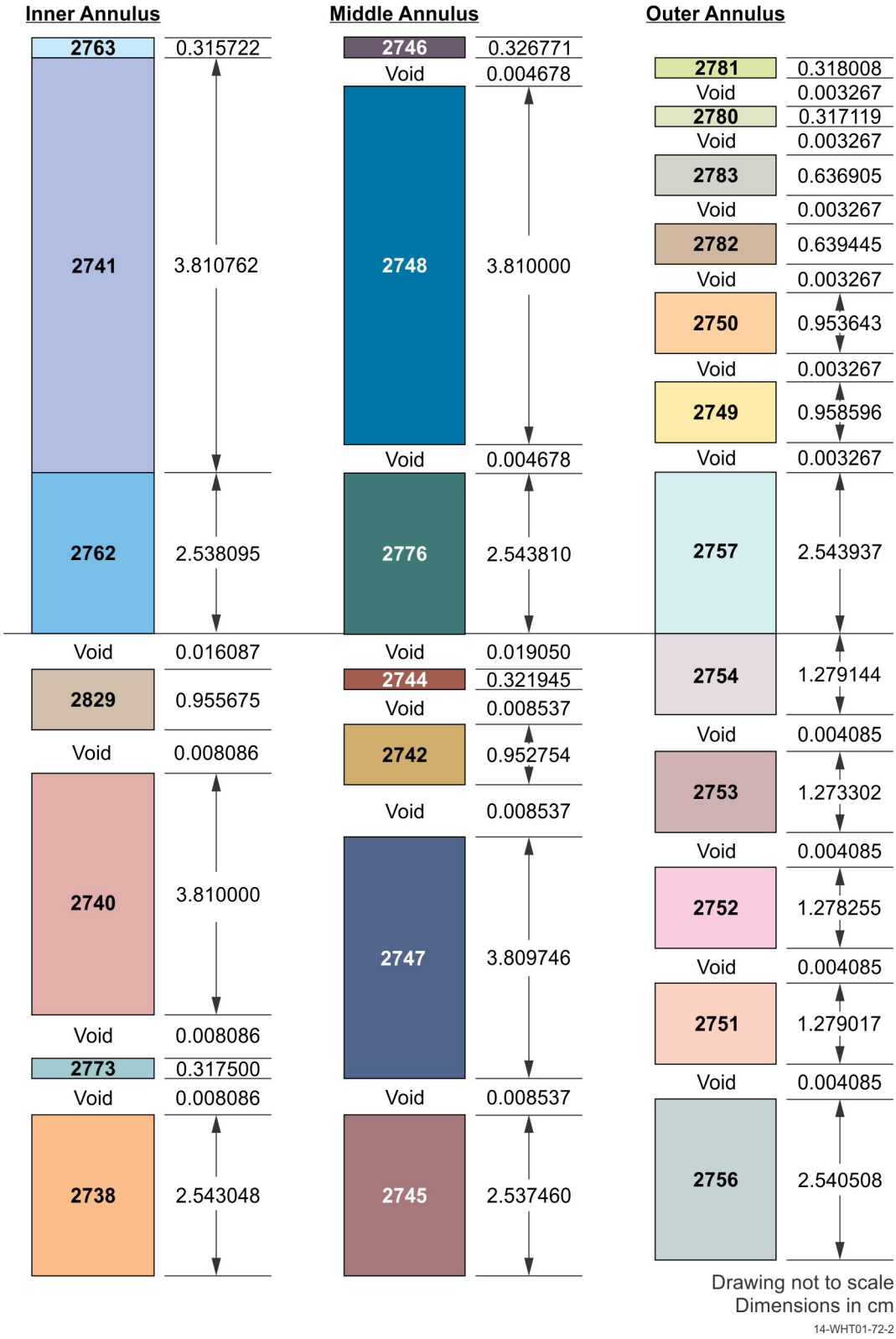

Figure 3.1-2. Gap Placement between HEU Annuli for Detailed Benchmark Model.
(Note that gap heights are quite small and visually exaggerated for the benefit of the reader.)

Table 3.1-2. Properties of Detailed Benchmark Model HEU Annuli.

Annulus (Stack)	Part Number	Mass (g)	Inner Radius (cm)	Outer Radius (cm)	Height (cm)
13-11	2781	1449	13.973175	16.505873	0.318008
(Upper)	2780	1440	13.972540	16.504984	0.317119
	2783	2888	13.973810	16.504412	0.636905
	2782	2914	13.974445	16.504412	0.639445
	2750	4336	13.971905	16.503015	0.953643
	2749	4360	13.973810	16.504285	0.958596
	2757	11575	13.973175	16.504920	2.543937
11-9	2746	1238	11.432223	13.965555	0.326771
(Upper)	2748	14462	11.433175	13.966825	3.810000
	2776	9644	11.431905	13965555	2.543810
9-7	2763	953	8.894826	11.424666	0.315722
(Upper)	2741	11568	8.893175	11.425555	3.810762
	2762	7703	8.894763	11.425238	2.538095
13-11	2754	5826	13.975080	16.504031	1.279144
(Lower)	2753	5782	13.973810	16.505873	1.273302
	2752	5811	13.973175	16.504285	1.278255
	2751	5822	13.971905	16.504666	1.279017
	2756	11567	13.974572	16.505809	2.540508
11-9	2744	1223	11.438255	13.965936	0.321945
(Lower)	2742	3617	11.431905	13.965936	0.952754
	2747	14436	11.432540	13.965936	3.809746
	2745	9634	11.431270	13.965555	2.537460
9-7	2829	2895	8.894001	11.425238	0.955675
(Lower)	2740	11568	8.893175	11.425238	3.810000
	2773	962	8.891905	11.426190	0.317500
	2738	7710	8.894763	11.424603	2.543048

Table 3.1-3. Properties of Detailed Benchmark Model Stainless Steel Cans.

Property	Upper Can	Lower Can
Height (cm)	6.35	7.58317
Outer Diameter (cm)	17.71142	17.71015
Radial Thickness (cm)	0.15769082	0.156972
End Thickness (cm)	0.51308	0.51110388
Steel Mass (g)	2358	2424
Potassium Mass (g) (Case 2 only)	1064	1334
Gap Between Cans (cm)	0.083397	

3.1.2.2 Simple Model

Figure 3.1-3 shows the simple benchmark model depiction for Cases 1 and 2. It is labeled with dimensions and material types. The simple model dimensions are chosen to correspond to the nominal experiment dimensions. A summary of the simple benchmark model dimensions is also provided in Table 3.1-4.

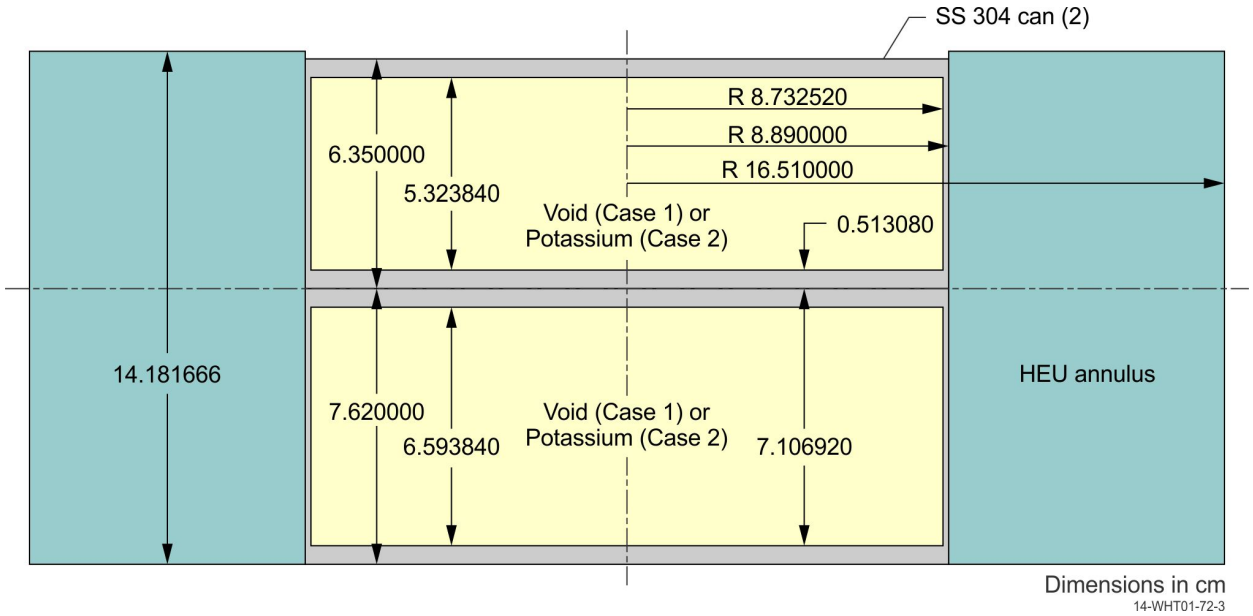

Figure 3.1-3. Simple Benchmark Model of Cases 1 and 2.

Table 3.1-4. Properties of Simple Benchmark Model Components.

Property	HEU Annulus	Upper Steel Can	Lower Steel Can
Inner Height (cm)	--	5.323840	6.593840
Outer Height (cm)	14.181666	6.350000	7.620000
Top/Bottom End Thickness (cm)	--	0.513080	
Inner Radius (cm)	8.890000	8.732520	
Outer Radius (cm)	16.51000	8.890000	
Radial Wall Thickness (cm)	--	0.157480	
Mass (g)	161383	4782 (stainless steel 304) 2398 (potassium, Case 2)	

3.1.3 Material Data

3.1.3.1 Detailed Model

Material mass densities were obtained by taking the individual mass of the uranium, steel, and potassium components divided by the individual volume they occupy in the detailed benchmark model.

The atom densities of the various uranium annuli are in Table 3.1-5, where part identifiers match the identifiers shown in Figures 3.1-1 and 3.1-2 and Table 3.1-2. The atom densities of the two stainless steel cans used in both cases and the potassium used in Case 2 are in Tables 3.1-6 and 3.1-7, respectively.

Table 3.1-5. Uranium Annuli Atom Densities (atoms/barns-cm) for the Detailed Benchmark Model.

Part Number	2781	2780	2783	2782	2750	2749
^{234}U	4.7355E-04	4.7200E-04	4.4760E-04	4.6445E-04	4.5842E-04	4.7313E-04
^{235}U	4.4839E-02	4.4663E-02	4.4655E-02	4.4898E-02	4.4743E-02	4.4799E-02
^{236}U	1.1978E-04	1.1938E-04	1.1930E-04	1.1033E-04	1.1961E-04	1.1967E-04
^{238}U	2.6509E-03	2.6706E-03	2.6687E-03	2.6684E-03	2.6947E-03	2.6486E-03
Ag	8.3915E-07	8.3640E-07	8.3580E-07	8.4017E-07	8.3800E-07	8.3841E-07
Ba	4.1196E-10	4.1061E-10	4.1032E-10	4.1246E-10	4.1140E-10	4.1160E-10
Bi	8.8794E-06	8.8503E-06	8.8439E-06	8.8902E-06	8.8672E-06	8.8715E-06
C	4.7103E-06	4.6948E-06	4.6915E-06	4.7160E-06	4.7038E-06	4.7061E-06
Ca	2.8232E-08	2.8139E-08	2.8119E-08	2.8266E-08	2.8193E-08	2.8207E-08
Cd	5.0328E-08	5.0163E-08	5.0127E-08	5.0389E-08	5.0258E-08	5.0283E-08
Co	9.5996E-07	9.5682E-07	9.5613E-07	9.6113E-07	9.5865E-07	9.5911E-07
Cr	1.5233E-06	1.5183E-06	1.5172E-06	1.5251E-06	1.5212E-06	1.5219E-06
Cu	4.4514E-06	4.4368E-06	4.4336E-06	4.4568E-06	4.4453E-06	4.4474E-06
K	2.8939E-08	2.8844E-08	2.8824E-08	2.8974E-08	2.8899E-08	2.8913E-08
Li	1.6301E-06	1.6248E-06	1.6236E-06	1.6321E-06	1.6279E-06	1.6287E-06
Mg	1.3966E-06	1.3920E-06	1.3910E-06	1.3983E-06	1.3947E-06	1.3954E-06
Mn	1.1533E-05	1.1496E-05	1.1487E-05	1.1547E-05	1.1518E-05	1.1523E-05
Mo	5.8968E-08	5.8774E-08	5.8732E-08	5.9039E-08	5.8887E-08	5.8915E-08
Na	1.3288E-05	1.3245E-05	1.3235E-05	1.3305E-05	1.3270E-05	1.3277E-05
Ni	1.9278E-05	1.9215E-05	1.9201E-05	1.9301E-05	1.9251E-05	1.9261E-05
Sb	3.5312E-06	3.5196E-06	3.5171E-06	3.5355E-06	3.5264E-06	3.5281E-06
Ti	2.3638E-07	2.3560E-07	2.3544E-07	2.3667E-07	2.3605E-07	2.3617E-07
O	1.4144E-05	1.4098E-05	1.4087E-05	1.4161E-05	1.4125E-05	1.4131E-05
N	2.4234E-05	2.4155E-05	2.4138E-05	2.4264E-05	2.4201E-05	2.4213E-05
Total	4.8194E-02	4.8035E-02	4.8001E-02	4.8252E-02	4.8127E-02	4.8151E-02
Mass Density (g/cm^3)	18.7887	18.7271	18.7137	18.8115	18.7629	18.7720

Table 3.1-5 (continued). Uranium Annuli Atom Densities (atoms/barns-cm) for the Detailed Benchmark Model.

Part Number	2757	2746	2748	2776	2763	2741
^{234}U	4.6342E-04	4.8204E-04	4.8285E-04	4.6302E-04	4.6147E-04	4.6364E-04
^{235}U	4.4798E-02	4.4681E-02	4.4757E-02	4.4740E-02	4.4601E-02	4.4810E-02
^{236}U	1.1008E-04	1.0515E-04	1.0533E-04	1.0999E-04	1.1915E-04	1.1972E-04
^{238}U	2.6625E-03	2.6966E-03	2.7012E-03	2.6792E-03	2.6513E-03	2.6638E-03
Ag	8.3830E-07	8.3711E-07	8.3853E-07	8.3759E-07	8.3479E-07	8.3872E-07
Ba	4.1155E-10	4.1096E-10	4.1166E-10	4.1119E-10	4.0982E-10	4.1175E-10
Bi	8.8704E-06	8.8578E-06	8.8728E-06	8.8628E-06	8.8332E-06	8.8748E-06
C	4.7055E-06	4.6988E-06	4.7068E-06	4.7015E-06	4.6858E-06	4.7078E-06
Ca	2.8203E-08	2.8163E-08	2.8211E-08	2.8179E-08	2.8085E-08	2.8217E-08
Cd	5.0277E-08	5.0205E-08	5.0290E-08	5.0234E-08	5.0066E-08	5.0301E-08
Co	9.5899E-07	9.5763E-07	9.5925E-07	9.5817E-07	9.5497E-07	9.5946E-07
Cr	1.5217E-06	1.5195E-06	1.5221E-06	1.5204E-06	1.5153E-06	1.5225E-06
Cu	4.4469E-06	4.4406E-06	4.4481E-06	4.4431E-06	4.4283E-06	4.4491E-06
K	2.8910E-08	2.8869E-08	2.8918E-08	2.8885E-08	2.8789E-08	2.8924E-08
Li	1.6285E-06	1.6262E-06	1.6289E-06	1.6271E-06	1.6217E-06	1.6293E-06
Mg	1.3952E-06	1.3932E-06	1.3956E-06	1.3940E-06	1.3893E-06	1.3959E-06
Mn	1.1522E-05	1.1505E-05	1.1525E-05	1.1512E-05	1.1473E-05	1.1527E-05
Mo	5.8908E-08	5.8824E-08	5.8924E-08	5.8858E-08	5.8661E-08	5.8937E-08
Na	1.3275E-05	1.3256E-05	1.3279E-05	1.3264E-05	1.3219E-05	1.3282E-05
Ni	1.9258E-05	1.9231E-05	1.9263E-05	1.9242E-05	1.9177E-05	1.9268E-05
Sb	3.5276E-06	3.5226E-06	3.5286E-06	3.5246E-06	3.5128E-06	3.5294E-06
Ti	2.3614E-07	2.3580E-07	2.3620E-07	2.3594E-07	2.3515E-07	2.3626E-07
O	1.4130E-05	1.4110E-05	1.4133E-05	1.4118E-05	1.4070E-05	1.4137E-05
N	2.4210E-05	2.4175E-05	2.4216E-05	2.4189E-05	2.4108E-05	2.4222E-05
Total	4.8145E-02	4.8076E-02	4.8157E-02	4.8103E-02	4.7943E-02	4.8168E-02
Mass Density (g/cm^3)	18.7697	18.7430	18.7747	18.7536	18.6910	18.7789

Table 3.1-5 (continued). Uranium Annuli Atom Densities (atoms/barns-cm) for the Detailed Benchmark Model.

Part Number	2762	2754	2753	2752	2751	2756
^{234}U	4.6870E-04	4.6438E-04	4.5759E-04	4.7278E-04	4.7310E-04	4.4929E-04
^{235}U	4.4808E-02	4.4843E-02	4.4662E-02	4.4737E-02	4.4767E-02	4.4823E-02
^{236}U	1.2935E-04	1.3429E-04	1.1940E-04	1.1480E-04	1.1488E-04	1.1975E-04
^{238}U	2.6745E-03	2.6918E-03	2.6898E-03	2.6798E-03	2.6816E-03	2.6788E-03
Ag	8.3911E-07	8.4005E-07	8.3648E-07	8.3780E-07	8.3836E-07	8.3896E-07
Ba	4.1194E-10	4.1240E-10	4.1065E-10	4.1130E-10	4.1157E-10	4.1187E-10
Bi	8.8790E-06	8.8888E-06	8.8511E-06	8.8650E-06	8.8710E-06	8.8774E-06
C	4.7101E-06	4.7153E-06	4.6953E-06	4.7027E-06	4.7058E-06	4.7092E-06
Ca	2.8230E-08	2.8262E-08	2.8142E-08	2.8186E-08	2.8205E-08	2.8225E-08
Cd	5.0325E-08	5.0381E-08	5.0167E-08	5.0246E-08	5.0280E-08	5.0316E-08
Co	9.5992E-07	9.6099E-07	9.5691E-07	9.5841E-07	9.5905E-07	9.5974E-07
Cr	1.5232E-06	1.5249E-06	1.5184E-06	1.5208E-06	1.5218E-06	1.5229E-06
Cu	4.4512E-06	4.4561E-06	4.4372E-06	4.4442E-06	4.4472E-06	4.4504E-06
K	2.8938E-08	2.8970E-08	2.8847E-08	2.8892E-08	2.8912E-08	2.8933E-08
Li	1.6301E-06	1.6319E-06	1.6249E-06	1.6275E-06	1.6286E-06	1.6298E-06
Mg	1.3965E-06	1.3981E-06	1.3921E-06	1.3943E-06	1.3953E-06	1.3963E-06
Mn	1.1533E-05	1.1546E-05	1.1497E-05	1.1515E-05	1.1523E-05	1.1531E-05
Mo	5.8965E-08	5.9031E-08	5.8780E-08	5.8872E-08	5.8912E-08	5.8954E-08
Na	1.3288E-05	1.3303E-05	1.3246E-05	1.3267E-05	1.3276E-05	1.3285E-05
Ni	1.9277E-05	1.9298E-05	1.9216E-05	1.9247E-05	1.9259E-05	1.9273E-05
Sb	3.5310E-06	3.5350E-06	3.5200E-06	3.5255E-06	3.5279E-06	3.5304E-06
Ti	2.3637E-07	2.3663E-07	2.3563E-07	2.3600E-07	2.3615E-07	2.3632E-07
O	1.4143E-05	1.4159E-05	1.4099E-05	1.4121E-05	1.4131E-05	1.4141E-05
N	2.4233E-05	2.4260E-05	2.4157E-05	2.4195E-05	2.4211E-05	2.4229E-05
Total	4.8191E-02	4.8244E-02	4.8040E-02	4.8115E-02	4.8148E-02	4.8182E-02
Mass Density (g/cm^3)	18.7878	18.8087	18.7289	18.7583	18.7709	18.7844

Table 3.1-5 (continued). Uranium Annuli Atom Densities (atoms/barns-cm) for the Detailed Benchmark Model.

Part Number	2744	2742	2747	2745	2829	2740
^{234}U	4.7461E-04	4.7324E-04	4.7245E-04	4.6359E-04	4.7734E-04	4.6863E-04
^{235}U	4.4915E-02	4.4785E-02	4.4720E-02	4.4815E-02	4.4697E-02	4.4821E-02
^{236}U	1.1044E-04	1.1012E-04	9.0820E-05	1.0534E-04	1.1474E-04	1.1497E-04
^{238}U	2.6902E-03	2.6824E-03	2.6874E-03	2.6682E-03	2.6878E-03	2.6694E-03
Ag	8.4103E-07	8.3860E-07	8.3721E-07	8.3862E-07	8.3732E-07	8.3900E-07
Ba	4.1288E-10	4.1169E-10	4.1101E-10	4.1170E-10	4.1106E-10	4.1189E-10
Bi	8.8992E-06	8.8735E-06	8.8588E-06	8.8738E-06	8.8600E-06	8.8778E-06
C	4.7208E-06	4.7072E-06	4.6994E-06	4.7073E-06	4.7000E-06	4.7094E-06
Ca	2.8295E-08	2.8213E-08	2.8166E-08	2.8214E-08	2.8170E-08	2.8227E-08
Cd	5.0440E-08	5.0294E-08	5.0211E-08	5.0296E-08	5.0218E-08	5.0318E-08
Co	9.6211E-07	9.5933E-07	9.5774E-07	9.5936E-07	9.5787E-07	9.5979E-07
Cr	1.5267E-06	1.5222E-06	1.5197E-06	1.5223E-06	1.5199E-06	1.5230E-06
Cu	4.4613E-06	4.4485E-06	4.4411E-06	4.4486E-06	4.4417E-06	4.4506E-06
K	2.9004E-08	2.8920E-08	2.8872E-08	2.8921E-08	2.8876E-08	2.8934E-08
Li	1.6338E-06	1.6291E-06	1.6264E-06	1.6291E-06	1.6266E-06	1.6298E-06
Mg	1.3997E-06	1.3957E-06	1.3934E-06	1.3957E-06	1.3935E-06	1.3963E-06
Mn	1.1559E-05	1.1526E-05	1.1507E-05	1.1526E-05	1.1508E-05	1.1531E-05
Mo	5.9100E-08	5.8929E-08	5.8831E-08	5.8930E-08	5.8839E-08	5.8957E-08
Na	1.3318E-05	1.3280E-05	1.3258E-05	1.3280E-05	1.3259E-05	1.3286E-05
Ni	1.9321E-05	1.9265E-05	1.9233E-05	1.9265E-05	1.9236E-05	1.9274E-05
Sb	3.5391E-06	3.5289E-06	3.5230E-06	3.5290E-06	3.5235E-06	3.5306E-06
Ti	2.3691E-07	2.3622E-07	2.3583E-07	2.3623E-07	2.3586E-07	2.3634E-07
O	1.4176E-05	1.4135E-05	1.4111E-05	1.4135E-05	1.4113E-05	1.4141E-05
N	2.4288E-05	2.4218E-05	2.4178E-05	2.4219E-05	2.4181E-05	2.4230E-05
Total	4.8301E-02	4.8161E-02	4.8082E-02	4.8163E-02	4.8088E-02	4.8185E-02
Mass Density (g/cm^3)	18.8307	18.7763	18.7452	18.7768	18.7477	18.7853

Table 3.1-5 (continued). Uranium Annuli Atom Densities (atoms/barns-cm) for the Detailed Benchmark Model.

Part Number	2773	2738
^{234}U	4.6726E-04	4.7317E-04
^{235}U	4.4689E-02	4.4783E-02
^{236}U	1.1463E-04	1.1489E-04
^{238}U	2.6616E-03	2.6725E-03
Ag	8.3654E-07	8.3848E-07
Ba	4.1068E-10	4.1163E-10
Bi	8.8517E-06	8.8723E-06
C	4.6956E-06	4.7065E-06
Ca	2.8144E-08	2.8209E-08
Cd	5.0171E-08	5.0287E-08
Co	9.5697E-07	9.5919E-07
Cr	1.5185E-06	1.5220E-06
Cu	4.4375E-06	4.4478E-06
K	2.8849E-08	2.8916E-08
Li	1.6251E-06	1.6288E-06
Mg	1.3922E-06	1.3955E-06
Mn	1.1498E-05	1.1524E-05
Mo	5.8784E-08	5.8920E-08
Na	1.3247E-05	1.3278E-05
Ni	1.9218E-05	1.9262E-05
Sb	3.5202E-06	3.5284E-06
Ti	2.3564E-07	2.3619E-07
O	1.4100E-05	1.4133E-05
N	2.4159E-05	2.4215E-05
Total	4.8043E-02	4.8155E-02
Mass Density (g/cm^3)	18.7302	18.7736

Table 3.1-6. Stainless Steel Type 304 Can Atom Densities (atoms/barns-cm) for the Detailed Benchmark Model.

Element	**Content (wt.%)**	Upper Can	Lower Can
C	0.05	1.9763E-04	1.9692E-04
Cr	19	1.7347E-02	1.7285E-02
Ni	10	8.0884E-03	8.0591E-03
Mn	1	8.6413E-04	8.6100E-04
Si	0.375	6.3387E-04	6.3158E-04
P	0.0225	3.4486E-05	3.4361E-05
S	0.015	2.2208E-05	2.2128E-05
N	0.05	1.6947E-04	1.6885E-04
Fe	69.4875	5.9071E-02	5.8857E-02
Total	100	8.6428E-02	8.6116E-02
Mass Density (g/cm^3)		7.8832	7.8547

Table 3.1-7. Potassium Atom Densities (atoms/barns-cm) for the Detailed Benchmark Model of Case 2.

Element	**Content (wt.%)**	Upper Can	Lower Can
K	100	1.2951E-02	1.3176E-02
Mass Density (g/cm^3)		0.84086	0.85544

3.1.3.2 Simple Model

Material mass densities were obtained by taking the total mass of the uranium, steel, and potassium components divided by the total volume they occupy in the simple benchmark model.

The atom densities of the uranium annulus are in Table 3.1-8. The density of the uranium annulus in the simple case is obtained by dividing the total uranium mass by the volume of the modeled annulus; this density of 18.7151 g/cm^3 is then multiplied by the factor 0.9995088 to account for the removal of impurities (Table 2.1-16). The isotopic content of the simple cases is obtained by taking the weight-averaged isotopic content of the individual HEU parts.

The atom densities of the stainless steel cans used in both cases, and the potassium used in Case 2, are in Tables 3.1-9 and 3.1-10, respectively.

Table 3.1-8. Uranium Annulus Composition.[(a)]

Isotope	Content (wt.%)	Atom Density (atoms/barns-cm)
^{234}U	0.968054	4.6572E-04
^{235}U	93.153679	4.4624E-02
^{236}U	0.236216	1.1267E-04
^{238}U	5.642051	2.6686E-03
Total	100	4.7871E-02
Mass Density (g/cm^3)		18.7059

(a) Impurities were replaced with void by multiplying the mass density of 18.7151 g/cm^3 by the factor 0.9995088.

Table 3.1-9. Stainless Steel 304 Can Composition.

Element	Content (wt.%)	Atom Density (atoms/barns-cm)
C	0.05	1.9542E-04
Cr	19	1.7153E-02
Ni	10	7.9979E-03
Mn	1	8.5446E-04
Si	0.375	6.2678E-04
P	0.0225	3.4100E-05
S	0.015	2.1960E-05
N	0.05	1.6757E-04
Fe	69.4875	5.8410E-02
Total	100	8.5461E-02
Mass Density (g/cm^3)		7.7950

Table 3.1-10. Potassium Composition.
(Case 2 Only)

Element	Content (wt.%)	Atom Density (atoms/barns-cm)
K	100	1.2937E-02
Mass Density (g/cm^3)		0.8399

3.1.4 Temperature Data

The temperature of all benchmark models is at room temperature, 300 K.

3.1.5 Experimental and Benchmark-Model k_{eff} and / or Subcritical Parameters

The experimental k_{eff} for Cases 1 and 2 was approximately at unity, maintained near delayed critical with the 1σ uncertainty summarized in Section 2.1.4. Measured corrections and simplification biases, with their associated bias uncertainties, are discussed in Section 3.1.1 and applied to the benchmark models. The benchmark k_{eff} is provided in Tables 3.1-11 and 3.1-12 for detailed and simple benchmark model, respectively, for both cases. The uncertainty in the benchmark k_{eff} value is obtained by summing under quadrature the total experimental uncertainty (Tables 2.1-27 and 2.1-28) and the total bias uncertainty (Table 3.1-1).

3.1.5.1 Detailed Model

Table 3.1-11. Experimental and Benchmark Eigenvalues, Biases, and Uncertainties for Detailed Benchmark Model.

Case	Steel Can Content	Experimental			Bias			Benchmark Experiment		
		k_{eff}	±	σ	Δk	±	σ	k_{eff}	±	σ
1	Void	0.99957	±	0.00037	-0.00145	±	0.00004	0.9981	±	0.0004
2	Potassium	1.00025	±	0.00037	-0.00138	±	0.00005	0.9989	±	0.0004

3.1.5.2 Simple Model

Table 3.1-12. Experimental and Benchmark Eigenvalues, Biases, and Uncertainties for Simple Benchmark Model.

Case	Steel Can Content	Experimental			Bias			Benchmark Experiment		
		k_{eff}	±	σ	Δk	±	σ	k_{eff}	±	σ
1	Void	0.99957	±	0.00037	-0.00157	±	0.00005	0.9980	±	0.0004
2	Potassium	1.00025	±	0.00037	-0.00153	±	0.00006	0.9987	±	0.0004

3.2 Benchmark-Model Specifications for Buckling and Extrapolation-Length Measurements

Buckling and extrapolation length measurements were not made.

3.3 Benchmark-Model Specifications for Spectral Characteristics Measurements

Spectral characteristics measurements were not made.

3.4 Benchmark-Model Specifications for Reactivity Effects Measurements

The two near-critical cases provided in Section 3.1 can be utilized to evaluate the effective worth of potassium, which is the single difference between the two configurations. This reactivity effects measurement has been evaluated as an acceptable benchmark measurement. Please note that this benchmark experiment value is derived from the two near-critical benchmark experiment configurations.

3.4.1 Description of the Benchmark Model Simplifications

Benchmark model simplifications are identical to those discussed in Section 3.1.1.

Model simplifications had similar impacts on each of the critical cases described in Section 3.1; however, the slight variances between the modifications to each assembly result in small biases attributed to the worth calculation of the potassium using either the detailed or simple models, with an increased bias uncertainty. A bias of +0.00007 ± 0.00003 (+1.1 ± 0.4 ¢) is applied to the detailed benchmark model and +0.00004 ± 0.00005 (+0.6 ± 0.7 ¢) to the simple benchmark model (Note: final bias values are rounded; however, unrounded values were carried through calculations to obtain the final values reported in cents). The bias uncertainty accounts for solely the neglect of potassium impurities in both the detailed and simple models and the simplification of the potassium geometry (within the stainless steel can) for the simple model. The uncertainty contributions from other bias sources are considered to be correlated and negligible.

To compute the detailed and simple biases for the benchmark models, the detailed and simple benchmark model eigenvalues in Section 3.1 (Tables 3.1-11 and 3.1-12, respectively) were input into the equation presented below in Section 3.4.5 to calculate a potassium worth. The bias is the difference between the computed detailed and simple worth values using the benchmark eigenvalues and the measured experiment worth of 0.00068 Δk.

3.4.2 Dimensions

The dimensions of the benchmark models for determination of the worth of the addition of 2398 g of potassium are identical to those of the critical cases described in Section 3.1.2. As both critical cases are identical except for the presence of potassium within the stainless steel cans of Case 2, the difference in the absolute reactivity between Cases 1 and 2 equate to the worth of potassium added to the system.

3.4.3 Material Data

The materials of the benchmark models for determination of the worth of the addition of 2398 g of potassium are identical to those of the cases described in Section 3.1.3.

3.4.4 Temperature Data

The temperature of all benchmark models is at room temperature, 300 K.

3.4.5 Experimental and Benchmark-Model Reactivity Effects Measurements

The potassium worth was experimentally determined as the difference between two nearly identical near-critical cases. Measured corrections and simplification biases, with their associated bias uncertainties, are discussed in Section 3.1.1 as applied to the criticality benchmark models, their estimated impact upon use of these models to assess the potassium worth is provided in Section 3.4-1. The benchmark worth is provided in Tables 3.4-1 and 3.4-2 for detailed and simple benchmark models, respectively. The uncertainty in the benchmark value is obtained by summing under quadrature the total experimental uncertainty (Section 2.4) and the total bias uncertainty (Section 3.4-1). The delayed neutron fraction, β_{eff},

is 0.0066 for conversion of reactivity, ρ, to reactivity in cents, ρ(¢). Reactivity is calculated using the following equation with k_1 and k_2 representing the eigenvalues for critical Cases 1 and 2, respectively:

$$\rho = \frac{k_1 - k_2}{k_1 k_2}.$$

3.4.5.1 Detailed Model

Table 3.4-1. Experimental and Benchmark Potassium Worth, Bias, and Uncertainties for Detailed Benchmark Model.

Case	Experimental			Bias			Benchmark Experiment		
	ρ(Δk/k)	**±**	**σ**	**Δρ(Δk/k)**	**±**	**σ**	**ρ(Δk/k)**	**±**	**σ**
1	0.00068	±	0.00006	0.00007	±	0.00003	0.00075	±	0.00007
	ρ(¢)	**±**	**σ**	**Δρ(¢)**	**±**	**σ**	**ρ(¢)**	**±**	**σ**
	10.3	±	1.1	1.1	±	0.4	11.4	±	1.2

3.4.5.2 Simple Model

Table 3.4-2. Experimental and Benchmark Potassium Worth, Bias, and Uncertainties for Simple Benchmark Model.

Case	Experimental			Bias			Benchmark Experiment		
	ρ(Δk/k)	**±**	**σ**	**Δρ(Δk/k)**	**±**	**σ**	**ρ(Δk/k)**	**±**	**σ**
1	0.00068	±	0.00006	0.00004	±	0.00005	0.00072	±	0.00008
	ρ(¢)	**±**	**σ**	**Δρ(¢)**	**±**	**σ**	**ρ(¢)**	**±**	**σ**
	10.3	±	1.1	0.6	±	0.7	11.0	±	1.3

3.4.5.3 Potassium Mass Coefficient

A potassium mass coefficient can be obtained as the difference between two nearly identical near-critical configurations divided by the total mass of potassium added to the system. The benchmark mass coefficient is provided in Tables 3.4-3 and 3.4-4 for detailed and simple benchmark models, respectively. The delayed neutron fraction, β_{eff}, is 0.0066 for conversion of reactivity, ρ, to reactivity in cents, ρ(¢). The mass coefficient is calculated using the following equation with k_1 and k_2 representing the eigenvalues for critical Case 1 and 2, respectively, and m representing the total mass of potassium (2398 g):

$$\rho = \frac{k_1 - k_2}{k_1 k_2} \times \frac{1}{m}.$$

Table 3.4-3. Experimental and Benchmark Potassium Mass Coefficient, Bias, and Uncertainties for Detailed Benchmark Model.

Case	Mass	Experimental			Bias			Benchmark Experiment		
	(g)	ρ_m(¢/g)	±	σ	$\Delta\rho_m$(¢/g)	±	σ	ρ_m(¢/g)	±	σ
1	2398	0.0043	±	0.0005	0.0005	±	0.0002	0.0048	±	0.0005

Table 3.4-4. Experimental and Benchmark Potassium Mass Coefficient, Bias, and Uncertainties for Simple Benchmark Model.

Case	Mass	Experimental			Bias			Benchmark Experiment		
	(g)	ρ_m(¢/g)	±	σ	$\Delta\rho_m$(¢/g)	±	σ	ρ_m(¢/g)	±	σ
1	2398	0.0043	±	0.0005	0.0003	±	0.0003	0.0046	±	0.0006

3.5 Benchmark-Model Specifications for Reactivity Coefficient Measurements

Reactivity coefficient measurements were not made.

3.6 Benchmark-Model Specifications for Kinetics Measurements

Kinetics measurements were not made.

3.7 Benchmark-Model Specifications for Reaction-Rate Distribution Measurements

Reaction-rate distribution measurements were not made.

3.8 Benchmark-Model Specifications for Power Distribution Measurements

Power distribution measurements were not made.

3.9 Benchmark-Model Specifications for Isotopic Measurements

Isotopic measurements were not made.

3.10 Benchmark-Model Specifications for Other Miscellaneous Types of Measurements

Other miscellaneous types of measurements were not made.

4.0 RESULTS OF SAMPLE CALCULATIONS

Results were calculated using MCNP6.1 and ENDF/B-VII.1, ENDF/B-VII.0, JEFF-3.1, and JENDL-3.3 neutron cross section libraries with the input decks and specifications provided in Appendix A. A comparison of the neutron spectral data between the detailed and simple models is provided in Appendix B. The cross section data for ^{16}O is used for ^{18}O in the input decks. Calculations were performed with 1,050 generations with 1,000,000 neutrons per generation. The k_{eff} estimates did not include the first 50 generations and are the result of 1,000,000,000 neutron histories. Isotopic abundances were taken from the 17th edition of the Chart of the Nuclides.[a]

As the calculated results for the potassium worth appear abnormal, additional investigation into cross section uncertainties and sensitivities were investigated. These are presented in Appendices C and D, respectively. Comparison of the available uncertainties in cross section data and sensitivities indicate that refinement of the cross section data could improve the quality of the calculated results.

4.1 Results of Calculations of the Critical or Subcritical Configurations

4.1.1 Detailed Benchmark Model

The calculated results for the detailed benchmark model are reported in Tables 4.1-1 and 4.1-2 for Cases 1 and 2, respectively. There is variability in the calculated results for the different libraries with most libraries calculating below the benchmark eigenvalue but all results within 1 %. The number of sigmas between the benchmark eigenvalue and the calculated eigenvalues is between approximately 5 and 15σ for Case 1, and between approximately 3 and 17 σ for Case 2, due to the small uncertainty in the benchmark experiment itself.

Table 4.1-1. Comparison of Detailed Benchmark and Calculated Eigenvalues (Case 1).

Analysis Code	Neutron Cross Section Library	Calculated k_{eff} ± σ	Benchmark Experiment k_{eff} ± σ	$\frac{C-E}{E}$ %
MCNP6	ENDF/B-VII.1	0.99554 ± 0.00002	0.9981 ± 0.0004	-0.26 ± 0.04
	ENDF/B-VII.0	0.99572 ± 0.00002		-0.24 ± 0.04
	JEFF-3.1	0.99243 ± 0.00002		-0.57 ± 0.04
	JENDL-3.3	0.99999 ± 0.00002		0.19 ± 0.04

Table 4.1-2. Comparison of Detailed Benchmark and Calculated Eigenvalues (Case 2).

Analysis Code	Neutron Cross Section Library	Calculated k_{eff} ± σ	Benchmark Experiment k_{eff} ± σ	$\frac{C-E}{E}$ %
MCNP6	ENDF/B-VII.1	0.99579 ± 0.00002	0.9989 ± 0.0004	-0.31 ± 0.04
	ENDF/B-VII.0	0.99592 ± 0.00002		-0.30 ± 0.04
	JEFF-3.1	0.99258 ± 0.00002		-0.63 ± 0.04
	JENDL-3.3	1.00015 ± 0.00002		0.13 ± 0.04

[a] E. M. Baum, M. C. Ernesti, H. D. Knox, T. R. Miller, and A. M. Watson, *Nuclides and Isotopes, Chart of the Nuclides: 17th Edition*, Knolls Atomic Power Laboratory (2009).

4.1.2 Simple Benchmark Model

The calculated results for the simple benchmark model is reported in Tables 4.1-3 and 4.1-4 for Cases 1 and 2, respectively. Comments discussed in the previous section regarding calculations of the detailed benchmark model also apply to calculations of the simple benchmark model. Additional calculations of the simple benchmark model were performed with both SERPENT-2.1.13 and KENO-VI using ENDF/B-VII.0 neutron cross section library data. Results are comparable to those obtained via MCNP6.1.

Table 4.1-3. Comparison of Simple Benchmark and Calculated Eigenvalues (Case 1).

Analysis Code	Neutron Cross Section Library	Calculated k_{eff} ± σ	Benchmark Experiment k_{eff} ± σ	$\frac{C-E}{E}$ %
MCNP6	ENDF/B-VII.1	0.99542 ± 0.00002	0.9980 ± 0.0004	-0.26 ± 0.04
	ENDF/B-VII.0	0.99556 ± 0.00002		-0.24 ± 0.04
	JEFF-3.1	0.99227 ± 0.00002		-0.57 ± 0.04
	JENDL-3.3	0.99982 ± 0.00002		0.18 ± 0.04
SERPENT2	ENDF/B-VII.0	0.99558 ± 0.00003		-0.24 ± 0.04
KENO-VI	ENDF/B-VII.0	0.99528 ± 0.00003		-0.27 ± 0.04

Table 4.1-4. Comparison of Simple Benchmark and Calculated Eigenvalues (Case 2).

Analysis Code	Neutron Cross Section Library	Calculated k_{eff} ± σ	Benchmark Experiment k_{eff} ± σ	$\frac{C-E}{E}$ %
MCNP6	ENDF/B-VII.1	0.99564 ± 0.00002	0.9987 ± 0.0004	-0.31 ± 0.04
	ENDF/B-VII.0	0.99577 ± 0.00002		-0.30 ± 0.04
	JEFF-3.1	0.99242 ± 0.00002		-0.63 ± 0.04
	JENDL-3.3	0.99996 ± 0.00002		0.12 ± 0.04
SERPENT2	ENDF/B-VII.0	0.99581 ± 0.00003		-0.29 ± 0.04
KENO-VI	ENDF/B-VII.0	0.99549 ± 0.00003		-0.32 ± 0.04

4.2 Results of Buckling and Extrapolation Length Calculations

Buckling and extrapolation length measurements were not made.

4.3 Results of Spectral-Characteristics Calculations

Spectral characteristics measurements were not made.

4.4 Results of Reactivity-Effects Calculations

4.4.1 Detailed Benchmark Model

The calculated results for the detailed benchmark model are reported in Table 4.4-1. The delayed neutron fraction, β_{eff}, is 0.0066 for conversion of reactivity, ρ, to reactivity in cents, ρ(¢). All calculations of the worth of the potassium are significantly lower than the benchmark worth (~70 – 80 %) by roughly 7σ to 8σ. Reactivity is calculated using the following equation with k_1 and k_2 representing the eigenvalues for critical configurations 1 and 2, respectively:

$$\rho = \frac{k_1 - k_2}{k_1 k_2}.$$

Table 4.4-1. Comparison of Detailed Benchmark Potassium Worth.

Analysis Code	Neutron Cross Section Library	Calculated ρ(¢) ± σ	Benchmark Experiment ρ(¢) ± σ	$\frac{C-E}{E}$ %
MCNP6	ENDF/B-VII.1	3.8 ± 0.4	11.4 ± 1.2	-67 ± 5
	ENDF/B-VII.0	3.1 ± 0.4		-73 ± 5
	JEFF-3.1	2.3 ± 0.4		-80 ± 4
	JENDL-3.3	2.4 ± 0.4		-79 ± 4

Results in Table 4.4-1 can be divided by the total potassium mass of 2398 g to obtain a mass coefficient in units of ¢/g according to the following formula (results shown in Table 4.4-2):

$$\rho = \frac{k_1 - k_2}{k_1 k_2} \times \frac{1}{m}.$$

Table 4.4-2. Comparison of Detailed Benchmark Potassium Mass Coefficient.

Analysis Code	Neutron Cross Section Library	Mass (g)	Calculated ρ_m(¢/g) ± σ	Benchmark Experiment ρ_m(¢/g) ± σ	$\frac{C-E}{E}$ %
MCNP6	ENDF/B-VII.1	2398	0.0016 ± 0.0002	0.0048 ± 0.0005	-67 ± 5
	ENDF/B-VII.0		0.0013 ± 0.0002		-73 ± 5
	JEFF-3.1		0.0010 ± 0.0002		-79 ± 5
	JENDL-3.3		0.0010 ± 0.0002		-79 ± 5

4.4.2 Simple Benchmark Model

The calculated results for the simple benchmark model are reported` in Tables 4.4-3 and 4.4-4. Comments discussed in the previous section regarding the detailed benchmark model also apply to the simple benchmark model. Additional calculations of the simple benchmark model were performed with both SERPENT-2.1.13 and KENO-VI using ENDF/B-VII.0 neutron cross section library data. Results are comparable to those obtained via MCNP6.1.

Table 4.4-3. Comparison of Simple Benchmark Potassium Worth.

Analysis Code	Neutron Cross Section Library	Calculated ρ(¢) ± σ	Benchmark Experiment ρ(¢) ± σ	$\frac{C-E}{E}$%
MCNP6	ENDF/B-VII.1	3.4 ± 0.4	11.0 ± 1.3	-69 ± 5
	ENDF/B-VII.0	3.2 ± 0.4		-71 ± 5
	JEFF-3.1	2.3 ± 0.4		-79 ± 4
	JENDL-3.3	2.1 ± 0.4		-81 ± 4
SERPENT2	ENDF/B-VII.0	3.6 ± 0.6		-67 ± 7
KENO-VI	ENDF/B-VII.0	3.2 ± 0.6		-71 ± 6

Table 4.4-4. Comparison of Simple Benchmark Potassium Mass Coefficient.

Analysis Code	Neutron Cross Section Library	Mass (g)	Calculated ρ_m(¢/g) ± σ	Benchmark Experiment ρ_m(¢/g) ± σ	$\frac{C-E}{E}$%
MCNP6	ENDF/B-VII.1	2398	0.0014 ± 0.0002	0.0046 ± 0.0006	-70 ± 6
	ENDF/B-VII.0		0.0013 ± 0.0002		-72 ± 6
	JEFF-3.1		0.0010 ± 0.0002		-78 ± 5
	JENDL-3.3		0.0009 ± 0.0002		-80 ± 5
SERPENT2	ENDF/B-VII.0		0.0015 ± 0.0003		-67 ± 8
KENO-VI	ENDF/B-VII.0		0.0013 ± 0.0003		-72 ± 7

4.5 Results of Reactivity Coefficient Calculations

Reactivity coefficient measurements were not made.

4.6 Results of Kinetics Parameter Calculations

Kinetics measurements were not made.

4.7 Results of Reaction-Rate Distribution Calculations

Reaction-rate distribution measurements were not made.

4.8 Results of Power Distribution Calculations

Power distribution measurements were not made.

4.9 Results of Isotopic Calculations

Isotopic measurements were not made.

4.10 Results of Calculations for Other Miscellaneous Types of Measurements

Other miscellaneous types of measurements were not made.

5.0 REFERENCES

1. J. T. Mihalczo and M. S. Wyatt, "Potassium Reactivity Worth in a ^{235}U Fission Spectrum Critical Assembly," *Trans. Am. Nucl. Soc.*, **76**, 359-360 (1997).

APPENDIX A: COMPUTER CODES, CROSS SECTIONS, AND TYPICAL INPUT LISTINGS

A.1 Critical/Subcritical Configurations

A.1.1 Name(s) of code system(s) used.

1. Monte Carlo n-Particle, version 6.1 (MCNP6).

A.1.2 Bibliographic references for the codes used.

1. J. T. Goorley, et al., "Initial MCNP6 Release Overview – MCNP6 version 1.0," LA-UR-13-22934, Los Alamos National Laboratory (2013).
2. D. F. Hollenbach, L. M. Petrie, S. Goluoglu, N. F. Landers, and M. E. Dunn, "KENO-VI: A General Quadratic Version of the KENO Program," ORNL/TM-2005/39 Version 6 Vol. II, Sect. F17, Oak Ridge National Laboratory (January 2009).
3. J. Leppänen, "Development of a New Monte Carlo Reactor Physics Code," D.C. Thesis, Helsinki University of Technology, VTT Publications 640, VTT Technical Research Centre, Finland, (2007).

A.1.3 Origin of cross-section data.

The Evaluated Neutron Data File library, ENDF/B-VII.1[a] was utilized in the benchmark model analysis. The European Joint Evaluated Fission and Fusion File, JEFF-3.1,[b] the Japanese Evaluated Nuclear Data Library, JENDL-3.3,[c] and ENDF/B-VII.0[d] were also included for a basic evaluative comparison.

A.1.4 Spectral calculations and data reduction methods used.

Not applicable.

A.1.5 Number of energy groups or if continuous-energy cross sections are used in the different phases of calculation.

1. Continuous-energy cross sections (MCNP and SERPENT)
2. 238-group cross sections (KENO)

A.1.6 Component calculations.

- Type of cell calculation – Stack annuli around cans
- Geometry – Annuli and cylinders
- Theory used – Not applicable
- Method used – Monte Carlo
- Calculation characteristics
    - MCNP/SERPENT/KENO – histories/cycles/cycles skipped = 1,000,000/1,050/50
      continuous-energy cross sections (MCNP/SERPENT) 238-group (KENO)

[a] M. B. Chadwick, et al., "ENDF/B-VII.1: Nuclear Data for Science and Technology: Cross Sections, Covariances, Fission Product Yields and Decay Data," *Nucl. Data Sheets*, **112**: 2887-2996 (2011).
[b] A. Koning, R. Forrest, M. Kellett, R. Mills, H. Henriksson, and Y. Rugama, "The JEFF-3.1 Nuclear Data Library," JEFF Report 21, Organisation for Economic Co-operation and Development, Paris (2006).
[c] K. Shibata, et al., "Japanese Evaluated Nuclear Data Library Version 3 Revision3: JENDL-3.3," *J. Nucl. Sci. Tech.*, **39**: 1125-1136 (November 2002).
[d] M. B. Chadwick, et al., "ENDF/B-VII.0: Next Generation Evaluated Nuclear Data Library for Nuclear Science and Technology," *Nucl. Data Sheets*, **107**: 2931-3060 (2006).

A.1.7 Other assumptions and characteristics.

Not applicable.

A.1.8 Typical input listings for each code system type.

The input decks provided below are for core Configuration 2; the content of the stainless steel cans can be voided to model Configuration 1.

Detailed Model: MCNP6 Input Deck for Configuration 2 (Potassium-Filled Steel Cans):

```
ORALLOY (93.15 235U) METAL ANNULI FOR POTASSIUM WORTH MEASUREMENT
c Case 1 = Empty SS Cans
c Case 2 = K-Filled SS Cans
c
c John Darrell Bess - Idaho National Laboratory
c Last Updated: June 4, 2014
c
c
c Cell Cards ******************************************************************
c ------ Steel Cans ------
1304  1304 8.6428E-02  1019 -1304  imp:n=1  $ Upper Can
2304  2304 8.6116E-02  2019 -2304  imp:n=1  $ Lower Can
1019  1019 1.2951E-02       -1019  imp:n=1  $ Upper Potassium
2019  2019 1.3176E-02       -2019  imp:n=1  $ Lower Potassium
c
c ------ 7"-9" HEU Annulus ------
2763  2763 4.7943E-02  9763 -2763  imp:n=1  $ Top/Upper
2741  2741 4.8168E-02  9741 -2741  imp:n=1
2762  2762 4.8191E-02  9762 -2762  imp:n=1  $ Bottom/Upper
2829  2829 4.8088E-02  9829 -2829  imp:n=1  $ Top/Lower
2740  2740 4.8185E-02  9740 -2740  imp:n=1
2773  2773 4.8043E-02  9773 -2773  imp:n=1
2738  2738 4.8155E-02  9738 -2738  imp:n=1  $ Bottom/Lower
c
c ------ 9"-11" HEU Annulus ------
2746  2746 4.8076E-02  9746 -2746  imp:n=1  $ Top/Upper
2748  2748 4.8157E-02  9748 -2748  imp:n=1
2776  2776 4.8103E-02  9776 -2776  imp:n=1  $ Bottom/Upper
2744  2744 4.8301E-02  9744 -2744  imp:n=1  $ Top/Lower
2742  2742 4.8161E-02  9742 -2742  imp:n=1
2747  2747 4.8082E-02  9747 -2747  imp:n=1
2745  2745 4.8163E-02  9745 -2745  imp:n=1  $ Bottom/Lower
c
c ------ 11"-13" HEU Annulus ------
2781  2781 4.8194E-02  9781 -2781  imp:n=1  $ Top/Upper
2780  2780 4.8035E-02  9780 -2780  imp:n=1
2783  2783 4.8001E-02  9783 -2783  imp:n=1
2782  2782 4.8252E-02  9782 -2782  imp:n=1
2750  2750 4.8127E-02  9750 -2750  imp:n=1
2749  2749 4.8151E-02  9749 -2749  imp:n=1
2757  2757 4.8145E-02  9757 -2757  imp:n=1  $ Bottom/Upper
2754  2754 4.8244E-02  9754 -2754  imp:n=1  $ Top/Lower
2753  2753 4.8040E-02  9753 -2753  imp:n=1
2752  2752 4.8115E-02  9752 -2752  imp:n=1
2751  2751 4.8148E-02  9751 -2751  imp:n=1
2756  2756 4.8182E-02  9756 -2756  imp:n=1  $ Bottom/Lower
c
c ------ Void Spaces------
29    0  1304 2304
         #2763 #2741 #2762 #2829 #2740 #2773 #2738
         #2746 #2748 #2776 #2744 #2742 #2747 #2745
         #2781 #2780 #2783 #2782 #2750 #2749 #2757 #2754 #2753 #2752 #2751 #2756
         -9999  imp:n=1 $ Gaps
30    0   9999  imp:n=0 $ The Great Void

c Surface Cards ***************************************************************
c ------ Steel Cans ------
1304  rcc 0 0  0.000000 0 0 6.35000 8.855710  $ Outer/Upper, 2.5"
2304  rcc 0 0 -7.666567 0 0 7.58317 8.855075  $ Outer/Lower, 3"
1019  rcc 0 0  0.513080 0 0 5.32384 8.698019  $ Inner/Upper, 2.5"
```

```
2019  rcc 0 0 -7.155463 0 0 6.56096 8.698103  $ Inner/Lower, 3"
c
c ------ 7"-9" HEU Annulus ------
c --------- Outer Surfaces ---------
2763  rcc 0 0  6.348857 0 0 0.315722 11.424666  $ Top/Upper
2741  rcc 0 0  2.538095 0 0 3.810762 11.425555
2762  rcc 0 0  0.000000 0 0 2.538095 11.425238  $ Bottom/Upper
2829  rcc 0 0 -0.971762 0 0 0.955675 11.425238  $ Top/Lower
2740  rcc 0 0 -4.789847 0 0 3.810000 11.425238
2773  rcc 0 0 -5.115433 0 0 0.317500 11.426190
2738  rcc 0 0 -7.666567 0 0 2.543048 11.424603  $ Bottom/Lower
c --------- Inner Surfaces ---------
9763  cz 8.894826
9741  cz 8.893175
9762  cz 8.894763
9829  cz 8.894001
9740  cz 8.893175
9773  cz 8.891905
9738  cz 8.894763
c
c ------ 9"-11" HEU Annulus ------
c --------- Outer Surfaces ---------
2746  rcc 0 0  6.363166 0 0 0.326771 13.965555  $ Top/Upper
2748  rcc 0 0  2.548488 0 0 3.810000 13.966825
2776  rcc 0 0  0.000000 0 0 2.543810 13.965555  $ Bottom/Upper
2744  rcc 0 0 -0.340995 0 0 0.321945 13.965936  $ Top/Lower
2742  rcc 0 0 -1.302286 0 0 0.952754 13.965936
2747  rcc 0 0 -5.120569 0 0 3.809746 13.965936
2745  rcc 0 0 -7.666567 0 0 2.537460 13.965555  $ Bottom/Lower
c --------- Inner Surfaces ---------
9746  cz 11.432223
9748  cz 11.433175
9776  cz 11.431905
9744  cz 11.438255
9742  cz 11.431905
9747  cz 11.432540
9745  cz 11.431270
c
c ------ 11"-13" HEU Annulus ------
c --------- Outer Surfaces ---------
2781  rcc 0 0  6.069245 0 0 0.318008 16.505873  $ Top/Upper
2780  rcc 0 0  5.748860 0 0 0.317119 16.504984
2783  rcc 0 0  5.108688 0 0 0.636905 16.504412
2782  rcc 0 0  4.465976 0 0 0.639445 16.504412
2750  rcc 0 0  3.509066 0 0 0.953643 16.503015
2749  rcc 0 0  2.547204 0 0 0.958596 16.504285
2757  rcc 0 0  0.000000 0 0 2.543937 16.504920  $ Bottom/Upper
2754  rcc 0 0 -1.279144 0 0 1.279144 16.504031  $ Top/Lower
2753  rcc 0 0 -2.556531 0 0 1.273302 16.505873
2752  rcc 0 0 -3.838871 0 0 1.278255 16.504285
2751  rcc 0 0 -5.121974 0 0 1.279017 16.504666
2756  rcc 0 0 -7.666567 0 0 2.540508 16.505809  $ Bottom/Lower
c --------- Inner Surfaces ---------
9781  cz 13.973175
9780  cz 13.972540
9783  cz 13.973810
9782  cz 13.974445
9750  cz 13.971905
9749  cz 13.973810
9757  cz 13.973175
9754  cz 13.975080
9753  cz 13.973810
9752  cz 13.973175
9751  cz 13.971905
9756  cz 13.974572
c
c ------ Problem Boundary ------
9999  rcc 0 0 -8.000000 0 0 15.000000 17.000000
c

c Data Cards ******************************************************************
c --- Material Cards ------------------------------------------------------------
c ------ Stainless Steel 304 Cans ------
c --------- Upper, 2.5" ---------
m1304   6000.80c 1.9763E-04  24050.80c 7.5374E-04  24052.80c 1.4535E-02
```

```
       24053.80c 1.6482E-03  24054.80c 4.1027E-04  28058.80c 5.5063E-03
       28060.80c 2.1210E-03  28061.80c 9.2199E-05  28062.80c 2.9397E-04
       28064.80c 7.4866E-05  25055.80c 8.6413E-04  15031.80c 5.8457E-04
       16032.80c 2.9697E-05  16033.80c 1.9599E-05  16034.80c 3.4486E-05
       16036.80c 2.1095E-05  14028.80c 1.6656E-07  14029.80c 9.4384E-07
       14030.80c 2.2208E-09   7014.80c 1.6885E-04   7015.80c 6.1686E-07
       26054.80c 3.4527E-03  26056.80c 5.4200E-02  26057.80c 1.2517E-03
       26058.80c 1.6658E-04
c          Total 8.6428E-02
mt1304 fe56.22t
c
c --------- Lower, 3" ---------
m2304   6000.80c 1.9692E-04  24050.80c 7.5102E-04  24052.80c 1.4483E-02
       24053.80c 1.6422E-03  24054.80c 4.0878E-04  28058.80c 5.4864E-03
       28060.80c 2.1134E-03  28061.80c 9.1866E-05  28062.80c 2.9291E-04
       28064.80c 7.4595E-05  25055.80c 8.6100E-04  15031.80c 5.8246E-04
       16032.80c 2.9589E-05  16033.80c 1.9528E-05  16034.80c 3.4361E-05
       16036.80c 2.1019E-05  14028.80c 1.6596E-07  14029.80c 9.4043E-07
       14030.80c 2.2128E-09   7014.80c 1.6824E-04   7015.80c 6.1463E-07
       26054.80c 3.4402E-03  26056.80c 5.4004E-02  26057.80c 1.2472E-03
       26058.80c 1.6598E-04
c         Total 8.6116E-02
mt2304 fe56.22t
c
c ------ Potassium ------
c --------- Upper, 2.5" ---------
m1019  19039.80c 1.2078E-02  19040.80c 1.5153E-06  19041.80c 8.7165E-04
c          Total 1.2951E-02
c
c --------- Lower, 3" ---------
m2019  19039.80c 1.2288E-02  19040.80c 1.5416E-06  19041.80c 8.8676E-04
c          Total 1.3176E-02
c
c ------ 7"-9" HEU Annulus ------
m2763  92234.80c 4.6147E-04  92235.80c 4.4601E-02  92236.80c 1.1915E-04
       92238.80c 2.6513E-03  47107.80c 4.3275E-07  47109.80c 4.0204E-07
       56130.80c 4.3441E-13  56132.80c 4.1392E-13  56134.80c 9.9054E-12
       56135.80c 2.7015E-11  56136.80c 3.2187E-11  56137.80c 4.6031E-11
       56138.80c 2.9383E-10  83209.80c 8.8332E-06   6000.80c 4.6858E-06
       20040.80c 2.7226E-08  20042.80c 1.8171E-10  20043.80c 3.7915E-11
       20044.80c 5.8585E-10  20046.80c 1.1234E-12  20048.80c 5.2519E-11
       48106.80c 6.2582E-10  48108.80c 4.4559E-10  48110.80c 6.2532E-09
       48111.80c 6.4084E-09  48112.80c 1.2081E-08  48113.80c 6.1180E-09
       48114.80c 1.4384E-08  48116.80c 3.7499E-09  27059.80c 9.5497E-07
       24050.80c 6.5841E-08  24052.80c 1.2697E-06  24053.80c 1.4397E-07
       24054.80c 3.5838E-08  29063.80c 3.0621E-06  29065.80c 1.3661E-06
       19039.80c 2.6848E-08  19040.80c 3.3683E-12  19041.80c 1.9375E-09
        3006.80c 1.2308E-07   3007.80c 1.4986E-06  12024.80c 1.0974E-06
       12025.80c 1.3893E-07  12026.80c 1.5297E-07  25055.80c 1.1473E-05
       42092.80c 8.6643E-09  42094.80c 5.4144E-09  42095.80c 9.3271E-09
       42096.80c 9.7847E-09  42097.80c 5.6080E-09  42098.80c 1.4190E-08
       42100.80c 5.6725E-09  11023.80c 1.3219E-05  28058.80c 1.3055E-05
       28060.80c 5.0289E-06  28061.80c 2.1860E-07  28062.80c 6.9701E-07
       28064.80c 1.7751E-07  51121.80c 2.0097E-06  51123.80c 1.5031E-06
       22046.80c 1.9400E-08  22047.80c 1.7495E-08  22048.80c 1.7335E-07
       22049.80c 1.2722E-08  22050.80c 1.2181E-08   8016.80c 1.4065E-05
        8017.80c 5.3468E-09   7014.80c 2.4021E-05   7015.80c 8.7754E-08
c          Total 4.7943E-02
c
m2741  92234.80c 4.6364E-04  92235.80c 4.4810E-02  92236.80c 1.1972E-04
       92238.80c 2.6638E-03  47107.80c 4.3478E-07  47109.80c 4.0393E-07
       56130.80c 4.3645E-13  56132.80c 4.1587E-13  56134.80c 9.9520E-12
       56135.80c 2.7142E-11  56136.80c 3.2339E-11  56137.80c 4.6248E-11
       56138.80c 2.9522E-10  83209.80c 8.8748E-06   6000.80c 4.7078E-06
       20040.80c 2.7354E-08  20042.80c 1.8256E-10  20043.80c 3.8093E-11
       20044.80c 5.8861E-10  20046.80c 1.1287E-12  20048.80c 5.2766E-11
       48106.80c 6.2877E-10  48108.80c 4.4768E-10  48110.80c 6.2826E-09
       48111.80c 6.4386E-09  48112.80c 1.2138E-08  48113.80c 6.1468E-09
       48114.80c 1.4452E-08  48116.80c 3.7676E-09  27059.80c 9.5946E-07
       24050.80c 6.6151E-08  24052.80c 1.2757E-06  24053.80c 1.4465E-07
       24054.80c 3.6006E-08  29063.80c 3.0765E-06  29065.80c 1.3725E-06
       19039.80c 2.6974E-08  19040.80c 3.3841E-12  19041.80c 1.9467E-09
        3006.80c 1.2366E-07   3007.80c 1.5056E-06  12024.80c 1.1026E-06
       12025.80c 1.3959E-07  12026.80c 1.5368E-07  25055.80c 1.1527E-05
       42092.80c 8.7050E-09  42094.80c 5.4399E-09  42095.80c 9.3710E-09
```

```
        42096.80c 9.8307E-09  42097.80c 5.6344E-09  42098.80c 1.4257E-08
        42100.80c 5.6992E-09  11023.80c 1.3282E-05  28058.80c 1.3117E-05
        28060.80c 5.0526E-06  28061.80c 2.1963E-07  28062.80c 7.0028E-07
        28064.80c 1.7834E-07  51121.80c 2.0192E-06  51123.80c 1.5102E-06
        22046.80c 1.9491E-08  22047.80c 1.7577E-08  22048.80c 1.7417E-07
        22049.80c 1.2781E-08  22050.80c 1.2238E-08   8016.80c 1.4131E-05
         8017.80c 5.3719E-09   7014.80c 2.4133E-05   7015.80c 8.8167E-08
c          Total 4.8168E-02
c
m2762   92234.80c 4.6870E-04  92235.80c 4.4808E-02  92236.80c 1.2935E-04
        92238.80c 2.6745E-03  47107.80c 4.3499E-07  47109.80c 4.0413E-07
        56130.80c 4.3666E-13  56132.80c 4.1606E-13  56134.80c 9.9567E-12
        56135.80c 2.7155E-11  56136.80c 3.2354E-11  56137.80c 4.6270E-11
        56138.80c 2.9536E-10  83209.80c 8.8790E-06   6000.80c 4.7101E-06
        20040.80c 2.7367E-08  20042.80c 1.8265E-10  20043.80c 3.8111E-11
        20044.80c 5.8889E-10  20046.80c 1.1292E-12  20048.80c 5.2791E-11
        48106.80c 6.2906E-10  48108.80c 4.4789E-10  48110.80c 6.2856E-09
        48111.80c 6.4416E-09  48112.80c 1.2143E-08  48113.80c 6.1497E-09
        48114.80c 1.4458E-08  48116.80c 3.7694E-09  27059.80c 9.5992E-07
        24050.80c 6.6182E-08  24052.80c 1.2763E-06  24053.80c 1.4472E-07
        24054.80c 3.6023E-08  29063.80c 3.0780E-06  29065.80c 1.3732E-06
        19039.80c 2.6987E-08  19040.80c 3.3857E-12  19041.80c 1.9476E-09
         3006.80c 1.2372E-07   3007.80c 1.5063E-06  12024.80c 1.1031E-06
        12025.80c 1.3965E-07  12026.80c 1.5376E-07  25055.80c 1.1533E-05
        42092.80c 8.7091E-09  42094.80c 5.4425E-09  42095.80c 9.3754E-09
        42096.80c 9.8354E-09  42097.80c 5.6371E-09  42098.80c 1.4264E-08
        42100.80c 5.7019E-09  11023.80c 1.3288E-05  28058.80c 1.3123E-05
        28060.80c 5.0550E-06  28061.80c 2.1974E-07  28062.80c 7.0061E-07
        28064.80c 1.7843E-07  51121.80c 2.0201E-06  51123.80c 1.5109E-06
        22046.80c 1.9500E-08  22047.80c 1.7586E-08  22048.80c 1.7425E-07
        22049.80c 1.2787E-08  22050.80c 1.2244E-08   8016.80c 1.4138E-05
         8017.80c 5.3744E-09   7014.80c 2.4145E-05   7015.80c 8.8209E-08
c          Total 4.8191E-02
c
m2829   92234.80c 4.7734E-04  92235.80c 4.4697E-02  92236.80c 1.1474E-04
        92238.80c 2.6878E-03  47107.80c 4.3406E-07  47109.80c 4.0326E-07
        56130.80c 4.3573E-13  56132.80c 4.1518E-13  56134.80c 9.9354E-12
        56135.80c 2.7097E-11  56136.80c 3.2285E-11  56137.80c 4.6171E-11
        56138.80c 2.9473E-10  83209.80c 8.8600E-06   6000.80c 4.7000E-06
        20040.80c 2.7308E-08  20042.80c 1.8226E-10  20043.80c 3.8030E-11
        20044.80c 5.8763E-10  20046.80c 1.1268E-12  20048.80c 5.2678E-11
        48106.80c 6.2772E-10  48108.80c 4.4694E-10  48110.80c 6.2722E-09
        48111.80c 6.4279E-09  48112.80c 1.2118E-08  48113.80c 6.1366E-09
        48114.80c 1.4428E-08  48116.80c 3.7613E-09  27059.80c 9.5787E-07
        24050.80c 6.6041E-08  24052.80c 1.2735E-06  24053.80c 1.4441E-07
        24054.80c 3.5946E-08  29063.80c 3.0714E-06  29065.80c 1.3703E-06
        19039.80c 2.6929E-08  19040.80c 3.3785E-12  19041.80c 1.9434E-09
         3006.80c 1.2346E-07   3007.80c 1.5031E-06  12024.80c 1.1008E-06
        12025.80c 1.3935E-07  12026.80c 1.5343E-07  25055.80c 1.1508E-05
        42092.80c 8.6905E-09  42094.80c 5.4309E-09  42095.80c 9.3554E-09
        42096.80c 9.8144E-09  42097.80c 5.6250E-09  42098.80c 1.4233E-08
        42100.80c 5.6897E-09  11023.80c 1.3259E-05  28058.80c 1.3095E-05
        28060.80c 5.0442E-06  28061.80c 2.1927E-07  28062.80c 6.9912E-07
        28064.80c 1.7805E-07  51121.80c 2.0158E-06  51123.80c 1.5077E-06
        22046.80c 1.9459E-08  22047.80c 1.7548E-08  22048.80c 1.7388E-07
        22049.80c 1.2760E-08  22050.80c 1.2218E-08   8016.80c 1.4108E-05
         8017.80c 5.3630E-09   7014.80c 2.4093E-05   7015.80c 8.8020E-08
c          Total 4.8088E-02
c
m2740   92234.80c 4.6863E-04  92235.80c 4.4821E-02  92236.80c 1.1497E-04
        92238.80c 2.6694E-03  47107.80c 4.3493E-07  47109.80c 4.0407E-07
        56130.80c 4.3660E-13  56132.80c 4.1601E-13  56134.80c 9.9554E-12
        56135.80c 2.7152E-11  56136.80c 3.2350E-11  56137.80c 4.6263E-11
        56138.80c 2.9532E-10  83209.80c 8.8778E-06   6000.80c 4.7094E-06
        20040.80c 2.7363E-08  20042.80c 1.8263E-10  20043.80c 3.8106E-11
        20044.80c 5.8881E-10  20046.80c 1.1291E-12  20048.80c 5.2784E-11
        48106.80c 6.2898E-10  48108.80c 4.4783E-10  48110.80c 6.2848E-09
        48111.80c 6.4408E-09  48112.80c 1.2142E-08  48113.80c 6.1489E-09
        48114.80c 1.4456E-08  48116.80c 3.7689E-09  27059.80c 9.5979E-07
        24050.80c 6.6173E-08  24052.80c 1.2761E-06  24053.80c 1.4470E-07
        24054.80c 3.6018E-08  29063.80c 3.0776E-06  29065.80c 1.3730E-06
        19039.80c 2.6983E-08  19040.80c 3.3853E-12  19041.80c 1.9473E-09
         3006.80c 1.2370E-07   3007.80c 1.5061E-06  12024.80c 1.1030E-06
        12025.80c 1.3963E-07  12026.80c 1.5374E-07  25055.80c 1.1531E-05
        42092.80c 8.7080E-09  42094.80c 5.4417E-09  42095.80c 9.3742E-09
```

```
        42096.80c 9.8341E-09  42097.80c 5.6363E-09  42098.80c 1.4262E-08
        42100.80c 5.7012E-09  11023.80c 1.3286E-05  28058.80c 1.3121E-05
        28060.80c 5.0543E-06  28061.80c 2.1971E-07  28062.80c 7.0052E-07
        28064.80c 1.7840E-07  51121.80c 2.0198E-06  51123.80c 1.5107E-06
        22046.80c 1.9498E-08  22047.80c 1.7583E-08  22048.80c 1.7423E-07
        22049.80c 1.2786E-08  22050.80c 1.2242E-08   8016.80c 1.4136E-05
         8017.80c 5.3737E-09   7014.80c 2.4142E-05   7015.80c 8.8197E-08
c          Total 4.8185E-02
c
m2773   92234.80c 4.6726E-04  92235.80c 4.4689E-02  92236.80c 1.1463E-04
        92238.80c 2.6616E-03  47107.80c 4.3365E-07  47109.80c 4.0289E-07
        56130.80c 4.3532E-13  56132.80c 4.1479E-13  56134.80c 9.9262E-12
        56135.80c 2.7072E-11  56136.80c 3.2255E-11  56137.80c 4.6128E-11
        56138.80c 2.9445E-10  83209.80c 8.8517E-06   6000.80c 4.6956E-06
        20040.80c 2.7283E-08  20042.80c 1.8209E-10  20043.80c 3.7994E-11
        20044.80c 5.8708E-10  20046.80c 1.1258E-12  20048.80c 5.2629E-11
        48106.80c 6.2714E-10  48108.80c 4.4652E-10  48110.80c 6.2663E-09
        48111.80c 6.4219E-09  48112.80c 1.2106E-08  48113.80c 6.1309E-09
        48114.80c 1.4414E-08  48116.80c 3.7578E-09  27059.80c 9.5697E-07
        24050.80c 6.5979E-08  24052.80c 1.2723E-06  24053.80c 1.4427E-07
        24054.80c 3.5913E-08  29063.80c 3.0686E-06  29065.80c 1.3690E-06
        19039.80c 2.6904E-08  19040.80c 3.3753E-12  19041.80c 1.9416E-09
         3006.80c 1.2334E-07   3007.80c 1.5017E-06  12024.80c 1.0997E-06
        12025.80c 1.3922E-07  12026.80c 1.5329E-07  25055.80c 1.1498E-05
        42092.80c 8.6824E-09  42094.80c 5.4258E-09  42095.80c 9.3467E-09
        42096.80c 9.8052E-09  42097.80c 5.6198E-09  42098.80c 1.4220E-08
        42100.80c 5.6844E-09  11023.80c 1.3247E-05  28058.80c 1.3083E-05
        28060.80c 5.0395E-06  28061.80c 2.1906E-07  28062.80c 6.9847E-07
        28064.80c 1.7788E-07  51121.80c 2.0139E-06  51123.80c 1.5063E-06
        22046.80c 1.9441E-08  22047.80c 1.7532E-08  22048.80c 1.7372E-07
        22049.80c 1.2748E-08  22050.80c 1.2206E-08   8016.80c 1.4095E-05
         8017.80c 5.3580E-09   7014.80c 2.4071E-05   7015.80c 8.7938E-08
c          Total 4.8043E-02
c
m2738   92234.80c 4.7317E-04  92235.80c 4.4783E-02  92236.80c 1.1489E-04
        92238.80c 2.6725E-03  47107.80c 4.3466E-07  47109.80c 4.0382E-07
        56130.80c 4.3633E-13  56132.80c 4.1575E-13  56134.80c 9.9492E-12
        56135.80c 2.7135E-11  56136.80c 3.2330E-11  56137.80c 4.6235E-11
        56138.80c 2.9513E-10  83209.80c 8.8723E-06   6000.80c 4.7065E-06
        20040.80c 2.7346E-08  20042.80c 1.8251E-10  20043.80c 3.8082E-11
        20044.80c 5.8844E-10  20046.80c 1.1284E-12  20048.80c 5.2751E-11
        48106.80c 6.2859E-10  48108.80c 4.4756E-10  48110.80c 6.2809E-09
        48111.80c 6.4368E-09  48112.80c 1.2134E-08  48113.80c 6.1451E-09
        48114.80c 1.4447E-08  48116.80c 3.7665E-09  27059.80c 9.5919E-07
        24050.80c 6.6132E-08  24052.80c 1.2753E-06  24053.80c 1.4461E-07
        24054.80c 3.5996E-08  29063.80c 3.0757E-06  29065.80c 1.3722E-06
        19039.80c 2.6966E-08  19040.80c 3.3832E-12  19041.80c 1.9461E-09
         3006.80c 1.2363E-07   3007.80c 1.5052E-06  12024.80c 1.1023E-06
        12025.80c 1.3955E-07  12026.80c 1.5364E-07  25055.80c 1.1524E-05
        42092.80c 8.7025E-09  42094.80c 5.4384E-09  42095.80c 9.3683E-09
        42096.80c 9.8279E-09  42097.80c 5.6328E-09  42098.80c 1.4253E-08
        42100.80c 5.6976E-09  11023.80c 1.3278E-05  28058.80c 1.3113E-05
        28060.80c 5.0512E-06  28061.80c 2.1957E-07  28062.80c 7.0009E-07
        28064.80c 1.7829E-07  51121.80c 2.0186E-06  51123.80c 1.5098E-06
        22046.80c 1.9486E-08  22047.80c 1.7572E-08  22048.80c 1.7412E-07
        22049.80c 1.2778E-08  22050.80c 1.2235E-08   8016.80c 1.4127E-05
         8017.80c 5.3704E-09   7014.80c 2.4127E-05   7015.80c 8.8142E-08
c          Total 4.8155E-02
c
c ------ 9"-11" HEU Annulus ------
m2746   92234.80c 4.8204E-04  92235.80c 4.4681E-02  92236.80c 1.0515E-04
        92238.80c 2.6966E-03  47107.80c 4.3395E-07  47109.80c 4.0316E-07
        56130.80c 4.3562E-13  56132.80c 4.1507E-13  56134.80c 9.9329E-12
        56135.80c 2.7091E-11  56136.80c 3.2277E-11  56137.80c 4.6159E-11
        56138.80c 2.9465E-10  83209.80c 8.8578E-06   6000.80c 4.6988E-06
        20040.80c 2.7302E-08  20042.80c 1.8222E-10  20043.80c 3.8020E-11
        20044.80c 5.8748E-10  20046.80c 1.1265E-12  20048.80c 5.2665E-11
        48106.80c 6.2756E-10  48108.80c 4.4683E-10  48110.80c 6.2706E-09
        48111.80c 6.4263E-09  48112.80c 1.2115E-08  48113.80c 6.1351E-09
        48114.80c 1.4424E-08  48116.80c 3.7604E-09  27059.80c 9.5763E-07
        24050.80c 6.6024E-08  24052.80c 1.2732E-06  24053.80c 1.4437E-07
        24054.80c 3.5937E-08  29063.80c 3.0707E-06  29065.80c 1.3699E-06
        19039.80c 2.6923E-08  19040.80c 3.3777E-12  19041.80c 1.9429E-09
         3006.80c 1.2343E-07   3007.80c 1.5027E-06  12024.80c 1.1005E-06
        12025.80c 1.3932E-07  12026.80c 1.5339E-07  25055.80c 1.1505E-05
```

```
        42092.80c 8.6884E-09  42094.80c 5.4295E-09  42095.80c 9.3531E-09
        42096.80c 9.8119E-09  42097.80c 5.6236E-09  42098.80c 1.4230E-08
        42100.80c 5.6883E-09  11023.80c 1.3256E-05  28058.80c 1.3092E-05
        28060.80c 5.0429E-06  28061.80c 2.1921E-07  28062.80c 6.9894E-07
        28064.80c 1.7800E-07  51121.80c 2.0153E-06  51123.80c 1.5073E-06
        22046.80c 1.9454E-08  22047.80c 1.7544E-08  22048.80c 1.7383E-07
        22049.80c 1.2757E-08  22050.80c 1.2215E-08   8016.80c 1.4104E-05
         8017.80c 5.3616E-09   7014.80c 2.4087E-05   7015.80c 8.7998E-08
c          Total 4.8076E-02
c
m2748   92234.80c 4.8285E-04  92235.80c 4.4757E-02  92236.80c 1.0533E-04
        92238.80c 2.7012E-03  47107.80c 4.3468E-07  47109.80c 4.0384E-07
        56130.80c 4.3636E-13  56132.80c 4.1577E-13  56134.80c 9.9497E-12
        56135.80c 2.7136E-11  56136.80c 3.2332E-11  56137.80c 4.6237E-11
        56138.80c 2.9515E-10  83209.80c 8.8728E-06   6000.80c 4.7068E-06
        20040.80c 2.7348E-08  20042.80c 1.8252E-10  20043.80c 3.8085E-11
        20044.80c 5.8848E-10  20046.80c 1.1284E-12  20048.80c 5.2754E-11
        48106.80c 6.2863E-10  48108.80c 4.4758E-10  48110.80c 6.2812E-09
        48111.80c 6.4371E-09  48112.80c 1.2135E-08  48113.80c 6.1454E-09
        48114.80c 1.4448E-08  48116.80c 3.7667E-09  27059.80c 9.5925E-07
        24050.80c 6.6136E-08  24052.80c 1.2754E-06  24053.80c 1.4462E-07
        24054.80c 3.5998E-08  29063.80c 3.0758E-06  29065.80c 1.3722E-06
        19039.80c 2.6968E-08  19040.80c 3.3834E-12  19041.80c 1.9462E-09
         3006.80c 1.2363E-07   3007.80c 1.5053E-06  12024.80c 1.1023E-06
        12025.80c 1.3956E-07  12026.80c 1.5365E-07  25055.80c 1.1525E-05
        42092.80c 8.7031E-09  42094.80c 5.4387E-09  42095.80c 9.3689E-09
        42096.80c 9.8285E-09  42097.80c 5.6331E-09  42098.80c 1.4254E-08
        42100.80c 5.6979E-09  11023.80c 1.3279E-05  28058.80c 1.3114E-05
        28060.80c 5.0514E-06  28061.80c 2.1958E-07  28062.80c 7.0013E-07
        28064.80c 1.7830E-07  51121.80c 2.0187E-06  51123.80c 1.5099E-06
        22046.80c 1.9487E-08  22047.80c 1.7573E-08  22048.80c 1.7413E-07
        22049.80c 1.2779E-08  22050.80c 1.2235E-08   8016.80c 1.4128E-05
         8017.80c 5.3707E-09   7014.80c 2.4128E-05   7015.80c 8.8147E-08
c          Total 4.8157E-02
c
m2776   92234.80c 4.6302E-04  92235.80c 4.4740E-02  92236.80c 1.0999E-04
        92238.80c 2.6792E-03  47107.80c 4.3420E-07  47109.80c 4.0339E-07
        56130.80c 4.3587E-13  56132.80c 4.1531E-13  56134.80c 9.9386E-12
        56135.80c 2.7106E-11  56136.80c 3.2295E-11  56137.80c 4.6185E-11
        56138.80c 2.9482E-10  83209.80c 8.8628E-06   6000.80c 4.7015E-06
        20040.80c 2.7317E-08  20042.80c 1.8232E-10  20043.80c 3.8042E-11
        20044.80c 5.8782E-10  20046.80c 1.1272E-12  20048.80c 5.2695E-11
        48106.80c 6.2792E-10  48108.80c 4.4708E-10  48110.80c 6.2742E-09
        48111.80c 6.4299E-09  48112.80c 1.2121E-08  48113.80c 6.1385E-09
        48114.80c 1.4432E-08  48116.80c 3.7625E-09  27059.80c 9.5817E-07
        24050.80c 6.6062E-08  24052.80c 1.2739E-06  24053.80c 1.4445E-07
        24054.80c 3.5958E-08  29063.80c 3.0724E-06  29065.80c 1.3707E-06
        19039.80c 2.6938E-08  19040.80c 3.3796E-12  19041.80c 1.9440E-09
         3006.80c 1.2350E-07   3007.80c 1.5036E-06  12024.80c 1.1011E-06
        12025.80c 1.3940E-07  12026.80c 1.5348E-07  25055.80c 1.1512E-05
        42092.80c 8.6933E-09  42094.80c 5.4326E-09  42095.80c 9.3584E-09
        42096.80c 9.8175E-09  42097.80c 5.6268E-09  42098.80c 1.4238E-08
        42100.80c 5.6915E-09  11023.80c 1.3264E-05  28058.80c 1.3099E-05
        28060.80c 5.0458E-06  28061.80c 2.1934E-07  28062.80c 6.9934E-07
        28064.80c 1.7810E-07  51121.80c 2.0164E-06  51123.80c 1.5082E-06
        22046.80c 1.9465E-08  22047.80c 1.7554E-08  22048.80c 1.7393E-07
        22049.80c 1.2764E-08  22050.80c 1.2222E-08   8016.80c 1.4112E-05
         8017.80c 5.3647E-09   7014.80c 2.4101E-05   7015.80c 8.8048E-08
c          Total 4.8103E-02
c
m2744   92234.80c 4.7461E-04  92235.80c 4.4915E-02  92236.80c 1.1044E-04
        92238.80c 2.6902E-03  47107.80c 4.3598E-07  47109.80c 4.0505E-07
        56130.80c 4.3766E-13  56132.80c 4.1701E-13  56134.80c 9.9794E-12
        56135.80c 2.7217E-11  56136.80c 3.2428E-11  56137.80c 4.6375E-11
        56138.80c 2.9603E-10  83209.80c 8.8992E-06   6000.80c 4.7208E-06
        20040.80c 2.7429E-08  20042.80c 1.8307E-10  20043.80c 3.8198E-11
        20044.80c 5.9023E-10  20046.80c 1.1318E-12  20048.80c 5.2911E-11
        48106.80c 6.3050E-10  48108.80c 4.4892E-10  48110.80c 6.3000E-09
        48111.80c 6.4563E-09  48112.80c 1.2171E-08  48113.80c 6.1638E-09
        48114.80c 1.4491E-08  48116.80c 3.7780E-09  27059.80c 9.6211E-07
        24050.80c 6.6333E-08  24052.80c 1.2792E-06  24053.80c 1.4505E-07
        24054.80c 3.6105E-08  29063.80c 3.0850E-06  29065.80c 1.3763E-06
        19039.80c 2.7048E-08  19040.80c 3.3935E-12  19041.80c 1.9520E-09
         3006.80c 1.2400E-07   3007.80c 1.5098E-06  12024.80c 1.1056E-06
        12025.80c 1.3997E-07  12026.80c 1.5411E-07  25055.80c 1.1559E-05
```

```
        42092.80c 8.7290E-09  42094.80c 5.4549E-09  42095.80c 9.3968E-09
        42096.80c 9.8578E-09  42097.80c 5.6499E-09  42098.80c 1.4296E-08
        42100.80c 5.7149E-09  11023.80c 1.3318E-05  28058.80c 1.3153E-05
        28060.80c 5.0665E-06  28061.80c 2.2024E-07  28062.80c 7.0221E-07
        28064.80c 1.7883E-07  51121.80c 2.0247E-06  51123.80c 1.5144E-06
        22046.80c 1.9545E-08  22047.80c 1.7626E-08  22048.80c 1.7465E-07
        22049.80c 1.2817E-08  22050.80c 1.2272E-08   8016.80c 1.4170E-05
         8017.80c 5.3867E-09   7014.80c 2.4200E-05   7015.80c 8.8410E-08
c          Total 4.8301E-02
c
m2742   92234.80c 4.7324E-04  92235.80c 4.4785E-02  92236.80c 1.1012E-04
        92238.80c 2.6824E-03  47107.80c 4.3472E-07  47109.80c 4.0388E-07
        56130.80c 4.3639E-13  56132.80c 4.1581E-13  56134.80c 9.9506E-12
        56135.80c 2.7139E-11  56136.80c 3.2334E-11  56137.80c 4.6241E-11
        56138.80c 2.9517E-10  83209.80c 8.8735E-06   6000.80c 4.7072E-06
        20040.80c 2.7350E-08  20042.80c 1.8254E-10  20043.80c 3.8088E-11
        20044.80c 5.8853E-10  20046.80c 1.1285E-12  20048.80c 5.2759E-11
        48106.80c 6.2868E-10  48108.80c 4.4762E-10  48110.80c 6.2818E-09
        48111.80c 6.4377E-09  48112.80c 1.2136E-08  48113.80c 6.1460E-09
        48114.80c 1.4450E-08  48116.80c 3.7670E-09  27059.80c 9.5933E-07
        24050.80c 6.6142E-08  24052.80c 1.2755E-06  24053.80c 1.4463E-07
        24054.80c 3.6001E-08  29063.80c 3.0761E-06  29065.80c 1.3724E-06
        19039.80c 2.6970E-08  19040.80c 3.3837E-12  19041.80c 1.9464E-09
         3006.80c 1.2365E-07   3007.80c 1.5054E-06  12024.80c 1.1024E-06
        12025.80c 1.3957E-07  12026.80c 1.5366E-07  25055.80c 1.1526E-05
        42092.80c 8.7038E-09  42094.80c 5.4391E-09  42095.80c 9.3697E-09
        42096.80c 9.8293E-09  42097.80c 5.6336E-09  42098.80c 1.4255E-08
        42100.80c 5.6984E-09  11023.80c 1.3280E-05  28058.80c 1.3115E-05
        28060.80c 5.0519E-06  28061.80c 2.1960E-07  28062.80c 7.0019E-07
        28064.80c 1.7832E-07  51121.80c 2.0189E-06  51123.80c 1.5100E-06
        22046.80c 1.9488E-08  22047.80c 1.7575E-08  22048.80c 1.7414E-07
        22049.80c 1.2780E-08  22050.80c 1.2236E-08   8016.80c 1.4129E-05
         8017.80c 5.3712E-09   7014.80c 2.4130E-05   7015.80c 8.8155E-08
c          Total 4.8161E-02
c
m2747   92234.80c 4.7245E-04  92235.80c 4.4720E-02  92236.80c 9.0820E-05
        92238.80c 2.6874E-03  47107.80c 4.3400E-07  47109.80c 4.0321E-07
        56130.80c 4.3567E-13  56132.80c 4.1512E-13  56134.80c 9.9341E-12
        56135.80c 2.7094E-11  56136.80c 3.2281E-11  56137.80c 4.6165E-11
        56138.80c 2.9469E-10  83209.80c 8.8588E-06   6000.80c 4.6994E-06
        20040.80c 2.7305E-08  20042.80c 1.8224E-10  20043.80c 3.8025E-11
        20044.80c 5.8755E-10  20046.80c 1.1267E-12  20048.80c 5.2671E-11
        48106.80c 6.2764E-10  48108.80c 4.4688E-10  48110.80c 6.2714E-09
        48111.80c 6.4270E-09  48112.80c 1.2116E-08  48113.80c 6.1358E-09
        48114.80c 1.4426E-08  48116.80c 3.7608E-09  27059.80c 9.5774E-07
        24050.80c 6.6032E-08  24052.80c 1.2734E-06  24053.80c 1.4439E-07
        24054.80c 3.5942E-08  29063.80c 3.0710E-06  29065.80c 1.3701E-06
        19039.80c 2.6926E-08  19040.80c 3.3780E-12  19041.80c 1.9432E-09
         3006.80c 1.2344E-07   3007.80c 1.5029E-06  12024.80c 1.1006E-06
        12025.80c 1.3934E-07  12026.80c 1.5341E-07  25055.80c 1.1507E-05
        42092.80c 8.6894E-09  42094.80c 5.4301E-09  42095.80c 9.3542E-09
        42096.80c 9.8131E-09  42097.80c 5.6243E-09  42098.80c 1.4231E-08
        42100.80c 5.6890E-09  11023.80c 1.3258E-05  28058.80c 1.3093E-05
        28060.80c 5.0435E-06  28061.80c 2.1924E-07  28062.80c 6.9903E-07
        28064.80c 1.7802E-07  51121.80c 2.0155E-06  51123.80c 1.5075E-06
        22046.80c 1.9456E-08  22047.80c 1.7546E-08  22048.80c 1.7385E-07
        22049.80c 1.2758E-08  22050.80c 1.2216E-08   8016.80c 1.4106E-05
         8017.80c 5.3623E-09   7014.80c 2.4090E-05   7015.80c 8.8009E-08
c          Total 4.8082E-02
c
m2745   92234.80c 4.6359E-04  92235.80c 4.4815E-02  92236.80c 1.0534E-04
        92238.80c 2.6682E-03  47107.80c 4.3473E-07  47109.80c 4.0389E-07
        56130.80c 4.3640E-13  56132.80c 4.1582E-13  56134.80c 9.9509E-12
        56135.80c 2.7139E-11  56136.80c 3.2335E-11  56137.80c 4.6242E-11
        56138.80c 2.9518E-10  83209.80c 8.8738E-06   6000.80c 4.7073E-06
        20040.80c 2.7351E-08  20042.80c 1.8254E-10  20043.80c 3.8089E-11
        20044.80c 5.8854E-10  20046.80c 1.1286E-12  20048.80c 5.2760E-11
        48106.80c 6.2870E-10  48108.80c 4.4763E-10  48110.80c 6.2819E-09
        48111.80c 6.4378E-09  48112.80c 1.2136E-08  48113.80c 6.1461E-09
        48114.80c 1.4450E-08  48116.80c 3.7671E-09  27059.80c 9.5936E-07
        24050.80c 6.6143E-08  24052.80c 1.2755E-06  24053.80c 1.4463E-07
        24054.80c 3.6002E-08  29063.80c 3.0762E-06  29065.80c 1.3724E-06
        19039.80c 2.6971E-08  19040.80c 3.3837E-12  19041.80c 1.9464E-09
         3006.80c 1.2365E-07   3007.80c 1.5055E-06  12024.80c 1.1025E-06
        12025.80c 1.3957E-07  12026.80c 1.5367E-07  25055.80c 1.1526E-05
```

```
       42092.80c 8.7040E-09  42094.80c 5.4393E-09  42095.80c 9.3699E-09
       42096.80c 9.8296E-09  42097.80c 5.6338E-09  42098.80c 1.4255E-08
       42100.80c 5.6986E-09  11023.80c 1.3280E-05  28058.80c 1.3115E-05
       28060.80c 5.0520E-06  28061.80c 2.1961E-07  28062.80c 7.0020E-07
       28064.80c 1.7832E-07  51121.80c 2.0189E-06  51123.80c 1.5100E-06
       22046.80c 1.9489E-08  22047.80c 1.7575E-08  22048.80c 1.7415E-07
       22049.80c 1.2780E-08  22050.80c 1.2237E-08   8016.80c 1.4130E-05
        8017.80c 5.3713E-09   7014.80c 2.4131E-05   7015.80c 8.8157E-08
c          Total 4.8163E-02
c
c ------ 11"-13" HEU Annulus ------
m2781  92234.80c 4.7355E-04  92235.80c 4.4839E-02  92236.80c 1.1978E-04
       92238.80c 2.6509E-03  47107.80c 4.3501E-07  47109.80c 4.0414E-07
       56130.80c 4.3668E-13  56132.80c 4.1608E-13  56134.80c 9.9572E-12
       56135.80c 2.7157E-11  56136.80c 3.2356E-11  56137.80c 4.6272E-11
       56138.80c 2.9537E-10  83209.80c 8.8794E-06   6000.80c 4.7103E-06
       20040.80c 2.7368E-08  20042.80c 1.8266E-10  20043.80c 3.8113E-11
       20044.80c 5.8892E-10  20046.80c 1.1293E-12  20048.80c 5.2793E-11
       48106.80c 6.2909E-10  48108.80c 4.4792E-10  48110.80c 6.2859E-09
       48111.80c 6.4419E-09  48112.80c 1.2144E-08  48113.80c 6.1500E-09
       48114.80c 1.4459E-08  48116.80c 3.7695E-09  27059.80c 9.5996E-07
       24050.80c 6.6185E-08  24052.80c 1.2763E-06  24053.80c 1.4472E-07
       24054.80c 3.6025E-08  29063.80c 3.0781E-06  29065.80c 1.3733E-06
       19039.80c 2.6988E-08  19040.80c 3.3859E-12  19041.80c 1.9477E-09
        3006.80c 1.2373E-07   3007.80c 1.5064E-06  12024.80c 1.1032E-06
       12025.80c 1.3966E-07  12026.80c 1.5377E-07  25055.80c 1.1533E-05
       42092.80c 8.7095E-09  42094.80c 5.4427E-09  42095.80c 9.3759E-09
       42096.80c 9.8358E-09  42097.80c 5.6373E-09  42098.80c 1.4264E-08
       42100.80c 5.7022E-09  11023.80c 1.3288E-05  28058.80c 1.3124E-05
       28060.80c 5.0552E-06  28061.80c 2.1975E-07  28062.80c 7.0065E-07
       28064.80c 1.7843E-07  51121.80c 2.0202E-06  51123.80c 1.5110E-06
       22046.80c 1.9501E-08  22047.80c 1.7587E-08  22048.80c 1.7426E-07
       22049.80c 1.2788E-08  22050.80c 1.2244E-08   8016.80c 1.4139E-05
        8017.80c 5.3747E-09   7014.80c 2.4146E-05   7015.80c 8.8213E-08
c          Total 4.8194E-02
c
m2780  92234.80c 4.7200E-04  92235.80c 4.4663E-02  92236.80c 1.1938E-04
       92238.80c 2.6706E-03  47107.80c 4.3358E-07  47109.80c 4.0282E-07
       56130.80c 4.3525E-13  56132.80c 4.1472E-13  56134.80c 9.9245E-12
       56135.80c 2.7068E-11  56136.80c 3.2250E-11  56137.80c 4.6120E-11
       56138.80c 2.9440E-10  83209.80c 8.8503E-06   6000.80c 4.6948E-06
       20040.80c 2.7278E-08  20042.80c 1.8206E-10  20043.80c 3.7988E-11
       20044.80c 5.8698E-10  20046.80c 1.1256E-12  20048.80c 5.2620E-11
       48106.80c 6.2703E-10  48108.80c 4.4645E-10  48110.80c 6.2653E-09
       48111.80c 6.4208E-09  48112.80c 1.2104E-08  48113.80c 6.1299E-09
       48114.80c 1.4412E-08  48116.80c 3.7572E-09  27059.80c 9.5682E-07
       24050.80c 6.5968E-08  24052.80c 1.2721E-06  24053.80c 1.4425E-07
       24054.80c 3.5907E-08  29063.80c 3.0681E-06  29065.80c 1.3688E-06
       19039.80c 2.6900E-08  19040.80c 3.3748E-12  19041.80c 1.9413E-09
        3006.80c 1.2332E-07   3007.80c 1.5015E-06  12024.80c 1.0996E-06
       12025.80c 1.3920E-07  12026.80c 1.5326E-07  25055.80c 1.1496E-05
       42092.80c 8.6810E-09  42094.80c 5.4249E-09  42095.80c 9.3451E-09
       42096.80c 9.8036E-09  42097.80c 5.6188E-09  42098.80c 1.4218E-08
       42100.80c 5.6835E-09  11023.80c 1.3245E-05  28058.80c 1.3081E-05
       28060.80c 5.0386E-06  28061.80c 2.1903E-07  28062.80c 6.9835E-07
       28064.80c 1.7785E-07  51121.80c 2.0136E-06  51123.80c 1.5061E-06
       22046.80c 1.9437E-08  22047.80c 1.7529E-08  22048.80c 1.7369E-07
       22049.80c 1.2746E-08  22050.80c 1.2204E-08   8016.80c 1.4092E-05
        8017.80c 5.3571E-09   7014.80c 2.4067E-05   7015.80c 8.7924E-08
c          Total 4.8035E-02
c
m2783  92234.80c 4.4760E-04  92235.80c 4.4655E-02  92236.80c 1.1930E-04
       92238.80c 2.6687E-03  47107.80c 4.3327E-07  47109.80c 4.0253E-07
       56130.80c 4.3494E-13  56132.80c 4.1442E-13  56134.80c 9.9174E-12
       56135.80c 2.7048E-11  56136.80c 3.2226E-11  56137.80c 4.6087E-11
       56138.80c 2.9419E-10  83209.80c 8.8439E-06   6000.80c 4.6915E-06
       20040.80c 2.7259E-08  20042.80c 1.8193E-10  20043.80c 3.7961E-11
       20044.80c 5.8656E-10  20046.80c 1.1248E-12  20048.80c 5.2583E-11
       48106.80c 6.2658E-10  48108.80c 4.4613E-10  48110.80c 6.2608E-09
       48111.80c 6.4162E-09  48112.80c 1.2096E-08  48113.80c 6.1255E-09
       48114.80c 1.4401E-08  48116.80c 3.7545E-09  27059.80c 9.5613E-07
       24050.80c 6.5921E-08  24052.80c 1.2712E-06  24053.80c 1.4415E-07
       24054.80c 3.5881E-08  29063.80c 3.0659E-06  29065.80c 1.3678E-06
       19039.80c 2.6880E-08  19040.80c 3.3724E-12  19041.80c 1.9399E-09
        3006.80c 1.2323E-07   3007.80c 1.5004E-06  12024.80c 1.0988E-06
```

```
        12025.80c 1.3910E-07  12026.80c 1.5315E-07  25055.80c 1.1487E-05
        42092.80c 8.6748E-09  42094.80c 5.4210E-09  42095.80c 9.3385E-09
        42096.80c 9.7966E-09  42097.80c 5.6148E-09  42098.80c 1.4207E-08
        42100.80c 5.6794E-09  11023.80c 1.3235E-05  28058.80c 1.3071E-05
        28060.80c 5.0350E-06  28061.80c 2.1887E-07  28062.80c 6.9785E-07
        28064.80c 1.7772E-07  51121.80c 2.0121E-06  51123.80c 1.5050E-06
        22046.80c 1.9423E-08  22047.80c 1.7516E-08  22048.80c 1.7356E-07
        22049.80c 1.2737E-08  22050.80c 1.2196E-08   8016.80c 1.4082E-05
         8017.80c 5.3532E-09   7014.80c 2.4050E-05   7015.80c 8.7861E-08
c          Total 4.8001E-02
c
m2782   92234.80c 4.6445E-04  92235.80c 4.4898E-02  92236.80c 1.1033E-04
        92238.80c 2.6684E-03  47107.80c 4.3554E-07  47109.80c 4.0463E-07
        56130.80c 4.3721E-13  56132.80c 4.1659E-13  56134.80c 9.9692E-12
        56135.80c 2.7190E-11  56136.80c 3.2395E-11  56137.80c 4.6328E-11
        56138.80c 2.9573E-10  83209.80c 8.8902E-06   6000.80c 4.7160E-06
        20040.80c 2.7401E-08  20042.80c 1.8288E-10  20043.80c 3.8159E-11
        20044.80c 5.8963E-10  20046.80c 1.1306E-12  20048.80c 5.2858E-11
        48106.80c 6.2986E-10  48108.80c 4.4846E-10  48110.80c 6.2935E-09
        48111.80c 6.4497E-09  48112.80c 1.2159E-08  48113.80c 6.1575E-09
        48114.80c 1.4477E-08  48116.80c 3.7741E-09  27059.80c 9.6113E-07
        24050.80c 6.6266E-08  24052.80c 1.2779E-06  24053.80c 1.4490E-07
        24054.80c 3.6069E-08  29063.80c 3.0819E-06  29065.80c 1.3749E-06
        19039.80c 2.7021E-08  19040.80c 3.3900E-12  19041.80c 1.9500E-09
         3006.80c 1.2388E-07   3007.80c 1.5082E-06  12024.80c 1.1045E-06
        12025.80c 1.3983E-07  12026.80c 1.5395E-07  25055.80c 1.1547E-05
        42092.80c 8.7201E-09  42094.80c 5.4493E-09  42095.80c 9.3873E-09
        42096.80c 9.8478E-09  42097.80c 5.6442E-09  42098.80c 1.4282E-08
        42100.80c 5.7091E-09  11023.80c 1.3305E-05  28058.80c 1.3140E-05
        28060.80c 5.0613E-06  28061.80c 2.2001E-07  28062.80c 7.0150E-07
        28064.80c 1.7865E-07  51121.80c 2.0227E-06  51123.80c 1.5128E-06
        22046.80c 1.9525E-08  22047.80c 1.7608E-08  22048.80c 1.7447E-07
        22049.80c 1.2804E-08  22050.80c 1.2259E-08   8016.80c 1.4156E-05
         8017.80c 5.3812E-09   7014.80c 2.4175E-05   7015.80c 8.8320E-08
c          Total 4.8252E-02
c
m2750   92234.80c 4.5842E-04  92235.80c 4.4743E-02  92236.80c 1.1961E-04
        92238.80c 2.6947E-03  47107.80c 4.3441E-07  47109.80c 4.0359E-07
        56130.80c 4.3608E-13  56132.80c 4.1551E-13  56134.80c 9.9435E-12
        56135.80c 2.7119E-11  56136.80c 3.2311E-11  56137.80c 4.6208E-11
        56138.80c 2.9496E-10  83209.80c 8.8672E-06   6000.80c 4.7038E-06
        20040.80c 2.7331E-08  20042.80c 1.8241E-10  20043.80c 3.8061E-11
        20044.80c 5.8811E-10  20046.80c 1.1277E-12  20048.80c 5.2721E-11
        48106.80c 6.2823E-10  48108.80c 4.4730E-10  48110.80c 6.2773E-09
        48111.80c 6.4331E-09  48112.80c 1.2127E-08  48113.80c 6.1416E-09
        48114.80c 1.4439E-08  48116.80c 3.7644E-09  27059.80c 9.5865E-07
        24050.80c 6.6094E-08  24052.80c 1.2746E-06  24053.80c 1.4453E-07
        24054.80c 3.5975E-08  29063.80c 3.0739E-06  29065.80c 1.3714E-06
        19039.80c 2.6951E-08  19040.80c 3.3812E-12  19041.80c 1.9450E-09
         3006.80c 1.2356E-07   3007.80c 1.5043E-06  12024.80c 1.1017E-06
        12025.80c 1.3947E-07  12026.80c 1.5355E-07  25055.80c 1.1518E-05
        42092.80c 8.6976E-09  42094.80c 5.4353E-09  42095.80c 9.3630E-09
        42096.80c 9.8223E-09  42097.80c 5.6296E-09  42098.80c 1.4245E-08
        42100.80c 5.6944E-09  11023.80c 1.3270E-05  28058.80c 1.3106E-05
        28060.80c 5.0483E-06  28061.80c 2.1944E-07  28062.80c 6.9969E-07
        28064.80c 1.7819E-07  51121.80c 2.0174E-06  51123.80c 1.5089E-06
        22046.80c 1.9474E-08  22047.80c 1.7562E-08  22048.80c 1.7402E-07
        22049.80c 1.2771E-08  22050.80c 1.2228E-08   8016.80c 1.4119E-05
         8017.80c 5.3673E-09   7014.80c 2.4113E-05   7015.80c 8.8092E-08
c          Total 4.8127E-02
c
m2749   92234.80c 4.7313E-04  92235.80c 4.4799E-02  92236.80c 1.1967E-04
        92238.80c 2.6486E-03  47107.80c 4.3462E-07  47109.80c 4.0379E-07
        56130.80c 4.3629E-13  56132.80c 4.1571E-13  56134.80c 9.9483E-12
        56135.80c 2.7132E-11  56136.80c 3.2327E-11  56137.80c 4.6231E-11
        56138.80c 2.9511E-10  83209.80c 8.8715E-06   6000.80c 4.7061E-06
        20040.80c 2.7344E-08  20042.80c 1.8250E-10  20043.80c 3.8079E-11
        20044.80c 5.8839E-10  20046.80c 1.1283E-12  20048.80c 5.2747E-11
        48106.80c 6.2854E-10  48108.80c 4.4752E-10  48110.80c 6.2803E-09
        48111.80c 6.4362E-09  48112.80c 1.2133E-08  48113.80c 6.1446E-09
        48114.80c 1.4446E-08  48116.80c 3.7662E-09  27059.80c 9.5911E-07
        24050.80c 6.6127E-08  24052.80c 1.2752E-06  24053.80c 1.4460E-07
        24054.80c 3.5993E-08  29063.80c 3.0754E-06  29065.80c 1.3720E-06
        19039.80c 2.6964E-08  19040.80c 3.3829E-12  19041.80c 1.9459E-09
         3006.80c 1.2362E-07   3007.80c 1.5051E-06  12024.80c 1.1022E-06
```

```
        12025.80c 1.3954E-07  12026.80c 1.5363E-07  25055.80c 1.1523E-05
        42092.80c 8.7018E-09  42094.80c 5.4379E-09  42095.80c 9.3675E-09
        42096.80c 9.8271E-09  42097.80c 5.6323E-09  42098.80c 1.4252E-08
        42100.80c 5.6971E-09  11023.80c 1.3277E-05  28058.80c 1.3112E-05
        28060.80c 5.0507E-06  28061.80c 2.1955E-07  28062.80c 7.0003E-07
        28064.80c 1.7828E-07  51121.80c 2.0184E-06  51123.80c 1.5097E-06
        22046.80c 1.9484E-08  22047.80c 1.7571E-08  22048.80c 1.7410E-07
        22049.80c 1.2777E-08  22050.80c 1.2234E-08   8016.80c 1.4126E-05
         8017.80c 5.3699E-09   7014.80c 2.4125E-05   7015.80c 8.8134E-08
c          Total 4.8151E-02
c
m2757   92234.80c 4.6342E-04  92235.80c 4.4798E-02  92236.80c 1.1008E-04
        92238.80c 2.6625E-03  47107.80c 4.3457E-07  47109.80c 4.0374E-07
        56130.80c 4.3624E-13  56132.80c 4.1566E-13  56134.80c 9.9471E-12
        56135.80c 2.7129E-11  56136.80c 3.2323E-11  56137.80c 4.6225E-11
        56138.80c 2.9507E-10  83209.80c 8.8704E-06   6000.80c 4.7055E-06
        20040.80c 2.7341E-08  20042.80c 1.8248E-10  20043.80c 3.8074E-11
        20044.80c 5.8832E-10  20046.80c 1.1281E-12  20048.80c 5.2740E-11
        48106.80c 6.2846E-10  48108.80c 4.4746E-10  48110.80c 6.2796E-09
        48111.80c 6.4354E-09  48112.80c 1.2132E-08  48113.80c 6.1438E-09
        48114.80c 1.4444E-08  48116.80c 3.7657E-09  27059.80c 9.5899E-07
        24050.80c 6.6118E-08  24052.80c 1.2750E-06  24053.80c 1.4458E-07
        24054.80c 3.5988E-08  29063.80c 3.0750E-06  29065.80c 1.3719E-06
        19039.80c 2.6961E-08  19040.80c 3.3825E-12  19041.80c 1.9457E-09
         3006.80c 1.2360E-07   3007.80c 1.5049E-06  12024.80c 1.1021E-06
        12025.80c 1.3952E-07  12026.80c 1.5361E-07  25055.80c 1.1522E-05
        42092.80c 8.7007E-09  42094.80c 5.4372E-09  42095.80c 9.3664E-09
        42096.80c 9.8259E-09  42097.80c 5.6316E-09  42098.80c 1.4250E-08
        42100.80c 5.6964E-09  11023.80c 1.3275E-05  28058.80c 1.3110E-05
        28060.80c 5.0501E-06  28061.80c 2.1952E-07  28062.80c 6.9994E-07
        28064.80c 1.7825E-07  51121.80c 2.0182E-06  51123.80c 1.5095E-06
        22046.80c 1.9482E-08  22047.80c 1.7569E-08  22048.80c 1.7408E-07
        22049.80c 1.2775E-08  22050.80c 1.2232E-08   8016.80c 1.4124E-05
         8017.80c 5.3693E-09   7014.80c 2.4122E-05   7015.80c 8.8124E-08
c          Total 4.8145E-02
c
m2754   92234.80c 4.6438E-04  92235.80c 4.4843E-02  92236.80c 1.3429E-04
        92238.80c 2.6918E-03  47107.80c 4.3547E-07  47109.80c 4.0457E-07
        56130.80c 4.3715E-13  56132.80c 4.1653E-13  56134.80c 9.9678E-12
        56135.80c 2.7186E-11  56136.80c 3.2390E-11  56137.80c 4.6321E-11
        56138.80c 2.9568E-10  83209.80c 8.8888E-06   6000.80c 4.7153E-06
        20040.80c 2.7397E-08  20042.80c 1.8285E-10  20043.80c 3.8154E-11
        20044.80c 5.8954E-10  20046.80c 1.1305E-12  20048.80c 5.2850E-11
        48106.80c 6.2976E-10  48108.80c 4.4839E-10  48110.80c 6.2926E-09
        48111.80c 6.4488E-09  48112.80c 1.2157E-08  48113.80c 6.1566E-09
        48114.80c 1.4474E-08  48116.80c 3.7735E-09  27059.80c 9.6099E-07
        24050.80c 6.6256E-08  24052.80c 1.2777E-06  24053.80c 1.4488E-07
        24054.80c 3.6063E-08  29063.80c 3.0814E-06  29065.80c 1.3747E-06
        19039.80c 2.7017E-08  19040.80c 3.3895E-12  19041.80c 1.9497E-09
         3006.80c 1.2386E-07   3007.80c 1.5080E-06  12024.80c 1.1043E-06
        12025.80c 1.3981E-07  12026.80c 1.5393E-07  25055.80c 1.1546E-05
        42092.80c 8.7188E-09  42094.80c 5.4485E-09  42095.80c 9.3859E-09
        42096.80c 9.8463E-09  42097.80c 5.6433E-09  42098.80c 1.4279E-08
        42100.80c 5.7083E-09  11023.80c 1.3303E-05  28058.80c 1.3138E-05
        28060.80c 5.0606E-06  28061.80c 2.1998E-07  28062.80c 7.0139E-07
        28064.80c 1.7862E-07  51121.80c 2.0224E-06  51123.80c 1.5126E-06
        22046.80c 1.9522E-08  22047.80c 1.7605E-08  22048.80c 1.7444E-07
        22049.80c 1.2802E-08  22050.80c 1.2257E-08   8016.80c 1.4154E-05
         8017.80c 5.3804E-09   7014.80c 2.4172E-05   7015.80c 8.8307E-08
c          Total 4.8244E-02
c
m2753   92234.80c 4.5759E-04  92235.80c 4.4662E-02  92236.80c 1.1940E-04
        92238.80c 2.6898E-03  47107.80c 4.3362E-07  47109.80c 4.0286E-07
        56130.80c 4.3529E-13  56132.80c 4.1476E-13  56134.80c 9.9255E-12
        56135.80c 2.7070E-11  56136.80c 3.2253E-11  56137.80c 4.6124E-11
        56138.80c 2.9443E-10  83209.80c 8.8511E-06   6000.80c 4.6953E-06
        20040.80c 2.7281E-08  20042.80c 1.8208E-10  20043.80c 3.7992E-11
        20044.80c 5.8704E-10  20046.80c 1.1257E-12  20048.80c 5.2625E-11
        48106.80c 6.2709E-10  48108.80c 4.4649E-10  48110.80c 6.2659E-09
        48111.80c 6.4214E-09  48112.80c 1.2105E-08  48113.80c 6.1305E-09
        48114.80c 1.4413E-08  48116.80c 3.7575E-09  27059.80c 9.5691E-07
        24050.80c 6.5975E-08  24052.80c 1.2723E-06  24053.80c 1.4426E-07
        24054.80c 3.5910E-08  29063.80c 3.0683E-06  29065.80c 1.3689E-06
        19039.80c 2.6902E-08  19040.80c 3.3751E-12  19041.80c 1.9415E-09
         3006.80c 1.2333E-07   3007.80c 1.5016E-06  12024.80c 1.0997E-06
```

```
        12025.80c 1.3921E-07  12026.80c 1.5328E-07  25055.80c 1.1497E-05
        42092.80c 8.6818E-09  42094.80c 5.4254E-09  42095.80c 9.3460E-09
        42096.80c 9.8045E-09  42097.80c 5.6194E-09  42098.80c 1.4219E-08
        42100.80c 5.6840E-09  11023.80c 1.3246E-05  28058.80c 1.3082E-05
        28060.80c 5.0391E-06  28061.80c 2.1905E-07  28062.80c 6.9842E-07
        28064.80c 1.7787E-07  51121.80c 2.0138E-06  51123.80c 1.5062E-06
        22046.80c 1.9439E-08  22047.80c 1.7531E-08  22048.80c 1.7370E-07
        22049.80c 1.2747E-08  22050.80c 1.2205E-08   8016.80c 1.4094E-05
         8017.80c 5.3576E-09   7014.80c 2.4069E-05   7015.80c 8.7932E-08
c          Total 4.8040E-02
c
m2752   92234.80c 4.7278E-04  92235.80c 4.4737E-02  92236.80c 1.1480E-04
        92238.80c 2.6798E-03  47107.80c 4.3430E-07  47109.80c 4.0349E-07
        56130.80c 4.3597E-13  56132.80c 4.1541E-13  56134.80c 9.9410E-12
        56135.80c 2.7113E-11  56136.80c 3.2303E-11  56137.80c 4.6197E-11
        56138.80c 2.9489E-10  83209.80c 8.8650E-06   6000.80c 4.7027E-06
        20040.80c 2.7324E-08  20042.80c 1.8236E-10  20043.80c 3.8051E-11
        20044.80c 5.8796E-10  20046.80c 1.1274E-12  20048.80c 5.2708E-11
        48106.80c 6.2808E-10  48108.80c 4.4719E-10  48110.80c 6.2757E-09
        48111.80c 6.4315E-09  48112.80c 1.2124E-08  48113.80c 6.1401E-09
        48114.80c 1.4436E-08  48116.80c 3.7634E-09  27059.80c 9.5841E-07
        24050.80c 6.6078E-08  24052.80c 1.2743E-06  24053.80c 1.4449E-07
        24054.80c 3.5967E-08  29063.80c 3.0732E-06  29065.80c 1.3710E-06
        19039.80c 2.6944E-08  19040.80c 3.3804E-12  19041.80c 1.9445E-09
         3006.80c 1.2353E-07   3007.80c 1.5040E-06  12024.80c 1.1014E-06
        12025.80c 1.3943E-07  12026.80c 1.5352E-07  25055.80c 1.1515E-05
        42092.80c 8.6955E-09  42094.80c 5.4339E-09  42095.80c 9.3607E-09
        42096.80c 9.8199E-09  42097.80c 5.6282E-09  42098.80c 1.4241E-08
        42100.80c 5.6930E-09  11023.80c 1.3267E-05  28058.80c 1.3102E-05
        28060.80c 5.0470E-06  28061.80c 2.1939E-07  28062.80c 6.9951E-07
        28064.80c 1.7815E-07  51121.80c 2.0169E-06  51123.80c 1.5086E-06
        22046.80c 1.9470E-08  22047.80c 1.7558E-08  22048.80c 1.7398E-07
        22049.80c 1.2767E-08  22050.80c 1.2225E-08   8016.80c 1.4116E-05
         8017.80c 5.3660E-09   7014.80c 2.4107E-05   7015.80c 8.8070E-08
c          Total 4.8115E-02
c
m2751   92234.80c 4.7310E-04  92235.80c 4.4767E-02  92236.80c 1.1488E-04
        92238.80c 2.6816E-03  47107.80c 4.3460E-07  47109.80c 4.0376E-07
        56130.80c 4.3627E-13  56132.80c 4.1569E-13  56134.80c 9.9477E-12
        56135.80c 2.7131E-11  56136.80c 3.2325E-11  56137.80c 4.6228E-11
        56138.80c 2.9509E-10  83209.80c 8.8710E-06   6000.80c 4.7058E-06
        20040.80c 2.7342E-08  20042.80c 1.8249E-10  20043.80c 3.8077E-11
        20044.80c 5.8836E-10  20046.80c 1.1282E-12  20048.80c 5.2743E-11
        48106.80c 6.2850E-10  48108.80c 4.4749E-10  48110.80c 6.2800E-09
        48111.80c 6.4358E-09  48112.80c 1.2133E-08  48113.80c 6.1442E-09
        48114.80c 1.4445E-08  48116.80c 3.7660E-09  27059.80c 9.5905E-07
        24050.80c 6.6123E-08  24052.80c 1.2751E-06  24053.80c 1.4459E-07
        24054.80c 3.5991E-08  29063.80c 3.0752E-06  29065.80c 1.3720E-06
        19039.80c 2.6963E-08  19040.80c 3.3827E-12  19041.80c 1.9458E-09
         3006.80c 1.2361E-07   3007.80c 1.5050E-06  12024.80c 1.1021E-06
        12025.80c 1.3953E-07  12026.80c 1.5362E-07  25055.80c 1.1523E-05
        42092.80c 8.7013E-09  42094.80c 5.4376E-09  42095.80c 9.3670E-09
        42096.80c 9.8265E-09  42097.80c 5.6320E-09  42098.80c 1.4251E-08
        42100.80c 5.6968E-09  11023.80c 1.3276E-05  28058.80c 1.3111E-05
        28060.80c 5.0504E-06  28061.80c 2.1954E-07  28062.80c 6.9998E-07
        28064.80c 1.7827E-07  51121.80c 2.0183E-06  51123.80c 1.5096E-06
        22046.80c 1.9483E-08  22047.80c 1.7570E-08  22048.80c 1.7409E-07
        22049.80c 1.2776E-08  22050.80c 1.2233E-08   8016.80c 1.4125E-05
         8017.80c 5.3696E-09   7014.80c 2.4123E-05   7015.80c 8.8129E-08
c          Total 4.8148E-02
c
m2756   92234.80c 4.4929E-04  92235.80c 4.4823E-02  92236.80c 1.1975E-04
        92238.80c 2.6788E-03  47107.80c 4.3491E-07  47109.80c 4.0405E-07
        56130.80c 4.3658E-13  56132.80c 4.1599E-13  56134.80c 9.9549E-12
        56135.80c 2.7150E-11  56136.80c 3.2348E-11  56137.80c 4.6261E-11
        56138.80c 2.9530E-10  83209.80c 8.8774E-06   6000.80c 4.7092E-06
        20040.80c 2.7362E-08  20042.80c 1.8262E-10  20043.80c 3.8104E-11
        20044.80c 5.8878E-10  20046.80c 1.1290E-12  20048.80c 5.2781E-11
        48106.80c 6.2895E-10  48108.80c 4.4781E-10  48110.80c 6.2845E-09
        48111.80c 6.4405E-09  48112.80c 1.2141E-08  48113.80c 6.1486E-09
        48114.80c 1.4456E-08  48116.80c 3.7687E-09  27059.80c 9.5974E-07
        24050.80c 6.6170E-08  24052.80c 1.2760E-06  24053.80c 1.4469E-07
        24054.80c 3.6017E-08  29063.80c 3.0774E-06  29065.80c 1.3729E-06
        19039.80c 2.6982E-08  19040.80c 3.3851E-12  19041.80c 1.9472E-09
         3006.80c 1.2370E-07   3007.80c 1.5061E-06  12024.80c 1.1029E-06
```

```
       12025.80c 1.3963E-07  12026.80c 1.5373E-07  25055.80c 1.1531E-05
       42092.80c 8.7076E-09  42094.80c 5.4415E-09  42095.80c 9.3737E-09
       42096.80c 9.8336E-09  42097.80c 5.6360E-09  42098.80c 1.4261E-08
       42100.80c 5.7009E-09  11023.80c 1.3285E-05  28058.80c 1.3121E-05
       28060.80c 5.0541E-06  28061.80c 2.1970E-07  28062.80c 7.0049E-07
       28064.80c 1.7839E-07  51121.80c 2.0197E-06  51123.80c 1.5107E-06
       22046.80c 1.9497E-08  22047.80c 1.7583E-08  22048.80c 1.7422E-07
       22049.80c 1.2785E-08  22050.80c 1.2242E-08   8016.80c 1.4135E-05
        8017.80c 5.3735E-09   7014.80c 2.4141E-05   7015.80c 8.8193E-08
c          Total 4.8182E-02
c
c --- Control Cards ---------------------------------------------------------
mode  n
kcode 1000000 1 50 1050
ksrc  0 13 2 0 -13 2 13 0 2 -13 0 4
      0 13 -2 0 -13 -2 13 0 -2 -13 0 -4
c print
c kopts blocksize=10 kinetics=yes precursor=yes
```

Simple Model: MCNP6 Input Deck for Configuration 2 (Potassium-Filled Steel Cans):

```
ORALLOY (93.15 235U) METAL ANNULI FOR POTASSIUM WORTH MEASUREMENT
c Case 1 = Empty SS Cans
c Case 2 = K-Filled SS Cans
c
c John Darrell Bess - Idaho National Laboratory
c Last Updated: June 4, 2014
c
c
c Cell Cards ******************************************************************
c ------ Steel Cans ------
1304  1304 8.5461E-02  1019 -1304  imp:n=1  $ Upper Can
2304  1304 8.5461E-02  2019 -2304  imp:n=1  $ Lower Can
1019  1019 1.2937E-02       -1019  imp:n=1  $ Upper Potassium
2019  1019 1.2937E-02       -2019  imp:n=1  $ Lower Potassium
c
c ------ HEU Annulus ------
1     1    4.7871E-02  9    -1     imp:n=1
c
c ------ Void Spaces------
29    0  1304 2304 #1 -9999  imp:n=1 $ Gaps
30    0   9999  imp:n=0 $ The Great Void

c Surface Cards ***************************************************************
c ------ Steel Cans ------
1304  rcc 0 0  0.000000 0 0 6.35000 8.890000  $ Outer/Upper, 2.5"
2304  rcc 0 0 -7.620000 0 0 7.62000 8.890000  $ Outer/Lower, 3"
1019  rcc 0 0  0.513080 0 0 5.32384 8.732520  $ Inner/Upper, 2.5"
2019  rcc 0 0 -7.106920 0 0 6.59384 8.732520  $ Inner/Lower, 3"
c
c ------ Annulus ------
c --------- Outer Surfaces ---------
1     rcc 0 0 -7.620000 0 0 14.181666 16.51    $ Top/Upper
c
c --------- Inner Surfaces ---------
9     cz 8.89
c
c ------ Problem Boundary ------
9999  rcc 0 0 -8.000000 0 0 15.000000 17.000000
c

c Data Cards ******************************************************************
c --- Material Cards ------------------------------------------------------
c ------ Stainless Steel 304 Cans ------
m1304   6000.80c 1.9542E-04  24050.80c 7.4531E-04  24052.80c 1.4373E-02
       24053.80c 1.6297E-03  24054.80c 4.0567E-04  28058.80c 5.4447E-03
       28060.80c 2.0973E-03  28061.80c 9.1168E-05  28062.80c 2.9068E-04
       28064.80c 7.4028E-05  25055.80c 8.5446E-04  15031.80c 5.7803E-04
       16032.80c 2.9365E-05  16033.80c 1.9380E-05  16034.80c 3.4100E-05
       16036.80c 2.0859E-05  14028.80c 1.6470E-07  14029.80c 9.3328E-07
       14030.80c 2.1960E-09   7014.80c 1.6696E-04   7015.80c 6.0996E-07
       26054.80c 3.4141E-03  26056.80c 5.3593E-02  26057.80c 1.2377E-03
       26058.80c 1.6472E-04
c          Total 8.5461E-02
mt1304 fe56.22t
c
c ------ Potassium ------
m1019  19039.80c 1.2064E-02  19040.80c 1.5136E-06  19041.80c 8.7065E-04
c          Total 1.2937E-02
c
c ------ HEU Annulus ------
m1     92234.80c 4.6572E-04  92235.80c 4.4624E-02  92236.80c 1.1267E-04
       92238.80c 2.6686E-03
c         Total 4.7871E-02
c
c --- Control Cards -------------------------------------------------------
mode  n
kcode 1000000 1 50 1050
ksrc  0 13 2 0 -13 2 13 0 2 -13 0 4
      0 13 -2 0 -13 -2 13 0 -2 -13 0 -4
c print
c kopts blocksize=10 kinetics=yes precursor=yes
```

Simple Model: SERPENT Input Deck for Configuration 2 (Potassium-Filled Steel Cans):

```
% ORALLOY (93.15 235U) METAL ANNULI FOR POTASSIUM WORTH MEASUREMENT
% Case 1 = Empty SS Cans
% Case 2 = K-Filled SS Cans
%
% John Darrell Bess - Idaho National Laboratory
% Last Updated: November 25, 2014
%
%
% Cell Cards ********************************************************************
% ------ Steel Cans ------
cell  c1304 0 m1304 1019 -1304  % Upper Can
cell  c2304 0 m1304 2019 -2304  % Lower Can
cell  c1019 0 m1019 -1019       % Upper Potassium
cell  c2019 0 m1019 -2019       % Lower Potassium
%
% ------ HEU Annulus ------
cell  1 0 m1 -1 9
%
% ------ Void Spaces------
cell  c29 0 void 1304 2304 -9  % Gaps
cell  c30 0 void 1 -9999       % Gaps
cell  c31 0 outside 9999       % The Great Void
% Surface Cards ****************************************************************
% ------ Steel Cans ------
surf  1304 cyl 0 0 8.89 0 6.35   % Outer/Upper, 2.5"
surf  2304 cyl 0 0 8.89 -7.62 0  % Outer/Lower, 3"
surf  1019 cyl 0 0 8.73252 0.51308 5.83692  % Inner/Upper, 2.5"
surf  2019 cyl 0 0 8.73252 -7.10692 -0.51308  % Inner/Lower, 3"
%
% ------ Annulus ------
% --------- Outer Surfaces ---------
surf  1 cyl 0 0 16.51 -7.62 6.561666
%
% --------- Inner Surfaces ---------
surf  9 cyl 0 0 8.89 -7.62 6.561666
%
% ------ Problem Boundary ------
surf  9999 cyl 0 0 17 -8 7
%
% Data Cards ********************************************************************
% --- Material Cards ----------------------------------------------------------
% ------ Stainless Steel 304 Cans ------
mat   m1304 sum
        6000.03c 1.9542E-04  24050.03c 7.4531E-04  24052.03c 1.4373E-02
       24053.03c 1.6297E-03  24054.03c 4.0567E-04  28058.03c 5.4447E-03
       28060.03c 2.0973E-03  28061.03c 9.1168E-05  28062.03c 2.9068E-04
       28064.03c 7.4028E-05  25055.03c 8.5446E-04  15031.03c 5.7803E-04
       16032.03c 2.9365E-05  16033.03c 1.9380E-05  16034.03c 3.4100E-05
       16036.03c 2.0859E-05  14028.03c 1.6470E-07  14029.03c 9.3328E-07
       14030.03c 2.1960E-09   7014.03c 1.6696E-04   7015.03c 6.0996E-07
       26054.03c 3.4141E-03  26056.03c 5.3593E-02  26057.03c 1.2377E-03
       26058.03c 1.6472E-04
%          Total 8.5461E-02
%
% ------ Potassium ------
mat   m1019 sum
       19039.03c 1.2064E-02  19040.03c 1.5136E-06  19041.03c 8.7065E-04
%          Total 1.2937E-02
%
% ------ HEU Annulus ------
mat   m1 sum
       92234.03c 4.6572E-04  92235.03c 4.4624E-02  92236.03c 1.1267E-04
       92238.03c 2.6686E-03
%         Total 4.7871E-02
%
% --- Control Cards -----------------------------------------------------------
set acelib "/home/bessjd/SERPENT/xsdata/xsdata_nf7"
% set opti 3
set ures 1
set bc 1  % Vacuum
set pop 1000000 1000 50 1.0
%
% plot  1 6800 3000 0 -17 17 -8 7
```

Simple Model: KENO-VI Input Deck for Configuration 2 (Potassium-Filled Steel Cans):

```
'Input generated by GeeWiz SCALE 6.1 Compiled on Tue Sep  6 15:23:32 2011
=csas6
simple heu-k benchmark w/ k
ce_v7_endf
read composition
 u-234       1 0 0.00046572 300   end
 u-235       1 0 0.044624 300   end
 u-236       1 0 0.00011267 300   end
 u-238       1 0 0.0026686 300   end
 c           2 0 0.00019542 300   end
 cr          2 0 0.017153 300   end
 ni          2 0 0.0079979 300   end
 mn          2 0 0.00085446 300   end
 si          2 0 0.00062678 300   end
 p           2 0 3.41e-05 300   end
 s           2 0 2.196e-05 300   end
 n           2 0 0.00016757 300   end
 fe          2 0 0.058461 300   end
 k           3 0 0.012937 300   end
end composition
read parameter
 gen=1050
 npg=1000000
 nsk=50
 htm=yes
end parameter
read geometry
global unit 1
 cylinder 1  8.73252  5.32384        0   origin  x=0 y=0 z=0.51308
 cylinder 2  8.73252  6.59384        0   origin  x=0 y=0 z=-7.10692
 cylinder 3     8.89     6.35        0
 cylinder 4     8.89     7.62        0   origin  x=0 y=0 z=-7.62
 cylinder 5     8.89  14.18167        0   origin  x=0 y=0 z=-7.62
 cylinder 6    16.51  14.18167        0   origin  x=0 y=0 z=-7.62
 media 0 1 1
 media 0 1 2
 media 2 1 -1 3
 media 2 1 -2 4
 media 0 1 -3 -4 5
 media 1 1 -5 6
 boundary 6
end geometry
end data
end
```

A.2 Buckling and Extrapolation Length Configurations

Buckling and extrapolation length measurements were not made.

A.3 Spectral-Characteristics Configurations

Spectral characteristics measurements were not made.

A.4 Reactivity-Effects Configurations

Models, details, and information provided in Appendix A.1 were also utilized to evaluate the reactivity-effect measurement.

A.5 Reactivity Coefficient Configurations

Reactivity coefficient measurements were not made.

A.6 Kinetics Parameter Configurations

Kinetics measurements were not made.

A.7 Reaction-Rate Configurations

Reaction-rate distribution measurements were not made.

A.8 Power Distribution Configurations

Power distribution measurements were not made.

A.9 Isotopic Configurations

Isotopic measurements were not made.

A.10 Configurations of Other Miscellaneous Types of Measurements

Other miscellaneous types of measurements were not made.

APPENDIX B: CALCULATED SPECTRAL DATA

The neutron spectral calculations provided below were obtained from the output files for the input decks used to obtain the results in Section 4.1. Spectral data using the ENDF/B-VII.1 neutron cross section library is provided here for the MCNP6 analysis and the ENDF/B-VII.0 (238-group and continuous energy) library for the KENO analyses.

B.1 MCNP-Calculated Spectral Data

A summary of the computed neutron spectral data using MCNP6 for the benchmark model is provided in Tables B.1-1 and B.1-2 for Configurations 1 and 2, respectively.

Table B.1-1. Neutron Spectral Data for Benchmark Model for Configuration 1.

Model		Detailed	Simple
Neutron Cross Section Library		ENDF/B-VII.1	ENDF/B-VII.1
$\mathbf{k_{eff}}$		0.99954	0.99542
$\mathbf{\pm\sigma_k}$		0.00002	0.00002
Neutron Leakage (%)[(a)]		57.14	57.15
Neutron Capture (%)		4.50	4.49
Neutron (x,xn) Reactions (%)		0.25	0.25
Neutron Fission (%)		38.11	38.11
Fission Fraction, by Energy (%)	**Thermal (<0.625 eV)**	0.00	0.00
	Intermediate	5.21	5.21
	Fast (>100 keV)	94.79	94.79
Average Number of Neutrons Produced per Fission		2.599	2.599
Energy of Average Neutron Lethargy Causing Fission (MeV)		0.82287	0.82335
Neutron Generation Time, Λ (nsec)		7.27910	7.24003
Rossi-α ($nsec^{-1}$)		-8.819E-04	-8.72E-04
$\mathbf{\beta_{eff}}$		0.00642	0.00636

(a) The neutron leakage is calculated using the neutron balance tables provided in the MCNP output file. The weight fraction of neutrons lost due to escaping the boundaries of the benchmark model are divided by the total weight fraction of neutron loss. Similar calculations are performed to evaluate neutron capture, (n,xn), and fission percentages.

Table B.1-2. Neutron Spectral Data for Benchmark Model for Configuration 2.

Model		Detailed	Simple
Neutron Cross Section Library		ENDF/B-VII.1	ENDF/B-VII.1
$\mathbf{k_{eff}}$		0.99579	0.99564
$\mathbf{\pm\sigma_k}$		0.00002	0.00002
Neutron Leakage (%)[(a)]		56.92	56.93
Neutron Capture (%)		4.69	4.69
Neutron (x,xn) Reactions (%)		0.25	0.25
Neutron Fission (%)		38.14	38.13
Fission Fraction, by Energy (%)	**Thermal (<0.625 eV)**	0.00	0.00
	Intermediate	5.24	5.24
	Fast (>100 keV)	94.76	94.76
Average Number of Neutrons Produced per Fission		2.598	2.598
Energy of Average Neutron Lethargy Causing Fission (MeV)		0.82000	0.82045
Neutron Generation Time, Λ (nsec)		7.29718	7.25363
Rossi-α ($nsec^{-1}$)		-8.786E-04	-8.847E-04
$\mathbf{\beta_{eff}}$		0.00641	0.00642

(a) The neutron leakage is calculated using the neutron balance tables provided in the MCNP output file. The weight fraction of neutrons lost due to escaping the boundaries of the benchmark model are divided by the total weight fraction of neutron loss. Similar calculations are performed to evaluate neutron capture, (n,xn), and fission percentages.

B.2 KENO-Calculated Spectral Data

A summary of the computed neutron spectral data using KENO-VI for the simple benchmark model is provided in Tables B.1-3 and B.1-4 for Configurations 1 and 2, respectively.

Table B.1-3. Neutron Spectral Data for Benchmark Model Case 1.

Neutron Cross Section Library	ENDF/B-VII.0 (238-group)
$\mathbf{k_{eff}}$	0.995275
$\pm\sigma_k$	0.000027
Energy of Average Neutron Lethargy Causing Fission (MeV)	0.825621
$\pm\sigma_{EALF}$	0.000032
Average Number of Neutrons Produced per Fission	2.59898
$\pm\sigma_\nu$	0.00001
Mean Free Path (cm)	2.01294
$\pm\sigma_\lambda$	0.00004

Table B.1-4. Neutron Spectral Data for Benchmark Model Case 2.

Neutron Cross Section Library	ENDF/B-VII.0 (238-group)
$\mathbf{k_{eff}}$	0.995486
$\pm\sigma_k$	0.000025
Energy of Average Neutron Lethargy Causing Fission (MeV)	0.822798
$\pm\sigma_{EALF}$	0.000031
Average Number of Neutrons Produced per Fission	2.59838
$\pm\sigma_\nu$	0.00001
Mean Free Path (cm)	2.44459
$\pm\sigma_\lambda$	0.00007

APPENDIX C: POTASSIUM CROSS SECTION UNCERTAINTIES

Discussions with Dr. A. C. (Skip) Kahler (November through December 2014) have resulted in the below uncertainty plots for ^{39}K and ^{41}K. No uncertainty data exists for ^{40}K. ^{39}K only has resonance parameter uncertainties that stop at 1 MeV; the quality is suspect near the approach to this upper energy limit and capture, in particular, appears small. The data for ^{41}K appears to be a little more complete. The charts below are for cross section processed using NJOY and provided by Skip Kahler from LANL.

The available data below are the following:

- Figure C.1-1. ^{39}K Correlation Matrix for Elastic Scattering,
- Figure C.1-2. ^{39}K Correlation Matrix for Capture and Elastic Scattering,
- Figure C.1-3. ^{39}K Correlation Matrix for Capture,
- Figure C.1-4. ^{41}K Correlation Matrix for Elastic Scattering,
- Figure C.1-5. ^{41}K Correlation Matrix for Capture and Elastic Scattering,
- Figure C.1-6. ^{41}K Correlation Matrix for Inelastic Scattering,
- Figure C.1-7. ^{41}K Correlation Matrix for n,2n, and
- Figure C.1-8. ^{41}K Correlation Matrix for Capture.

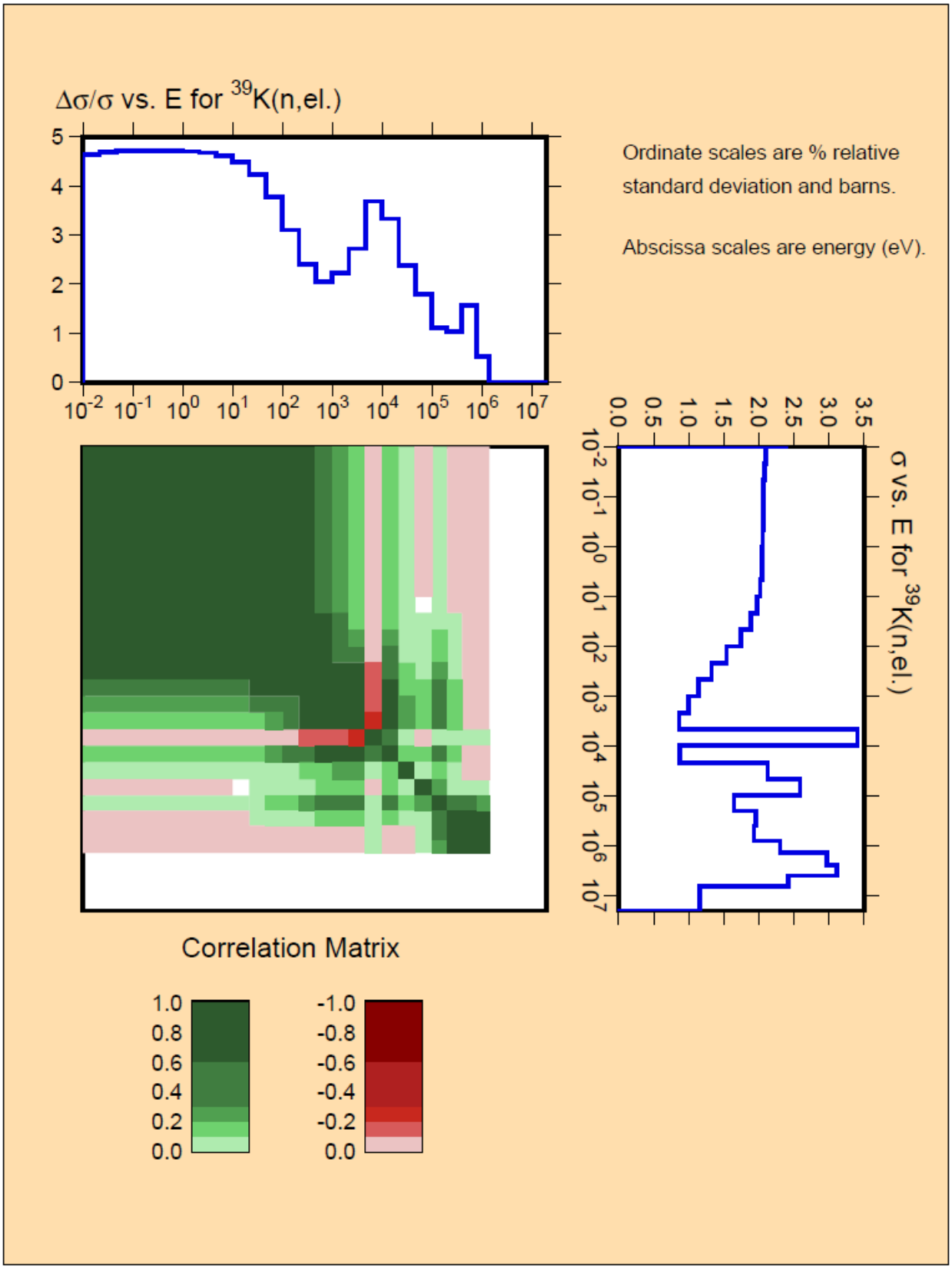

Figure C.1-1. ^{39}K Correlation Matrix for Elastic Scattering.

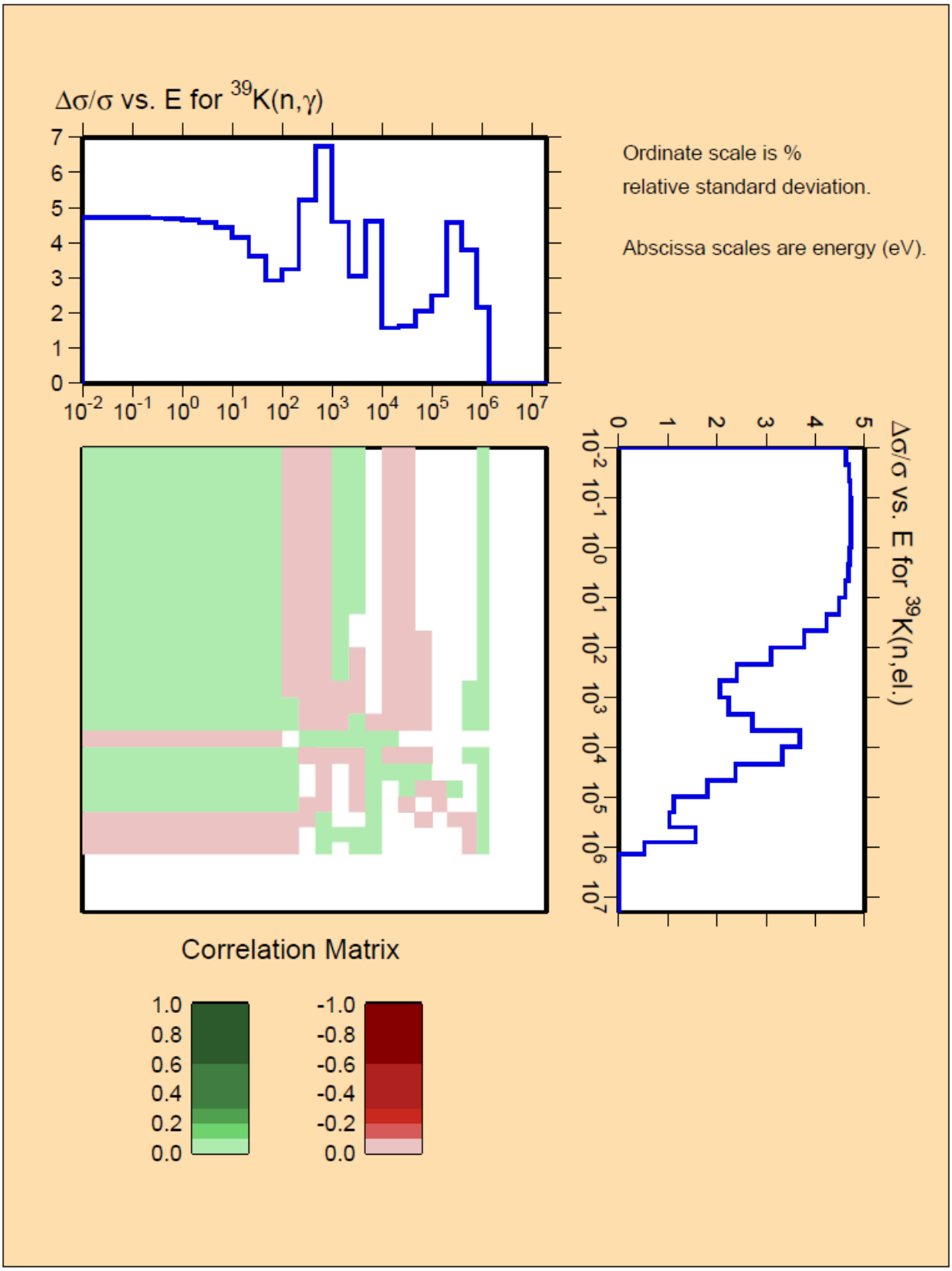

Figure C.1-2. ^{39}K Correlation Matrix for Capture and Elastic Scattering.

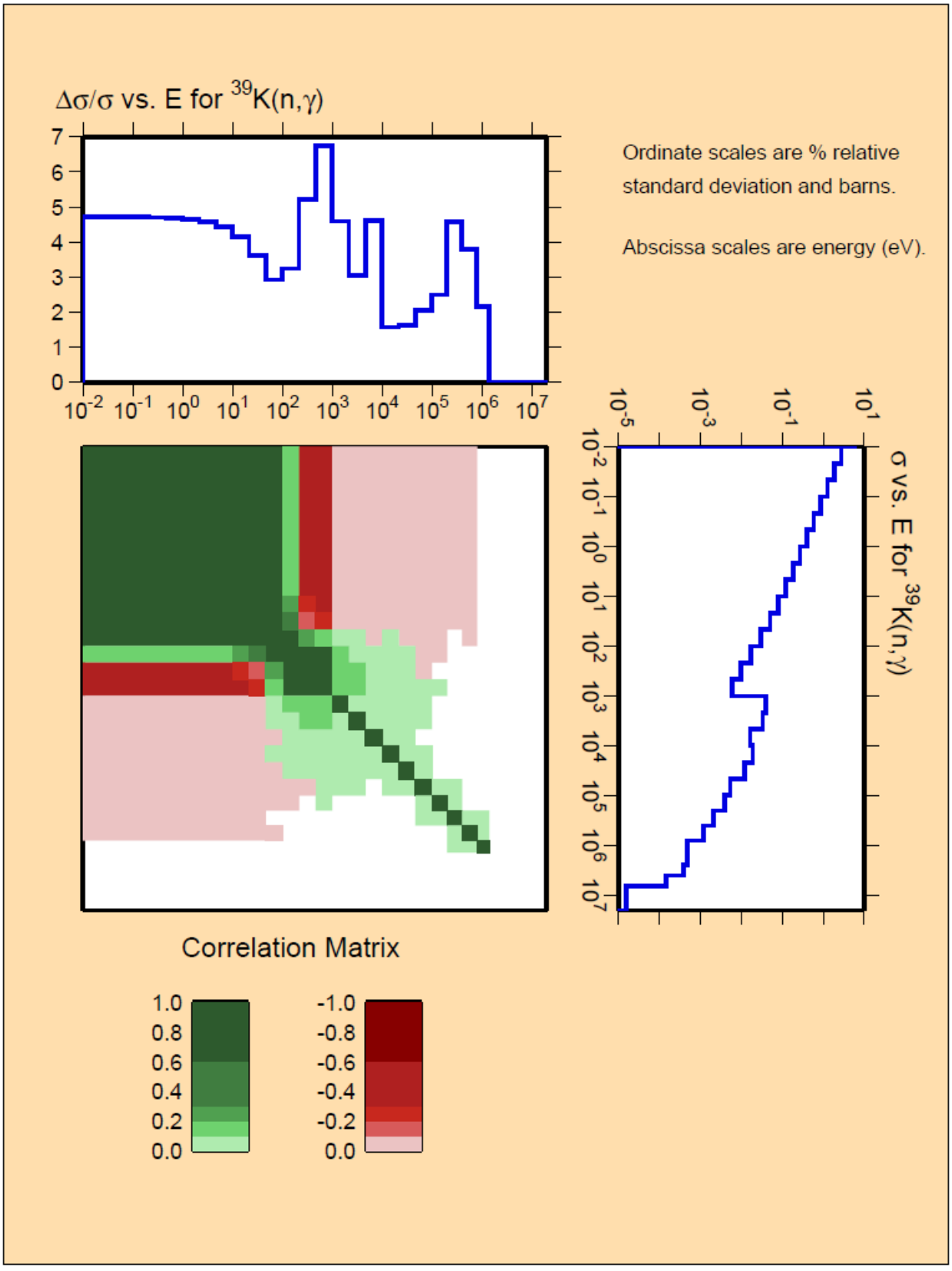

Figure C.1-3. ^{39}K Correlation Matrix for Capture.

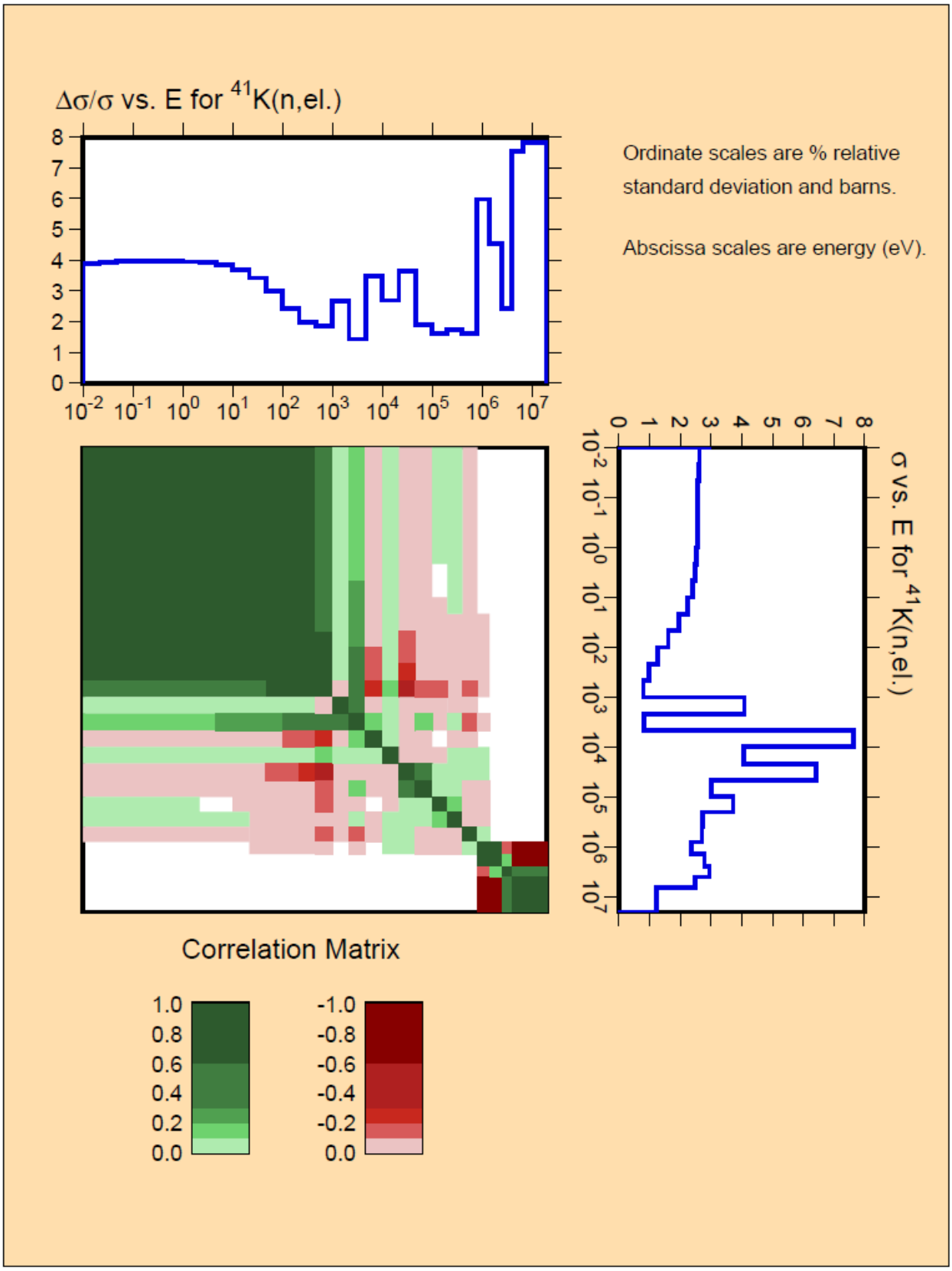

Figure C.1-4. ^{41}K Correlation Matrix for Elastic Scattering.

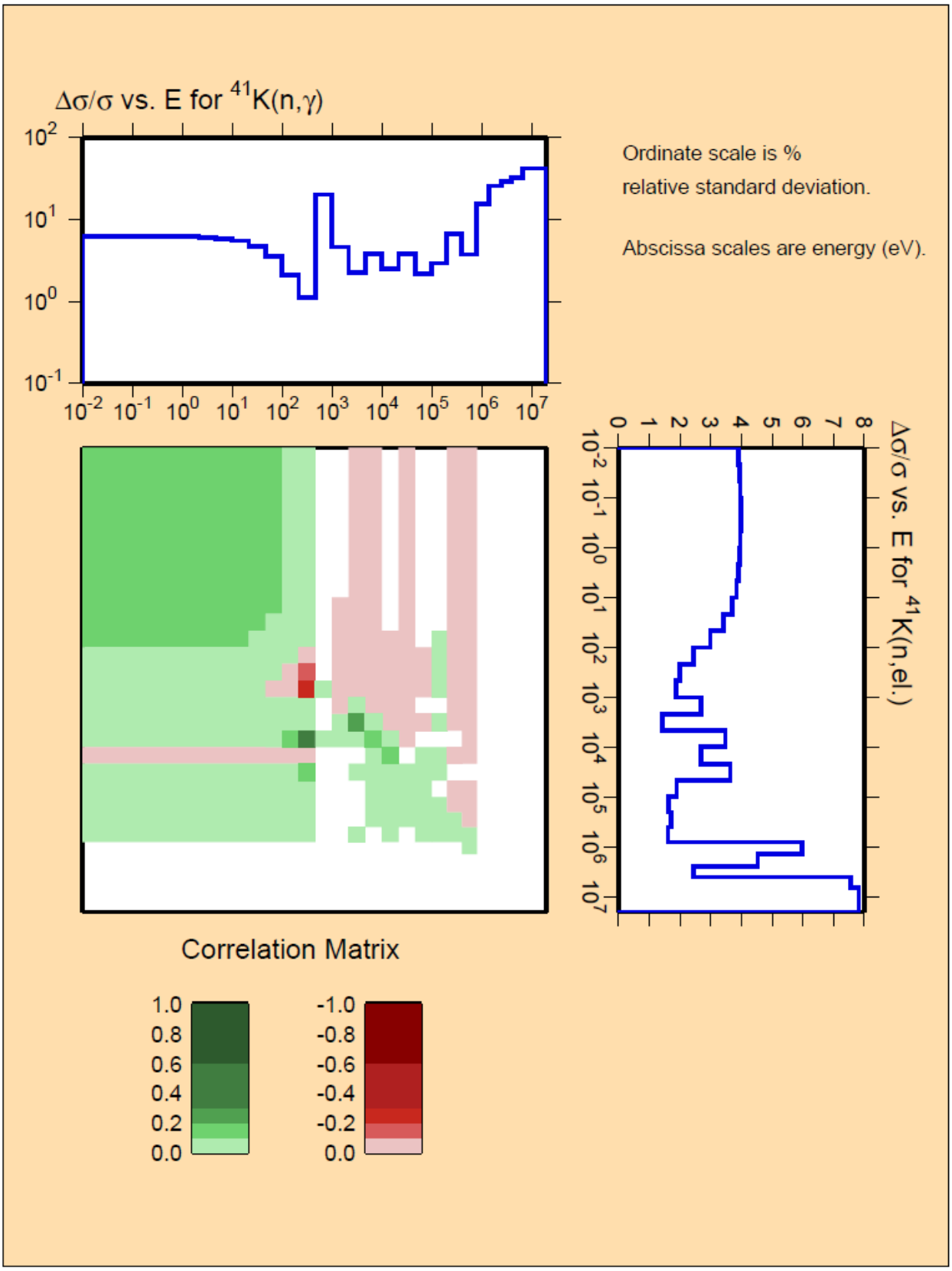

Figure C.1-5. ^{41}K Correlation Matrix for Capture and Elastic Scattering.

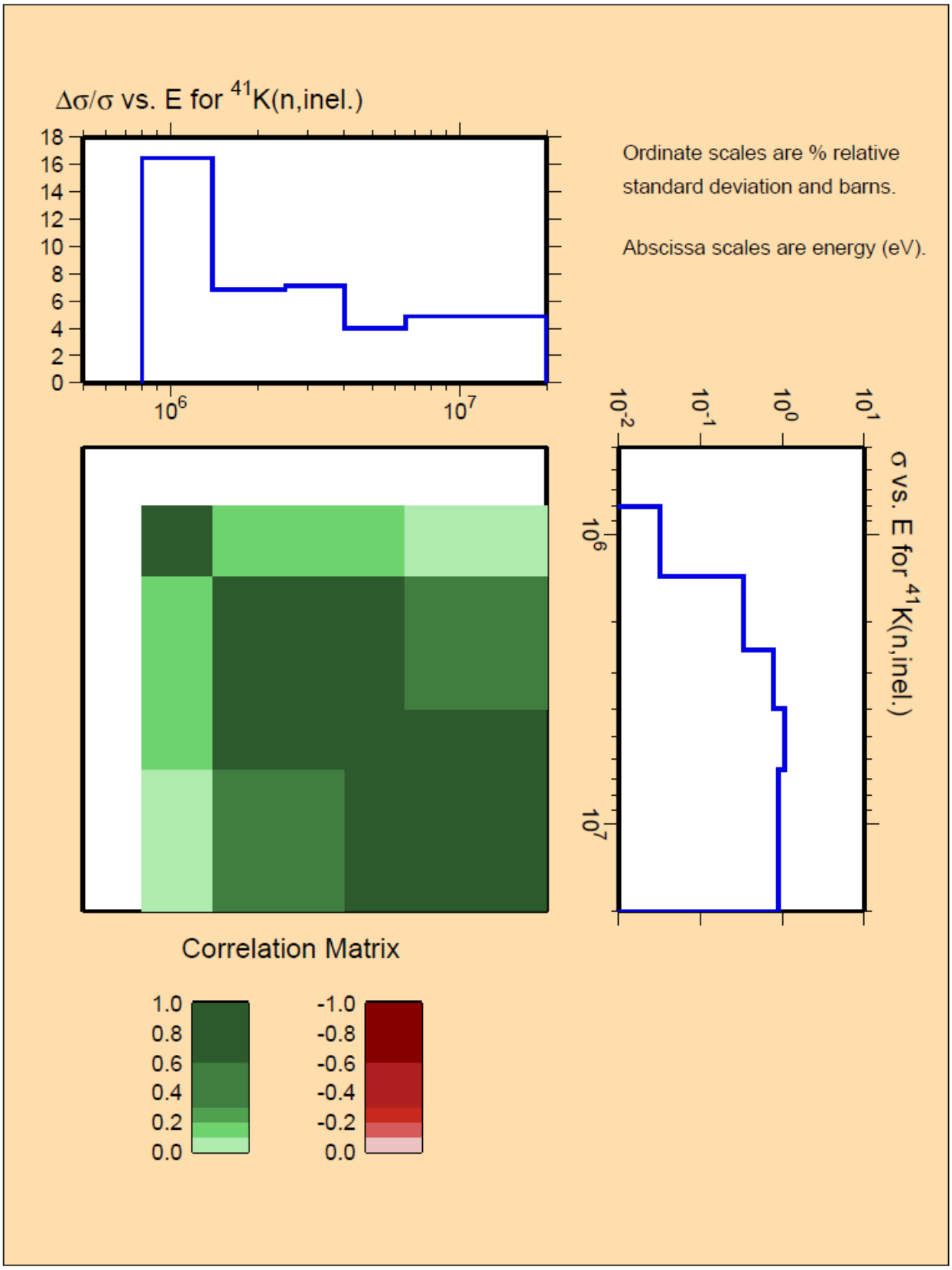

Figure C.1-6. ^{41}K Correlation Matrix for Inelastic Scattering.

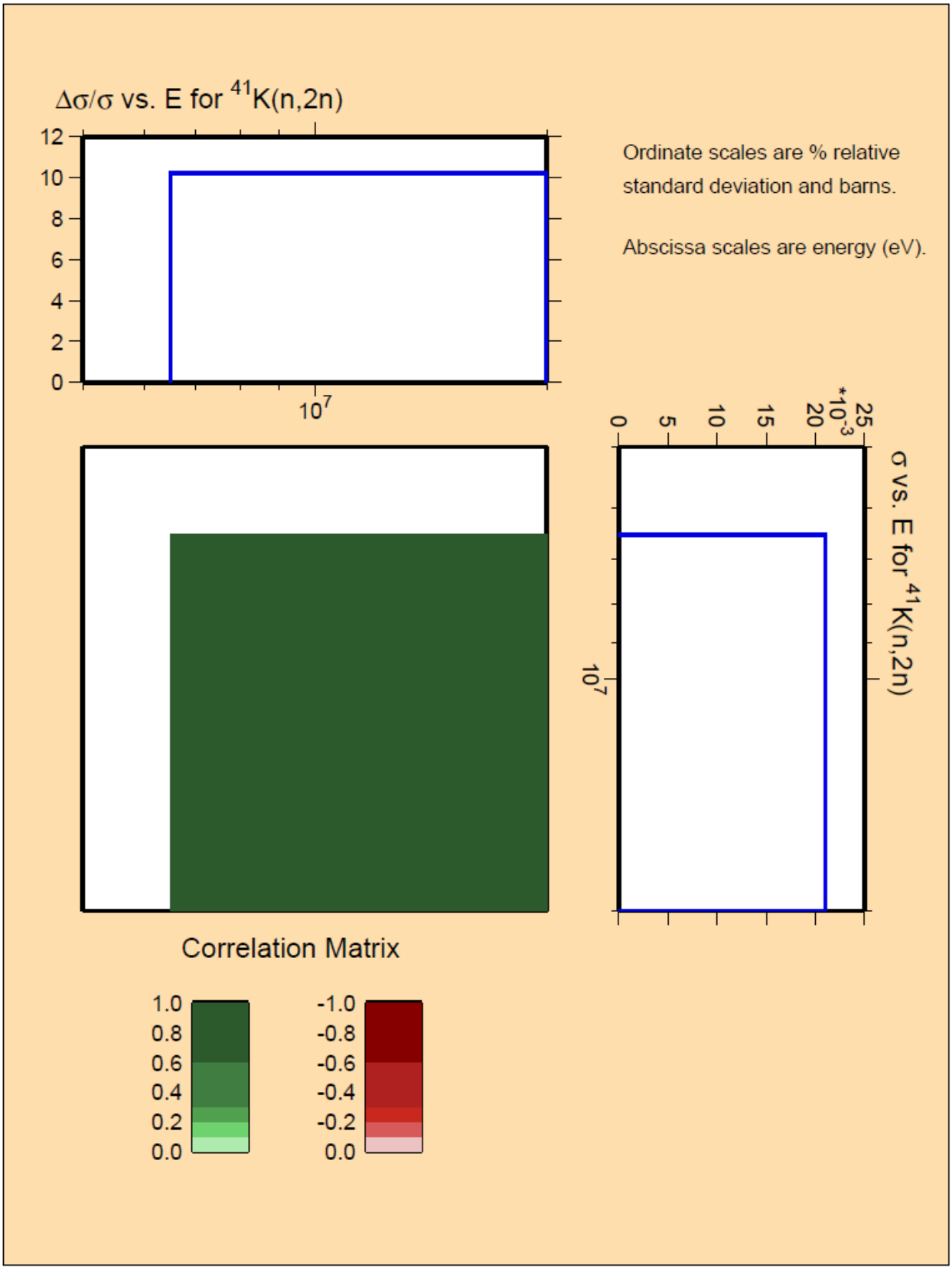

Figure C.1-7. ^{41}K Correlation Matrix for n,2n.

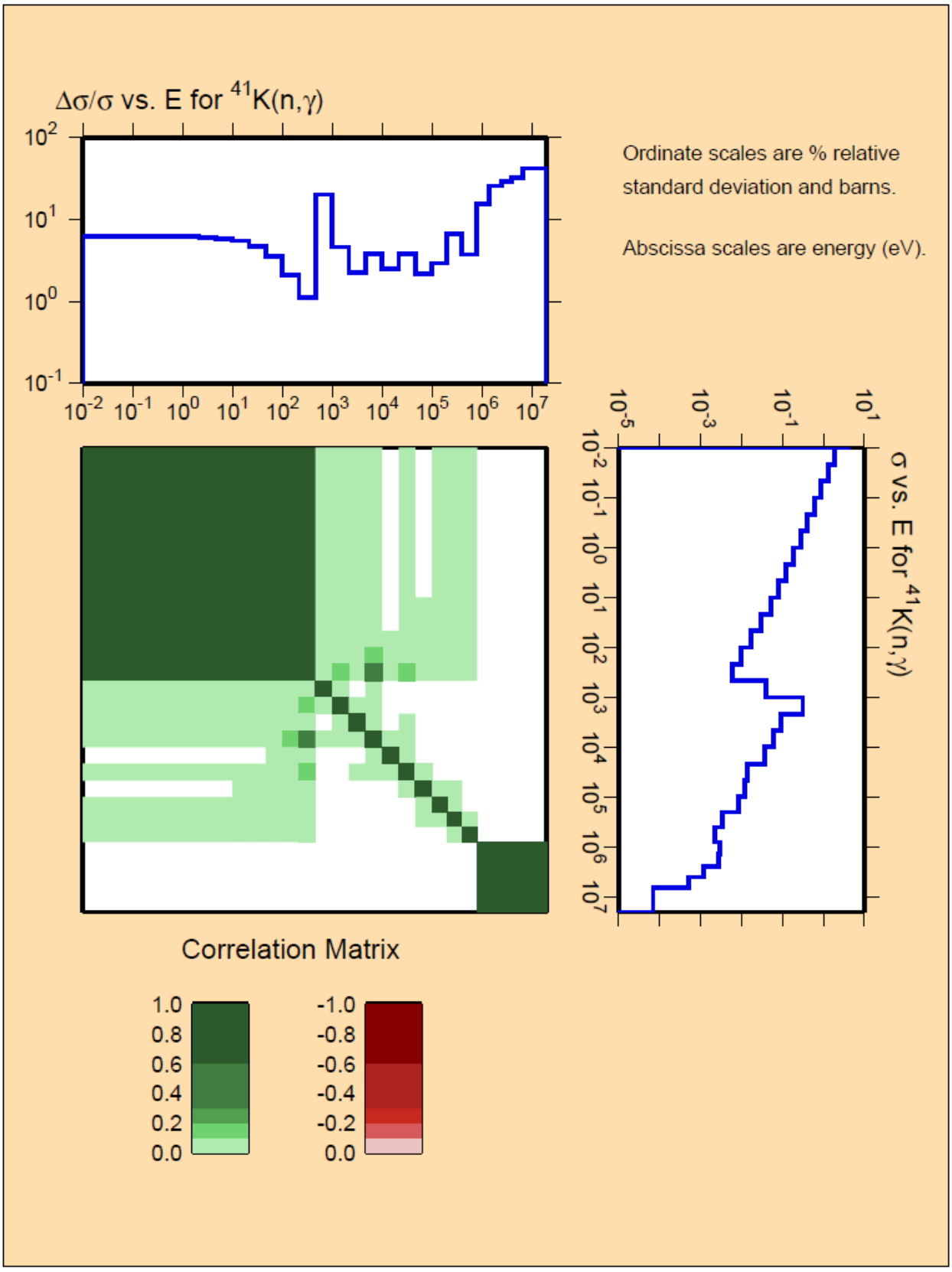

Figure C.1-8. ^{41}K Correlation Matrix for Capture.

APPENDIX D: SENSITIVITY STUDIES

Sensitivity studies were performed using the Simple Benchmark Model in TSUNAMI-3D (ENDF/B-VII.0) and MCNP6.1 (ENDF/B-VII.1). Approximately the top 20 to 30 contributors from the sensitivity data files are provided herein. MCNP6.1 can calculate sensitivities to scattering angles. The scattering (s), elastic (e), and/or inelastic (i) scattering angles in bins 0, 1, 2, and 3 (angles 180°-135°, 135°-90°, 90°-45°, and 45°-0°, respectively) are included when relevant. There are notable differences between the TSUNAMI and MCNP results in regards to absolute sensitivity and uncertainties for some of the isotope/reaction combinations. Because most of the potassium cross section sensitivities are very small, separate tables are provided with those sensitivities greater than 1×10^{-6} for the potassium isotopes. The absolute sensitivity in the potassium reactivity measurement, $\tilde{S}$, is computed using the following equation for a given sensitivity, S, isotope/reaction (i/j) combination divided by their respective calculated eigenvalue, k, where the subscripts 1 and 2 denote the benchmark model configurations without and with potassium in the steel cans, respectively:

$$\tilde{S} = \left|\frac{S_{i,j,1}}{k_1} - \frac{S_{i,j,2}}{k_2}\right|$$

The total sensitivity is calculated as the square-root of the sum of the squares of the individual sensitivities reported in the tables. The impact of neglecting the complete list of smaller sensitivities is considered negligible.

D.1 TSUNAMI-3D-Calculated Sensitivity Data

A summary of the computed sensitivity data using TSUNAMI-3D and ENDF/B-VII.0 neutron cross-section data for the benchmark model is provided in Tables D.1-1 and D.1-2 for Configurations 1 and 2, respectively. Table D.1-3 provides the sensitivity for just the potassium constituents in Configuration 2. Table D.1-4 provides the sensitivity for the potassium worth measurement.

Table D.1-1. Sensitivity Data for Configuration 1 (TSUNAMI-3D & ENDF/B-VII.0).

Nuclide	Reaction	Sensitivity	±	1σ
^{235}U	nubar	0.981180	±	0.000031
^{235}U	total	0.659700	±	0.000938
^{235}U	fission	0.627030	±	0.000327
^{235}U	scatter	0.073714	±	0.000605
^{235}U	elastic	0.041890	±	0.000177
^{235}U	n,gamma	-0.041048	±	0.000043
^{235}U	capture	-0.041048	±	0.000043
^{235}U	n,n'	0.029851	±	0.000463
^{238}U	total	0.010226	±	0.000051
^{238}U	nubar	0.010080	±	0.000001
^{234}U	nubar	0.007894	±	0.000000
^{238}U	fission	0.006588	±	0.000005
^{234}U	total	0.005498	±	0.000009
^{238}U	scatter	0.005206	±	0.000046
^{234}U	fission	0.005143	±	0.000003
^{238}U	elastic	0.003114	±	0.000013
^{39}K	total		--	
^{238}U	n,n'	0.001999	±	0.000036
^{39}K	capture		--	
^{238}U	n,gamma	-0.001568	±	0.000001
^{238}U	capture	-0.001568	±	0.000001
^{235}U	n,2n	0.001456	±	0.000008
^{39}K	n,p		--	
^{56}Fe	total	-0.001007	±	0.000038
TOTAL	**--**	**1.342740**	**±**	**0.001269**

Table D.1-2. Sensitivity Data for Configuration 2 (TSUNAMI-3D & ENDF/B-VII.0).

Nuclide	Reaction	Sensitivity	±	1σ
^{235}U	nubar	0.981230	±	0.000032
^{235}U	total	0.659840	±	0.000947
^{235}U	fission	0.626670	±	0.000331
^{235}U	scatter	0.074338	±	0.000612
^{235}U	elastic	0.042234	±	0.000178
^{235}U	n,gamma	-0.041170	±	0.000043
^{235}U	capture	-0.041170	±	0.000043
^{235}U	n,n'	0.030148	±	0.000469
^{238}U	total	0.010252	±	0.000051
^{238}U	nubar	0.010045	±	0.000001
^{234}U	nubar	0.007883	±	0.000000
^{238}U	fission	0.006564	±	0.000005
^{234}U	total	0.005496	±	0.000009
^{238}U	scatter	0.005261	±	0.000047
^{234}U	fission	0.005133	±	0.000003
^{238}U	elastic	0.003144	±	0.000013
^{39}K	total	-0.002038	±	0.000034
^{238}U	n,n'	0.002024	±	0.000037
^{39}K	capture	-0.001580	±	0.000006
^{238}U	n,gamma	-0.001573	±	0.000001
^{238}U	capture	-0.001573	±	0.000001
^{235}U	n,2n	0.001439	±	0.000008
^{39}K	n,p	-0.001141	±	0.000004
^{56}Fe	total	-0.000828	±	0.000037
TOTAL	**--**	**1.342740**	**±**	**0.001283**

Table D.1-3. Potassium Sensitivity Data for Configuration 2 (TSUNAMI-3D & ENDF/B-VII.0).

Nuclide	Reaction	Sensitivity	±	1σ
^{39}K	total	-0.002038	±	0.000034
^{39}K	capture	-0.001580	±	0.000006
^{39}K	n,p	-0.001141	±	0.000004
^{39}K	scatter	-0.000458	±	0.000031
^{39}K	elastic	-0.000417	±	0.000031
^{39}K	n,alpha	-0.000394	±	0.000002
^{41}K	total	-0.000053	±	0.000003
^{39}K	n,gamma	-0.000046	±	0.000000
^{41}K	scatter	-0.000042	±	0.000003
^{39}K	n,n'	-0.000037	±	0.000002
^{41}K	elastic	-0.000030	±	0.000002
^{41}K	capture	-0.000012	±	0.000000
^{41}K	n,n'	-0.000011	±	0.000001
^{41}K	n,gamma	-0.000009	±	0.000000
^{41}K	n,p	-0.000001	±	0.000000
^{41}K	n,alpha	-0.000001	±	0.000000
TOTAL	**--**	**0.002915**	**±**	**0.000056**

Table D.1-4. Sensitivity Data for Potassium Worth Measurement (TSUNAMI-3D & ENDF/B-VII.0).

Nuclide	Reaction	Sensitivity	±	1σ
^{235}U	nubar	0.000159	±	0.000056
^{235}U	total	0.000000	±	0.001339
^{235}U	fission	0.000495	±	0.000468
^{235}U	scatter	0.000611	±	0.000865
^{235}U	elastic	0.000337	±	0.000252
^{235}U	n,gamma	0.000114	±	0.000061
^{235}U	capture	0.000114	±	0.000061
^{235}U	n,n'	0.000292	±	0.000662
^{238}U	total	0.000024	±	0.000073
^{238}U	nubar	0.000037	±	0.000001
^{234}U	nubar	0.000012	±	0.000001
^{238}U	fission	0.000025	±	0.000008
^{234}U	total	0.000004	±	0.000012
^{238}U	scatter	0.000054	±	0.000066
^{234}U	fission	0.000011	±	0.000004
^{238}U	elastic	0.000030	±	0.000019
^{39}K	total	0.002047	±	0.000034
^{238}U	n,n'	0.000025	±	0.000052
^{39}K	capture	0.001587	±	0.000006
^{238}U	n,gamma	0.000004	±	0.000002
^{238}U	capture	0.000004	±	0.000002
^{235}U	n,2n	0.000018	±	0.000011
^{39}K	n,p	0.001146	±	0.000004
^{56}Fe	total	0.000179	±	0.000053
TOTAL	**--**	**0.002989**	**±**	**0.001814**

D.2 MCNP-Calculated Sensitivity Data

A summary of the computed sensitivity data using MCNP6.1 and ENDF/B-VII.1 neutron cross-section data for the benchmark model is provided in Tables D.1-5 and D.1-6 for Configurations 1 and 2, respectively. Table D.1-7 provides the sensitivity for just the potassium constituents in Configuration 2. Table D.1-8 provides the sensitivity for the potassium worth measurement.

Table D.1-5. Sensitivity Data for Configuration 1 (MCNP6.1 & ENDF/B-VII.1).

Nuclide	Reaction	Sensitivity	±	1σ
^{235}U	nubar	0.981273	±	0.000004
^{235}U	total	0.741136	±	0.000006
^{235}U	fission	0.643930	±	0.000004
^{235}U	elastic	0.077152	±	0.000004
^{235}U	inelastic	0.058189	±	0.000002
^{235}U	n,gamma	-0.039780	±	0.000000
^{235}U	capture	-0.039780	±	0.000000
^{235}U	s45°-0°	-0.040658	±	0.000002
^{235}U	s135°-90°	0.028434	±	0.000002
^{238}U	total	0.015382	±	0.000001
^{238}U	nubar	0.010028	±	0.000000
^{235}U	s180°-135°	0.019096	±	0.000001
^{235}U	i180°-135°	0.007686	±	0.000001
^{234}U	nubar	0.007869	±	0.000000
^{235}U	i90°-45°	-0.007523	±	0.000001
^{235}U	i45°-0°	-0.007121	±	0.000001
^{235}U	i135°-90°	0.006958	±	0.000001
^{238}U	fission	0.006769	±	0.000000
^{234}U	total	0.006428	±	0.000001
^{238}U	elastic	0.005847	±	0.000001
^{234}U	fission	0.005289	±	0.000000
^{56}Fe	total	0.005306	±	0.000000
^{56}Fe	elastic	0.004643	±	0.000001
^{238}U	inelastic	0.004165	±	0.000001
^{235}U	s90°-45°	0.006872	±	0.000002
^{238}U	s45°-0°	-0.002725	±	0.000001
^{39}K	elastic		--	
^{235}U	n,2n	0.001647	±	0.000000
^{238}U	n,gamma	-0.001519	±	0.000000
^{238}U	capture	-0.001519	±	0.000000
^{56}Fe	e180°-135°	0.001285	±	0.000000
^{52}Cr	total	0.001520	±	0.000000
^{56}Fe	e45°-0°	-0.001105	±	0.000000
^{52}Cr	elastic	0.001382	±	0.000000
^{39}K	capture		--	
^{39}K	e180°-135°		--	
^{238}U	s135°-90°	0.001974	±	0.000001
^{234}U	elastic	0.001016	±	0.000000
^{238}U	s180°-135°	0.001457	±	0.000000
TOTAL	**--**	**1.393937**	**±**	**0.000011**

Table D.1-6. Sensitivity Data for Configuration 2 (MCNP6.1 & ENDF/B-VII.1).

Nuclide	Reaction	Sensitivity	±	1σ
^{235}U	nubar	0.981304	±	0.000004
^{235}U	total	0.740626	±	0.000006
^{235}U	fission	0.643442	±	0.000004
^{235}U	elastic	0.077482	±	0.000004
^{235}U	inelastic	0.057963	±	0.000002
^{235}U	n,gamma	-0.039955	±	0.000000
^{235}U	capture	-0.039955	±	0.000000
^{235}U	s45°-0°	-0.024556	±	0.000002
^{235}U	s135°-90°	0.017382	±	0.000002
^{238}U	total	0.015407	±	0.000001
^{238}U	nubar	0.010006	±	0.000000
^{235}U	s180°-135°	0.009027	±	0.000001
^{235}U	i180°-135°		--	
^{234}U	nubar	0.007861	±	0.000000
^{235}U	i90°-45°		--	
^{235}U	i45°-0°		--	
^{235}U	i135°-90°		--	
^{238}U	fission	0.006761	±	0.000000
^{234}U	total	0.006377	±	0.000001
^{238}U	elastic	0.005793	±	0.000001
^{234}U	fission	0.005284	±	0.000000
^{56}Fe	total	0.005248	±	0.000001
^{56}Fe	elastic	0.004448	±	0.000001
^{238}U	inelastic	0.004268	±	0.000001
^{235}U	s90°-45°	-0.001853	±	0.000002
^{238}U	s45°-0°	-0.001717	±	0.000001
^{39}K	elastic	0.001698	±	0.000001
^{235}U	n,2n	0.001690	±	0.000000
^{238}U	n,gamma	-0.001525	±	0.000000
^{238}U	capture	-0.001525	±	0.000000
^{56}Fe	e180°-135°	0.001481	±	0.000000
^{52}Cr	total	0.001451	±	0.000000
^{56}Fe	e45°-0°	-0.001314	±	0.000000
^{52}Cr	elastic	0.001296	±	0.000000
^{39}K	capture	-0.001296	±	0.000000
^{39}K	e180°-135°	0.001238	±	0.000000
^{238}U	s135°-90°	0.001164	±	0.000000
^{234}U	elastic	0.000993	±	0.000000
^{238}U	s180°-135°	0.000709	±	0.000000
TOTAL	**--**	**1.392727**	**±**	**0.000010**

Table D.1-7. Potassium Sensitivity Data for Configuration 2 (MCNP6.1 & ENDF/B-VII.1).

Nuclide	Reaction	Sensitivity	±	1σ
^{39}K	elastic	0.001698	±	0.000001
^{39}K	capture	-0.001296	±	0.000000
^{39}K	e180°-135°	0.001238	±	0.000000
^{39}K	e90°-45°	-0.000781	±	0.000000
^{39}K	e45°-0°	-0.000594	±	0.000000
^{39}K	total	0.000397	±	0.000001
^{41}K	elastic	0.000192	±	0.000000
^{41}K	total	0.000189	±	0.000000
^{39}K	e135°-90°	0.000137	±	0.000000
^{41}K	e180°-135°	0.000119	±	0.000000
^{41}K	e90°-45°	-0.000069	±	0.000000
^{41}K	e45°-0°	-0.000064	±	0.000000
^{39}K	n,gamma	-0.000018	±	0.000000
^{41}K	e135°-90°	0.000014	±	0.000000
^{41}K	capture	-0.000005	±	0.000000
^{41}K	n,gamma	-0.000004	±	0.000000
^{39}K	inelastic	-0.000002	±	0.000000
^{41}K	inelastic	0.000002	±	0.000000
^{40}K	s45°-0°	0.000001	±	0.000000
^{40}K	s90°-45°	-0.000001	±	0.000000
TOTAL	**--**	**0.002708**	**±**	**0.000001**

Table D.1-8. Sensitivity Data for Potassium Worth Measurement (MCNP6.1 & ENDF/B-VII.1).

Nuclide	Reaction	Sensitivity	±	1σ
^{235}U	nubar	0.000197	±	0.000029
^{235}U	total	0.000684	±	0.000023
^{235}U	fission	0.000640	±	0.000019
^{235}U	elastic	0.000314	±	0.000006
^{235}U	inelastic	0.000240	±	0.000003
^{235}U	n,gamma	0.000167	±	0.000001
^{235}U	capture	0.000167	±	0.000001
^{235}U	s45°-0°	0.016182	±	0.000003
^{235}U	s135°-90°	0.011107	±	0.000003
^{238}U	total	0.000022	±	0.000001
^{238}U	nubar	0.000024	±	0.000000
^{235}U	s180°-135°	0.010118	±	0.000001
^{235}U	i180°-135°	0.007722	±	0.000001
^{234}U	nubar	0.000010	±	0.000000
^{235}U	i90°-45°	0.007558	±	0.000001
^{235}U	i45°-0°	0.007154	±	0.000001
^{235}U	i135°-90°	0.006990	±	0.000001
^{238}U	fission	0.000010	±	0.000000
^{234}U	total	0.000053	±	0.000001
^{238}U	elastic	0.000056	±	0.000001
^{234}U	fission	0.000006	±	0.000000
^{56}Fe	total	0.000059	±	0.000001
^{56}Fe	elastic	0.000197	±	0.000001
^{238}U	inelastic	0.000102	±	0.000001
^{235}U	s90°-45°	0.008765	±	0.000003
^{238}U	s45°-0°	0.001013	±	0.000001
^{39}K	elastic	0.001705	±	0.000001
^{235}U	n,2n	0.000043	±	0.000000
^{238}U	n,gamma	0.000006	±	0.000000
^{238}U	capture	0.000006	±	0.000000
^{56}Fe	e180°-135°	0.000197	±	0.000000
^{52}Cr	total	0.000070	±	0.000000
^{56}Fe	e45°-0°	0.000210	±	0.000000
^{52}Cr	elastic	0.000087	±	0.000000
^{39}K	capture	0.001302	±	0.000000
^{39}K	e180°-135°	0.001243	±	0.000000
^{238}U	s135°-90°	0.000814	±	0.000001
^{234}U	elastic	0.000023	±	0.000000
^{238}U	s180°-135°	0.000752	±	0.000000
TOTAL	**--**	**0.028123**	**±**	**0.000042**

APPENDIX E: Support Structure Assembly Schematics

E.1 Drawings of Diaphragm and Low-Mass Support Structures

Additional drawings were provided by the experimenter[a] to preserve the dimensions of the support structure immediately surrounding the experiment. Figure E.1-1 represents the diaphragm and rings with its support structure. Figure E.1-2 represents the low-mass support structure. Both of these structures can be seen in Figure 1.1-3. These support structures were used in many other critical experiments with oralloy at ORCEF (see Section 1.0).

[a] Personal communication with John T. Mihalczo, February 2010.

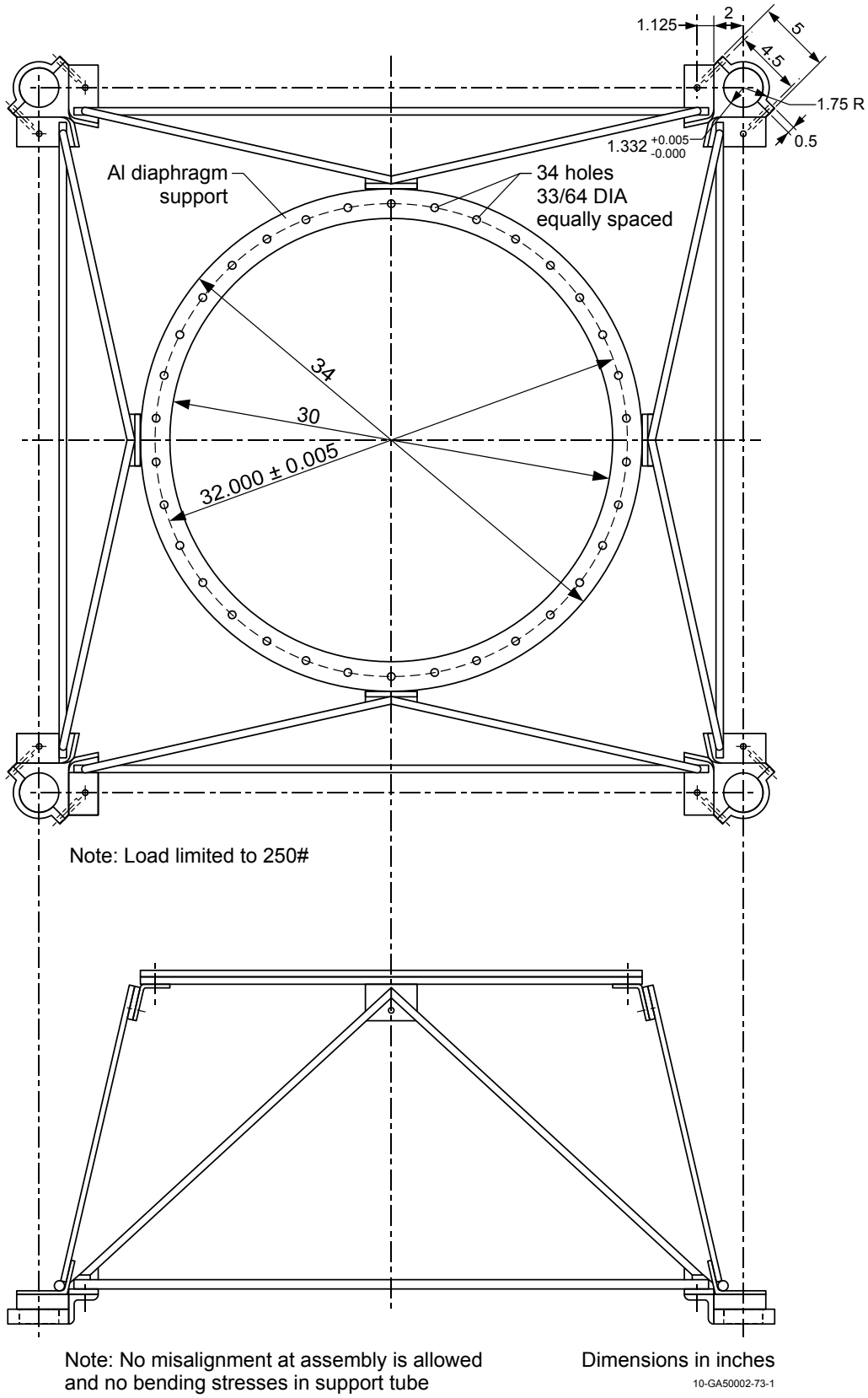

Figure E.1-1. Diaphragm Support Structure.

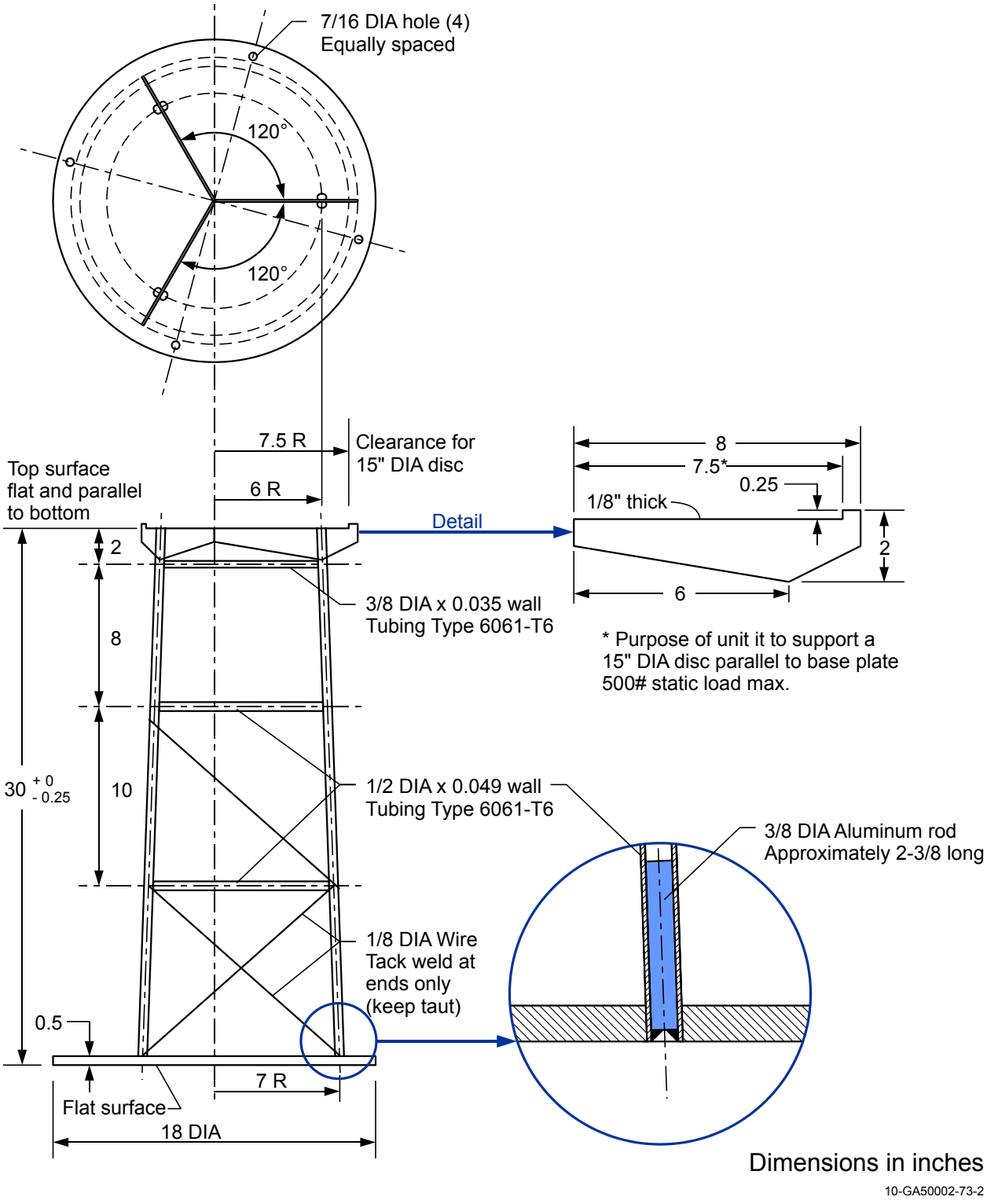

Figure E.1-2. Low-Mass Support Structure.